DOI: 10.1111/cgf.70498

EUROVIS 2026
A. Abdul-Rahman, M. Angelini, and B. Preim
(Guest Editors)

COMPUTER GRAPHICS *forum*
STAR – State of The Art Report

Survey on Visualization of Information Diffusion over Networks

T. Baumgartl[1], M. Sondag[1,5], V. Filipov[2], M. Tuscher[2], S. Rajendran[2],
S. Miksch[2], D. Archambault[3], A. Arleo[4,2], and T. von Landesberger[1]

[1]University of Cologne, Germany, [2]TU Wien, Austria, [3]School of Computing, Newcastle University, UK
[4]TU Eindhoven, the Netherlands, [5]Maastricht University, the Netherlands

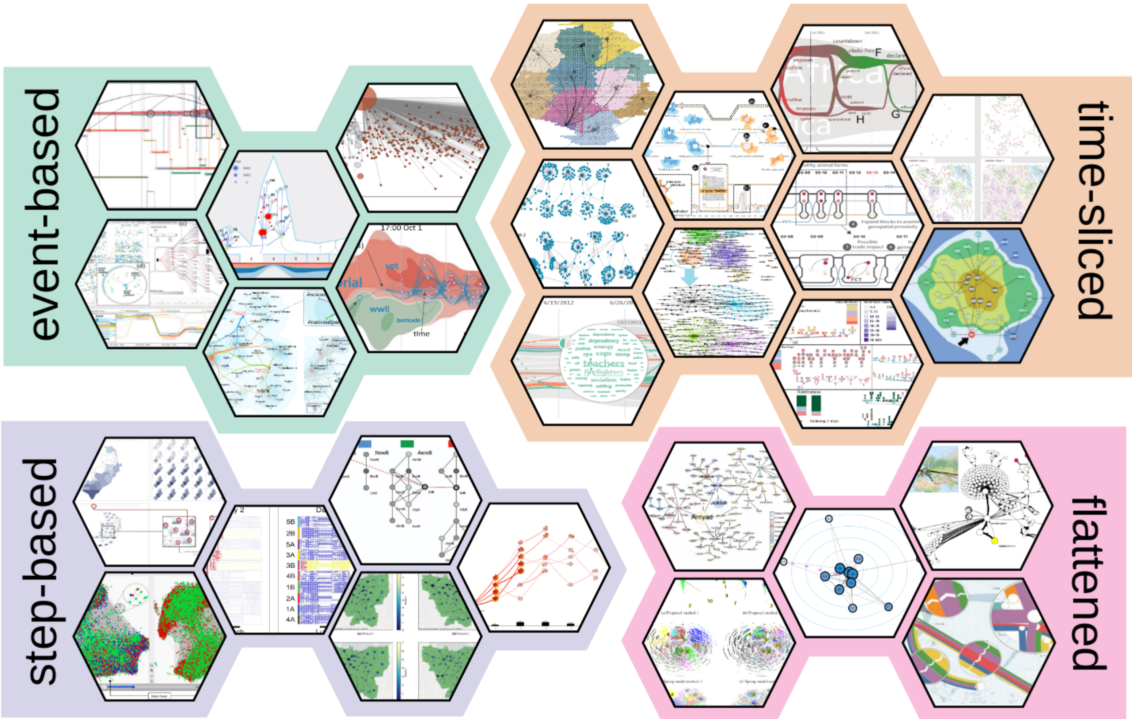

Figure 1: *Representative visualization examples of four common strategies for modeling and visualizing medium and transmission networks in information diffusion (ID). Each quadrant shows a collection of visualization thumbnails from the surveyed literature corresponding to the temporal abstractions. The colored backgrounds group the hexagonal tiles by their respective temporal modeling strategy. The number of hexagons per quadrant reflects the relative frequency of each strategy in the corpus. Typical designs include timeline-based representations for* ***event-based*** *approaches, small multiples for* ***time-sliced*** *approaches, step-wise or interactive views for* ***step-based*** *approaches, and aggregated, time-independent representations for* ***flattened*** *approaches. Together, these examples demonstrate both the diversity of visual designs and the distribution of temporal abstraction strategies in our survey.*

Abstract

Information Diffusion (ID) describes how a value (e.g., a pathogen, a rumor, a packet) spreads through an underlying "medium" network of elements (e.g., a social or computer network). Understanding the information diffusion process is essential to predicting trends, controlling misinformation, and enhancing decision-making as well as communication strategies. Visual Analytics has shown significant potential in supporting comprehension of ID processes in several domains. These approaches vary greatly in their design, both in terms of data and visual encodings. The variety of designs and application domains motivates this survey, which complements existing surveys with a focus on visualization of transmission processes in contrast to other surveys about visualizing networks. This survey defines types of transmission and medium networks, identifies common visualization principles, categorizes them, and identifies gaps–opportunities for future research.

1. Introduction

Diffusion processes are ubiquitous natural and anthropic phenomena, with a rich body of literature focusing on their combinatorial and modeling aspects. Specifically, Information Diffusion (ID) describes how a *value* spreads through an underlying *medium* network of elements. Connections between elements typically represent an opportunity for a value to transition (or be transmitted) from one node to another, progressing the diffusion process [BFR*25]. The portion of the medium network that contributes to the process makes up the *transmission* network. The diffusion process begins from a set of nodes in the medium network called *seeds* or *initiators*, but can also take other names depending on the semantics (e.g., “early adopters" or “influencers"). Therefore, an ID process can be described as a tuple of *what* is diffused (the value), *where* (the medium network), and *how* it spreads (the transmission network). The combination of these three elements makes it possible to model pathogen transmission on contact tracing networks, malware spread through networks of computers, academic papers' influence, vulnerability of finance networks, and many more.

Understanding the ID process is pivotal to analyzing the phenomenon evolution and extent, controlling misinformation, enhancing decision-making as well as communication strategies, and possibly predicting diffusion trends. Moreover, ID is intrinsically a dynamic and stochastic process: it evolves over time, usually depending on some kind of probabilistic influence metric encoded in the medium network connections. Therefore, analytical and combinatorial methods may not suffice in providing a tout-court perspective of the dynamics of diffusion. Visual Analytics (VA) has shown significant potential in supporting comprehension of ID processes across several domains ranging from pathogen transmission [AME11, AGJS*20, CSN*20, Guo07, WBv*19, STX*22, CARA*22, DARA*22], to viral news and memes [ZCW*14, WLY*14, CLY17, STP*17, YJZ*25], to financial contagion networks [vDBF15] and blockchain transactions [DBDDP*15]. VA supports the interactive exploration and analysis of diffusion processes, their patterns, characteristics, and context, in addition to (or agnostic of) the semantics of the medium network. Therefore, VA for ID is an intricate subject often involving multiple complex representations. Approaches vary greatly in their analysis methods, time modeling, and visual designs. The focus on the analysis also makes a profound difference: following the *effects* of the diffusion, like the overall spread and the interactions between the individual activated nodes (like the contacts between people [STX*22]), is profoundly different from looking at its *seed nodes* (as in tracing back to who brought the disease in the hospital ward [BPW*21]). In other cases, the scope is diffusion model development and analysis, where spread prediction, seed set selection, and customization are the goals of the analysis (how should I choose my influencers, so that my advertising spreads as far as possible [ADL*22]). A broad, organic perspective of the field would help in finding commonalities and differences in current methods, generalizing best and worst practices, and supporting researchers in complementing and expanding this field with their work.

This summarizes our motivation to survey related literature on visualizing ID processes over networks within VA literature. In light of our literature review, we categorize the body of literature according to the following aspects: (i) underlying (*medium*) network, (ii) ID process (*transmission network*) characteristics, (iii) presence and visual encodings of additional derived data, and (iv) special features, context, and semantics. These dimensions build a comprehensive yet flexible design space, providing an overview of what brings these VA methods together as well as what makes them unusual and innovative.

Contributions – With this survey, we contribute a practical resource for practitioners and researchers on the topic of visualizing ID over networks, specifically providing:

- A structured overview of papers published on the topic of visualizing ID processes over networks and a novel categorization of related work (see section 5 and section 6);
- Clarification and consolidation of terminology about ID processes in visualization, clearing ambiguities and establishing a common terminology (see section 2);
- A synthesis of the results, identification of research gaps, and highlighting of open future research directions (see section 7);

The remainder of the survey is structured as follows: section 2 consolidates the disperse usage of terms across literature resolving ambiguities; section 3 presents background, related work, and existing surveys; section 4 introduces our systematic literature review methodology, the exclusion, and inclusion criteria; section 5 and section 6 provide detailed overview of the current techniques with illustrative exemplars; section 7 synthesizes the results and outlines pressing directions for future research; section 8 concludes our survey.

2. Definitions

This section defines terminology that will be used throughout the paper and will be part of our proposed categorization.

2.1. Basic Definitions

Network. A network (or *graph* $G = (V,E)$) is a data structure composed of a set of nodes (or vertices) V and a set of relationships E that connect pairs of vertices. If those pairs are ordered, then the network is *directed*. The presence of a numerical value associated with nodes or edges makes it *weighted*. If V or E change over time (e.g., with nodes or edges appearing/disappearing), the network is *dynamic*, with time modeled in different ways (see definitions further below). For a complete treatment on the different facets typically associated with graphs, please refer to the survey by Hadlak et al. [HSS15].

Information Diffusion and Process. Information diffusion is a discipline that investigates diffusion processes. A *Diffusion* (also known as transmission or propagation) Process is a tuple $<$*information*, *medium*, *transmission*$>$. The *information* encodes the semantics and the context of the diffusion process, or, in other words, *what* is diffused. With *medium* and *transmission* we define two different networks. The medium network refers to the the structure on which the diffusion process takes place, while the transmission network consists only of the portions of the medium network on which a diffusion event was successful. Both concepts are explained in detail in subsection 2.2.

Transmission Event. Such an event happens when the information successfully traverses an edge from one previously activated node to another, previously inactive one. Formally, we define a diffusion as a transmission event *transition* $TR_{u,v}(t)$ that diffuses (transmits, transfers) the value a from a *source node* (N_u) to a *target node* (N_v) at a point in time (t) through the connecting edge $E_{u,v}$, assuming that N_u, N_v and $E_{u,v}$ all *exist* at time t. It is a directed edge event that causes diffusion from the source node to the target node. The value of the target node (N_v) from transmission event time t on, will be updated by the transition to the transmitted value a.

2.2. Why Distinguishing Between Medium and Transmission Networks Matters

The medium and transmission networks differ in structure, semantics, and temporal behavior.

The medium network (M-NW) provides the context and substrate of a diffusion process. The term medium is chosen from physics where it is the substance that transmits energy (light or sound) through it. It represents the set of *all pathways*, i.e., all possible routes along which a diffusion process could occur according to domain-specific constraints. In this context, a pathway denotes a possible connection between entities that enables transmission, such as physical contact, communication, or exposure. Examples of medium networks include patient contact tracing networks, a follower graph in social media, a financial exposure network, or a network topology in the context of cybersecurity.

The transmission network (T-NW) represents the realized diffusion process: the spread of a pathogen, rumor, or risk. They represent a sub-network of the medium, where its edges correspond to concrete transmission events from all the possible transmission events, represented by the edges of the medium network (see previous subsection). In other words, its vertex set contains all the vertices of the medium network that were activated by the diffusion process and the corresponding edges where transmission events took place.

From a visualization perspective, the transmission network defines the core object of analysis, as it determines how diffusion unfolds over time and space. Visual encodings must therefore support temporal ordering, progression, and accumulation of events, for example, through animation, time-slicing, path highlighting, or aggregation. The transmission process may terminate naturally or be bounded by observation windows or simulation constraints, which further influence how the diffusion is visually summarized and interpreted. Even when the transmission network is visualized in a flattened manner, there was always time and ordering behind its process, which differentiates it from the medium network.

2.3. Temporal Representation in Medium and Transmission Networks

Dynamicity is an intrinsic feature of ID. Therefore, the different methods and techniques that we report in the remainder of the paper model time in different ways for the medium and/or transmission networks. This depends on several factors, depending on the visualization design tasks, data characteristics, and general context. The temporal aspect is therefore a cornerstone in defining our paper categorization, as such a decision heavily influences the final visualization design. An overview of types of temporal representation is shown in Figure 2.

An **event-based** time representation represents the most natural method to represent time in networks. The term event-based has been used in the visualization community and is inspired by research in event sequence visualization [MLMdO*13, MLL*13] where each data element has its own individual time coordinate and the notion of the time-slice is rejected. In this instance, no temporal structure is imposed on the data and nodes/edges retain their original time information (e.g., start timestamp, duration). For ID, this has a profound impact. Event-based networks have been studied extensively for decades – known under the more general name of *temporal networks* [HS12] as they are a more natural representation of time and are easier to use when visualization is not the goal. Only recently have researchers looked at algorithms for drawing [SAK17, SAK20, AMA22, PS20] and visualizing [FCAA23, FCAA25, LAN19, LAN21] dynamic graphs in an event-based way directly. This said, methods have considered temporal networks that encode diffusion processes and have tried to visualize them in an event-based way.

Time-slicing sacrifices the precise order of nodes and edges by aggregating them into slices. Aggregating, however, inevitably means losing temporal information to quantization error and requires identifying a suitable temporal resolution but simplifies the visual representation. Consequently, time-sliced representations also constitute one of the richest historical foundations for M-NW and T-NW visualization, both within visualization research and in applied domains. The time-slice has been the primary mode for visualizing and drawing dynamic networks as it makes visualization computationally efficient and easier to conduct. It has been extensively studied in the context of dynamic graph drawing [BM11, DG02, EHK*03, FKN*04, DGK01, AP16a, AP12]. Time-slicing can also be non-uniform [TPL*25, WAH*19, PLFT21]. In this survey, we do not distinguish between uniform and non-uniform time-slicing as we found fewer non-uniform methods in our search.

Step-based time modeling focuses only on the order of the events. In other words, steps emphasize ordering and dependency, without including explicit temporal information – as it is more important to understand what came before/after rather than when in time. Depending on if the individual nodes or edges are ordered or if sets of them are ordered, step-based can be either time-sliced or not time-sliced.

With a **flattened** model (terminology adopted from Bach et al. [BDA*17]), the time dimension is collapsed into a single network representation whose node and edge sets aggregate all elements appearing over time. This definition directly applies to transmission networks, where temporally ordered events are often summarized into a single structure. For medium networks, the distinction between static and flattened is more nuanced.

A **static** network typically denotes a representation corresponding to a single time point or an explicitly time-independent dataset. In contrast, a flattened network results from collapsing temporal variations across multiple time points into a single representation.

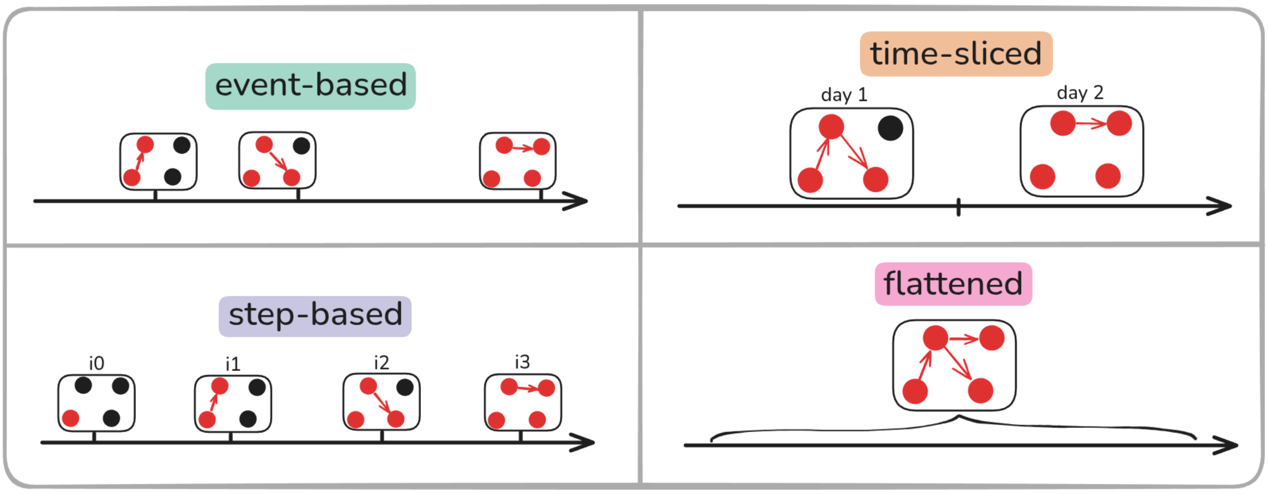

Figure 2: *Four common strategies for representing the temporal evolution of transmission networks. Red nodes are active/infected, red arrows visualize propagation.* ***Event-based*** *representations depict individual transmission events along a continuous time axis.* ***Time-sliced*** *representations aggregate transmissions within discrete temporal windows (e.g., days), yielding a sequence of network snapshots.* ***Step-based*** *representations organize transmissions into ordered propagation steps or iterations, independent of absolute time.* ***Flattened*** *representations collapse temporal information into a single, static network by aggregating all transmissions over time. Different temporal abstractions and temporal visualizations shape the visibility of transmission processes and their interpretation.*

In many application contexts, medium networks (e.g., follower-followee networks) evolve at a much slower rate than the transmission processes being analyzed. As a result, they are often treated as static for analytical and visualization purposes, even though they could also be interpreted as flattened representations over longer temporal scales.

Implicit medium network This special case is only for the M-NW. It is implicit, unknown, or intentionally omitted, while the transmission network T-NW is known and one of the previous temporal cases. In practice, this occurs when the medium structure is unavailable (e.g., missing or privacy restricted, such as in infection transmission, where the exact contact network is unavailable, only the infection information), when diffusion is modeled or inferred without an explicit medium (e.g., having only retweet information without underlying social structure of the individuals tweeting), or when the analytical focus lies primarily on outcomes and temporal phases rather than on structural mechanisms (e.g., interest is on the number of infections per geographic region, rather than exact pathways).

3. Related Work

Information diffusion research extensively investigated the factors that affect information diffusion, how information is disseminated, and how these aspects can be distilled into models that can be used to reliably simulate and replicate such complex behavior [LZ14]. As the goal of our survey is to discuss the intersection of ID with (network) visualization, it would be beneficial to discuss how that relates to computational diffusion modeling, and its applications in min/max related problems such as *influence maximization*. In the following, we frame our contributions in related literature, focusing on other surveys that, along with ours, help create a complete landscape of the topic.

Network and Graph Visualization. This discipline features a rich corpus of knowledge that evolved from simple network visualization techniques to advanced methods to cover complex, dynamic, multi-faceted data structures. As a comprehensive treatment of network visualization is beyond the scope of this paper, we summarize related work in this area, focusing on survey papers. In the early 2000s, Herman et al. [HMM00] presented a survey of graph drawing beyond its algorithmic aspects, speaking a language familiar to the visualization community. Techniques were discussed and classified according to the layout methods, interactions, navigation approaches, and methods to reduce visual complexity. The concept of "complex" or "large" network evolved significantly in a relatively short amount of time. Von Landesberger et al. [vKS*11] present a state-of-the-art review of large graph visualization, emphasizing scalability, interaction, and layout stability while noting challenges in visualizing dynamic structures. In the early 2010s, evolving networks gained traction and visibility in the research community. Beck et al. [BBDW17] survey visualization techniques on dynamic graphs, establishing a clear and widely accepted terminology. Bach et al. [BDA*17] survey dynamic data visualization and provide a terminology for describing operations that can be applied to space and time. Hadlak et al. [HSS15] introduce an overview of multi-faceted network visualization. These aspects (*facets*, i.e., dynamics, multivariate attributes, geospatial information) are particularly relevant to ID visualization, as diffusion data inherently exhibits one or multiple of these characteristics. Nobre et al. [NMSL19] review multivariate networks, McGee et al. [MGM*19] summarize contributions to multilayer network visualization, and Schöttler et al. [SYPB21] categorize work on (geo-)spatial network visualization. Kerracher et al. [KKC14] introduce the design space matrix, categorizing the visualization techniques for temporal networks based on their structural and temporal encoding strategies. Yoghourdjian et al. [YAD*18] survey the concept of visual complexity (i.e., visual scalability) in more detail, addressing how networks can be effectively visualized as they grow in both nodes and edges. We refer the reader to the survey by Filipov et al. [FAM23] for a synthesis of the broader landscape of network visualization research.

ID and Influence Maximization. ID processes and propagation models have been extensively reviewed from computational and mathematical perspectives (see, e.g., [GHFZ13, ZM14, MMH21, Sum13]). These surveys focus on understanding how structural and temporal properties of networks shape diffusion dynamics and have inspired computational models mimicking real-world spreading phenomena (e.g., [BGG19, CS14, FGRW*15, KKT05, MBZ22]). This effort in understanding and modeling diffusion acted as the cornerstone for tackling real-world optimization problems, such as in Influence Maximization (IM). In IM, the goal is to find the smallest set of initial seeds that maximizes the diffusion of a process under the assumptions of a diffusion model [KKT05, LZ14]. This has applications in viral marketing [CWW10, Tan18], social influence analysis [LFWT18], and social engineering [HFZW23, LZW25]. IM, however, is NP-Hard [KKT03] - in this, visualization, and network visualization in particular, can play a significant role in analyzing which aspects of the network can influence the spread, leading to increased confidence and user feedback in the seed set selection [ADL*22].

Specific Diffusion Domains. Visualization research on ID is emphasized as a necessity throughout domain-specific studies. Research on infectious disease transmission and epidemiology [BGG*11], particularly COVID-19 [KDB*24, ZSG*23, LLJ*24, CARA*22, DARA*22], highlights challenges in visualizing dynamic and real-time events while ensuring accuracy and interpretability. In parallel, the rise of social media has catalyzed extensive research on visualizing information diffusion, including identifying influential key players, understanding spreading patterns, and reasoning about information propagation [GHFZ13, CLS*12, CCW*16, CCL*17, CCW*18, CLCY19, WDC*22] and sentiment [KPK18]. Chen et al. [CLY17] categorize visualization techniques for social media analysis according to a range of VA tasks, illustrating how research in this domain has shifted and evolved over time. Research on information diffusion extends to socio-economic contexts such as public policy adoption to analyze how policies spread across the states [AL20].

Survey Structure. Surveys in visualization and visual analytics domain are commonly structured along different primary dimensions, including the underlying data to be visualized [vKS*11, FAM23, HSS15, MGM*19], the type of visualization used [BBDW17, YAD*18, SYPB21, BDA*17], or the part of the visual analytic workflow addressed [HKPC18, MOM*24] using an interrogative approach. Often surveys combine these aspects – for instance, the type of visualization aspect and the data type, such as layout and graph type, as done by von Landesberger et al. [vKS*11]. Given the complexity of the data that is visualized in ID processes – M-NW and T-NW as well as several types of time aspects – we have decided to use the data type as the main aspect of the survey categorization. Lower levels are categorized according to the type of visualization and application domain. While section 5 focuses on the used visualization designs, additional analytical aspects such as derived values and additional charts, interaction, layouts, and tasks and requirements are discussed in section 6.

With this literature survey, we wanted to review both the network visualization and ID literature to support our motivation in writing this paper. Within visualization literature, there is no comprehensive survey systematically examining how ID processes over networks are visualized across domains and techniques. Usul and Arleo [UA24] showcase exemplar systems and outline the need for such analysis. Our survey addresses this by providing a systematic literature review of VA for ID processes, examining how visualization represents both the underlying medium networks and the diffusion dynamics that unfold upon them.

4. Methodology

We followed the PRISMA statement [PMB*21] to collect related publications. We started our search by abstracting keywords from an initial set of 114 papers that relate to the visualization of ID processes. We divided the keywords into three categories: (1) synonyms for **ID** (*31 keywords, like contagion, spread*), (2) **(temporal) graphs** (*8 keywords, like dynamic graph or network*), and (3) **visualization** (*3 keywords, like visual analytics*). Table 1 shows all the keywords we used. For the search terms, keywords were combined across the three categories. We utilized seven different data sources for papers with all 792 search combinations of these keywords: the Scopus [Els25], CrossRef [Cro25], and Semantic Scholar [LWN*20] APIs, and the VISPUB [IHK*16], VISPUBs [Lan24], CGF [Eur25], and DBLP [Ley02] databases. The databases cover all major visualization conferences, and the APIs allow us to search for papers of interest outside the direct visualization domain. We filtered out certain document types that do not represent peer-reviewed research contributions, including books, book chapters, datasets, dissertations, editorials, notes, and retracted or posted content, ensured that the remaining papers were deemed relevant by the scientific community (≥ 1 citation per year of publication), and were written in the English language. To make sure they were sufficiently relevant for our purposes, we required the papers requested via the APIs and DBLP to be found at least three times, which means using at least three different combinations of keywords. This resulted in a total of 5,377 unique papers with very limited overlap across the seven data sources. We verified that this set included all our initial 114 papers, indicating that the coverage is sufficient. No paper was retrieved by all sources, and only a single paper appeared in six sources.

Analyzing the overlap among the three API-based sources (Scopus, CrossRef, and Semantic Scholar) further revealed substantial disparities in coverage (see Figure 3): 2,616 (out of 5,377) papers were identified by these three API's, with only five papers shared by all three sources. Of these 2,616 papers. 1,699 papers were retrieved exclusively from Scopus, 605 exclusively from Semantic Scholar, and 84 exclusively from CrossRef, with notably asymmetric pairwise overlaps. Similar patterns of low overlap were observed for the curated databases (DBLP, CGF, VISPUB, and VIS-

Information Diffusion				(Temporal) Graphs	Visualization
diffusion	event	receive	interrelationship	graph	visualization
contagion	scheduling	pathway	interplay	network	visualisation
spread	cascade	route	interrelated	dynamic graph	visual analytics
connectivity	transfer	trace | tracing back | backtracing	influence	dynamic network	
propagation	dissemination	branching	sequence	temporal graph	
temporal paths	flow	secondary delays	messaging	temporal network	
infections	transmission	reconstruct	gatekeepers	static graph	
dynamic paths	send	contract tracing		static network	

Table 1: *The 31 keywords for Information Diffusion, 8 for (Temporal) Graphs, and 3 for Visualization that were used as search terms.*

PUBs), where the majority of retrieved papers were unique to a single source. These findings indicate that a substantial portion of relevant literature would not have been captured if fewer data sources had been considered. Due to the resulting corpus size, an initial title-based screening assessed potential relevance. A paper was considered potentially relevant if, based on its title, it could plausibly address the visualization of information diffusion processes on networks. To mitigate individual interpretation bias at this early stage, the screening was performed independently by two co-authors. Papers were kept if at least one of the two co-authors marked them as potentially relevant. There were 207 papers determined to be relevant by both authors, 662 papers were determined to be relevant by one of the authors, and 4,508 papers were deemed irrelevant by both. Papers deemed irrelevant by both co-authors were filtered out, leaving 890 papers. Of these, 22 papers were inaccessible (none of the authors had free access to the papers' content) and filtered out, for a total of 868 papers deemed potentially relevant. These 868 papers were redistributed to six co-authors, with each paper being assigned to two co-authors to skim-read it and determine whether it would be included or excluded for categorization. One of the remaining co-authors served as a tie-breaker.

Inclusion and Exclusion Criteria. In the following, we will describe the criteria we used for including and excluding papers.

Inclusion:

I1 The paper contains **visualizations**.
I2 The visualization shows a **network-based representation**
I3 The visualization shows at least one explicit **transmission, propagation, or diffusion event** occurring **on the network**

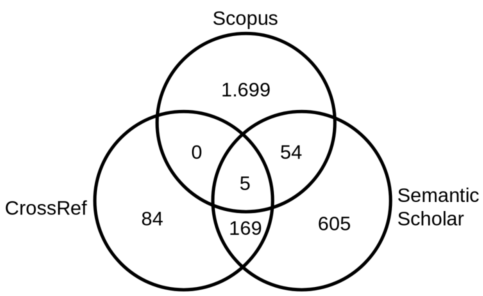

Figure 3: *Set visualization of the overlap between Scopus, CrossRef, and Semantic Scholar, the low overlap between them.*

A visualization of the *transmission network* alone is sufficient for inclusion. The presence of a separate visualization of the *medium network* is not required. The transmission network does not need to be complete (e.g., local subgraphs), provided that the transmission is explicitly represented as occurring between network entities.

In contrast to purely structural network visualizations, included papers must visualize the **process of propagation or diffusion itself**, rather than only the underlying medium network typology.

Exclusion:

E1 Papers only showing medium networks (no transmissions).
E2 Papers visualizing transmissions or flows that are **not modeled on an underlying network** (e.g., particle systems, vector fields, continuous flow simulations).
E3 Papers about transmission processes, but no visualizations.
E4 Survey papers about network diffusion.

Consequently, we excluded citation networks and bibliographic visualizations that only show the structure of the literature and do not analyze the propagation of ideas (E1), traffic networks that do not contain, e.g., propagation of delays (E1), software dependency and data provenance networks where edges represent deterministic dependencies rather than stochastic transmission events (E1), neural (brain) networks (E1, E2, E3), event sequence visualizations without propagation (E1), vector fields and particle visualizations (E2), family trees and similar hierarchical structures without specific transmissions (E1), circuit diagrams (E1), and general survey papers about diffusion without visualization (E4). We further excluded networks with "coincidental" transmissions, meaning that the transmission process was not the focus of the paper or only present in certain use cases. For example, Liu et al. [LWW*13] visualize storylines of different movies. One of these is "The Lord of the Rings" where two incidents are shown in which the ring is transmitted from one character to another. The transmission is neither a central analytics concept nor consistently present across examples. Therefore, the paper was excluded.

Finally, after an initial skim reading of all papers using these inclusion and exclusion criteria, 201 papers were deemed relevant enough to be included for the categorization. The complete categorization of the papers was conducted by eight co-authors, with each paper being categorized by one co-author, except in difficult cases, which were discussed among multiple co-authors. Of the 201 papers, 92 papers have been included in the final categorization. The remaining 109 were excluded after a full read of the paper.

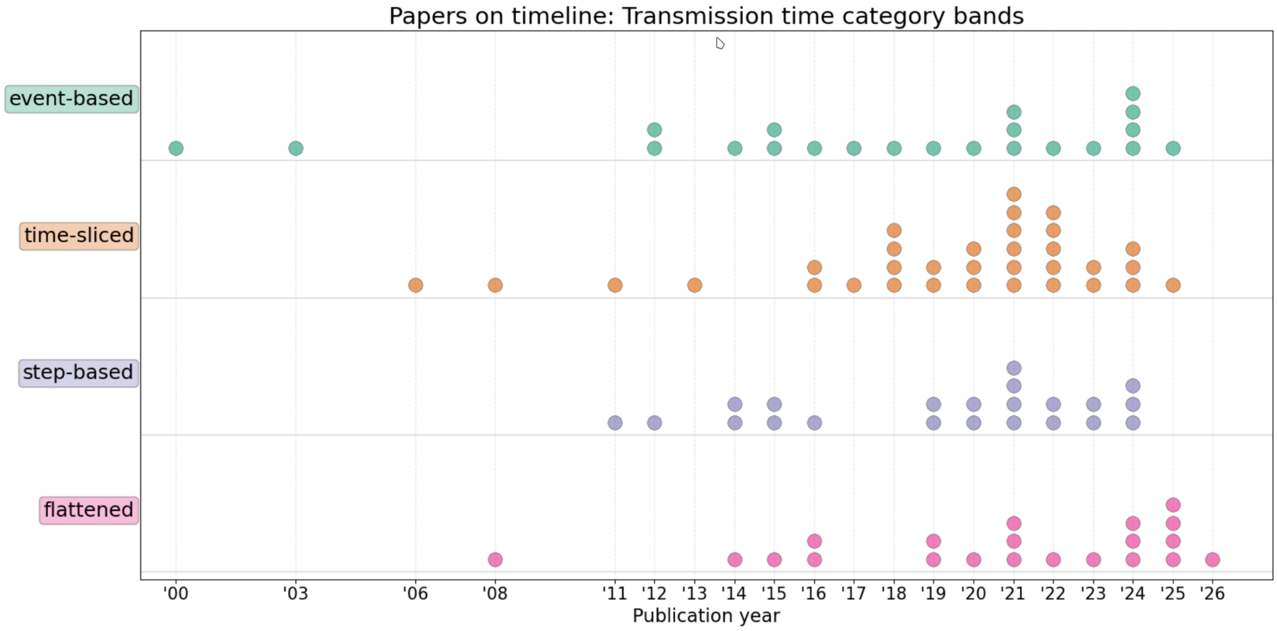

Figure 4: *Distribution of surveyed papers over time by transmission network temporal category. Each point represents a paper positioned by its publication year (x-axis) and assigned to one of four temporal categories (y-axis bands): event-based, time-sliced, step-based, and flattened. Colors redundantly encode the same categories as the vertical positioning. The x-axis uses abbreviated year labels (e.g., '00 for 2000, '15 for 2015), and stacked points indicate multiple papers per year and category. Empty years are not plotted.*

Figure 4 demonstrates that the visualization of ID processes is a recent and ongoing research trend of the last two decades. The figure shows temporal trends in the number and type of published papers. In general, time-sliced networks form the largest group of papers, which makes sense due to the commonly used sliced-type of data collection and type of propagation simulation. The figure also shows that the number of publications heavily picked up with/after the COVID-19 pandemic. This trend is the same across all temporal types of networks.

Limitations and Scope – Our categorization is shaped by the methodological choices made in this state-of-the-art report.

First, the primary perspective we use for the proposed categorization is the way in which time is modeled and represented in the visualization approaches. This temporal focus is motivated by the fact that diffusion and transmission processes are inherently temporal, as they are defined by ordered events unfolding over time.

Second, we intentionally exclude simulation models and algorithms from the categorization. While these publications present significant contributions to information diffusion, our focus is tightly coupled with how this diffusion is visually presented and encoded.

Finally, in this survey, we primarily review and discuss related literature and VA approaches for two-dimensional displays, such as desktops and large-screen environments. Virtual and augmented reality approaches were not explicitly excluded (nor did we directly query these using keywords), they are simply underrepresented in the queried literature and remain a direction for future research. Additionally, recent developments in generative AI and large language models are not explicitly covered in this survey. These approaches were not part of our search scope and are not yet sufficiently represented in the literature on visualization of information diffusion to support a systematic analysis within this work.

Extension for Recent Publications (2025 – 2026). As our initial search was conducted on literature up to 2024, we repeated the identical search procedure in March 2026 to include more recent publications. We used the same keyword combinations, data sources, and inclusion/exclusion criteria as described above, restricting the query to publications from 2025 and 2026. This resulted in an additional 653 unique papers, of which 17 were deemed potentially relevant after title-based screening, and 6 papers were finally included after full-text review. These papers were integrated into the final corpus and categorization without modifying the methodology or classification scheme, resulting in 98 papers total.

5. Visualizing Information Diffusion over Networks

Visualizing information diffusion requires understanding not only *what* is spread, but also *where* and *when* spreading was possible. Therefore, diffusion processes are fundamentally shaped by two distinct but interdependent network structures, the medium and transmission network (see section 2).

Although many visualization papers reference both implicitly, they are rarely made explicit as separate conceptual objects. In this survey, we explicitly distinguish whether a visualization depicts the *potential* for diffusion encoded by the underlying network structure (medium network), the *actual* diffusion events that occurred on that structure (transmission network), or a combination of both. While this separation is often not directly stated in the literature, it can be inferred from how visualizations encode structure and events. Making this distinction explicit is essential for correctly interpreting what is being visualized, for reasoning about causality and constraints in diffusion processes, and for comparing visualization techniques that encode fundamentally different aspects of diffusion.

5.1. Structure of this section

In the remainder of this section, we categorize diffusion visualizations over networks according to the **temporal structure of the transmission network**. The categorization is organized as a time-matrix, in which columns correspond to the temporal models of the transmission network (event-based, sliced, step-based, flattened), and rows correspond to the temporal models of the medium network (event-based, sliced, step-based, flattened, implicit).

The structure of this section follows this matrix column by column (see Table 2). For each transmission network temporal model, we discuss how diffusion is visualized across the different temporal representations of the medium network. Within each transmission network (T-NW) and medium network (M-NW) combination, we summarize the main trends for application domains and types of visualizations. We then provide details on the existing techniques grouped by application domain. This enables an overview of techniques per transmission semantic and similar data type. This organization provides a systematic traversal of the design space and facilitates direct comparison of different visualization techniques and choices between temporal combinations.

5.2. Event-Based Transmission Network Visualization

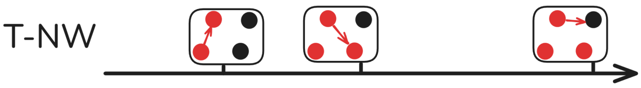

Event-based Transmission Network (T-NW) visualizations represent each diffusion event (node or edge) with precise timestamps (see also section 2). In contrast to discretized or aggregated models, timestamps in event-based T-NWs are typically irregular, unevenly spaced, and have high temporal granularity. This allows for strict temporal ordering of events and supports reasoning about causality and fine-grained temporal relationships. As such, event-based representations are the richest and most informative temporal model for T-NWs, which distinguishes them from the other time representations (see also section 2).

In this section, we discuss **22 approaches** that employ event-based T-NWs in combination with different temporal abstractions of the Medium Network (M-NW).

These works predominantly appear in **application domains** where precise timing and causality are central, including epidemiology, infection control, and medicine (5 of 22) [BPW*21, LCZ*24, JPAP21, VBF*17, GJG*19], social media, information diffusion, and citation analysis (8 of 22) [CLS*12, LLZ*16, LHS*15, HSS*20, BBB24, WLY*14, MB18, VRHGM*24], financial transactions and investments (2 of 22) [DBDDP*15, TLZ*23], event-centric computer network analysis (3 of 22) [USK21, TMW03, KSBT12], transportation (1 of 22) [XSS*24], geospatial network phenomena (1 of 22) [DWL*22], power infrastructure (1 of 22) [OW00], and a generalized approach (1 of 22) [OGGB25], which is demonstrated using datasets from several domaisn as examples. Across these domains, event-based T-NWs are used to trace concrete diffusion instances rather than aggregated trends.

From a **visualization perspective**, event-based T-NWs rely on representations that explicitly encode temporal ordering. Node-link diagrams remain common (13 of 22) [TMW03, KSBT12, LLZ*16, DBDDP*15, LHS*15, BBB24, TLZ*23, VBF*17, USK21, JPAP21, GJG*19, VRHGM*24, BPW*21, OGGB25], but are frequently augmented with timeline-based layouts (6 of 13) [LHS*15, BPW*21, TLZ*23, VRHGM*24, DBDDP*15, OGGB25], storyline-inspired designs, or flow-oriented metaphors to mitigate clutter and support temporal reasoning. For example, storyline-like layouts align entities along a temporal axis and depict transmission events as crossings or arcs (2 of 22) [BPW*21, LCZ*24], while radial or flow-based designs emphasize propagation direction and pace (3 of 22) [CLS*12, HSS*20, LHS*15]. Because individual events are visible, event-based T-NWs support detailed path tracing, but often require interaction (filtering, zooming, brushing) to remain interpretable at scale.

Temporal precision and causal structure are emphasized by special encodings in event-based T-NW visualizations. Time is typically mapped to a spatial axis or ordering (9 of 22) [DBDDP*15, LHS*15, BPW*21, TLZ*23, WLY*14, DWL*22, CLS*12, VRHGM*24, HSS*20, OGGB25], while color encodes state changes (e.g., infected, informed, invested) (15 of 22) [TMW03, KSBT12, BBB24, TLZ*23, XSS*24, VBF*17, OW00, WLY*14, USK21, GJG*19, LCZ*24, LHS*15, HSS*20, BPW*21, VRHGM*24], and edge directionality represents transmission direction (14 of 22) [TMW03, KSBT12, LLZ*16, DBDDP*15, LHS*15, HSS*20, BPW*21, VBF*17, OW00, WLY*14, DWL*22, VRHGM*24, CLS*12, XSS*24].

Additional attributes such as uncertainty, confidence, or sentiment may be encoded through opacity, glyphs, or animated motion (7 of 22) [CLS*12, BPW*21, HSS*20, TMW03, LHS*15, LCZ*24, VRHGM*24].

With respect to the **combinations of M-NW with event-based T-NWs**: event-based T-NWs: are most frequently combined with either event-based or flattened M-NWs. Event-based M-NWs (6 of 22) [LHS*15, BPW*21, TLZ*23, GJG*19, CLS*12, DBDDP*15] appear when both the potential interaction structure and the realized transmissions are logged and visualized at event resolution, such as patient transfers in hospitals or communication events in social media [LHS*15, BPW*21]. Flattened M-NWs (7 of 22) [BBB24, OW00, USK21, TMW03, KSBT12, LLZ*16, HSS*20] are common when the underlying medium structure is assumed stable or secondary, shifting analytical focus toward the dynamics of the transmission process itself. In several cases (8 of 22) [VBF*17, WLY*14, MB18, JPAP21, DWL*22, VRHGM*24, XSS*24, OGGB25], the M-NW remains implicit, with visual emphasis placed almost exclusively on the observed diffusion events

Transmission Network Time (columns) / **Medium Network Time** (rows)

Medium Network Time	subsection 5.2 event-based	subsection 5.3 time-sliced	subsection 5.4 step-based	subsection 5.5 flattened
event-based	subsubsection 5.2.1 [DBDDP*15]; [LHS*15]; [BPW*21]; [TLZ*23]; [GJG*19]; [CLS*12];			
time-sliced	subsubsection 5.2.2 [LCZ*24];	subsubsection 5.3.1 [YJZ*25]; [HWZ19]; [CLYL18]; [YZGW22]; [FBL*18]; [DC24]; [ZCW21]; [USK19]; [KLM24]; [CDBM*06]; [AC17]; [ZL21]; [WLS*22]; [XWW*13]; [NCZZ18]; [BDPC20]; [HBY*23]; [RWZ*20]; [STX*22];	subsubsection 5.4.1 [NW14]; [RRP*21]; [PVL21]; [PVL22];	
step-based			subsubsection 5.4.2 [Wu21];	
flattened	subsubsection 5.2.3 [HSS*20]; [BBB24]; [OW00]; [USK21]; [TMW03]; [KSBT12]; [LLZ*16];	subsubsection 5.3.2 [SKKS08]; [CCW*16]; [CSNW24]; [CAD21]; [HXF*21]; [SMSR20]; [TGA*23]; [FNV22]; [SPL*18]; [GGZZ22];	subsubsection 5.4.3 [WYG*11]; [SGM*23]; [ZXL23]; [XZX*24]; [ADL*22]; [AP16b]; [vDBF15]; [WBv*19];	subsubsection 5.5.1 [MZK19]; [AAA*24]; [RBJ*23]; [FH16]; [WTF*16]; [PMA*22]; [SV20];
implicit	subsubsection 5.2.4 [XSS*24]; [VBF*17]; [WLY*14]; [MB18]; [JPAP21]; [DWL*22]; [VRHGM*24]; [OGGB25];	subsubsection 5.3.3 [WLC*16]; [ASGK21]; [AME11]; [Yan21];	subsubsection 5.4.4 [LLM*19]; [SKOM12]; [BASD21]; [Gro24]; [VKPM15]; [NSS*24]; [DWC*20]; [LKB*14]; [PnABP20];	subsubsection 5.5.2 [BLRM19]; [SKM08]; [SYM24]; [SSXS15]; [DCX*24]; [TMK14]; [WM21]; [Wue21]; [LMJ*21]; [CSS*25]; [QHD26]; [GNX25]; [YLZ*25]; [RIDS25];

Paper count (cell): 0 – 19

Table 2: *Overview matrix of categorized papers. Sections and citations inside cells are clickable.*

rather than the enabling structure. A single case (1 of 22) [LCZ*24] was found, in which the M-NW is represented in a time-sliced manner.

Missing T-NW and M-NW combinations. We did not identify any examples where the T-NW is event-based while the M-NW is step-based (i.e., ordered but without time coordinates). A likely reason is that precise event timestamps in the T-NW are difficult to justify when the underlying M-NW provides only ordering information without temporal reference.

In the following subsections, we further differentiate event-based T-NW visualizations according to the temporal abstraction of the M-NW. For each combination, we summarize the number of papers, dominant application domains, and characteristic visualization strategies. Temporal combinations for which no literature was found are omitted.

5.2.1. Event-Based Transmission Network and Event-Based Medium Network

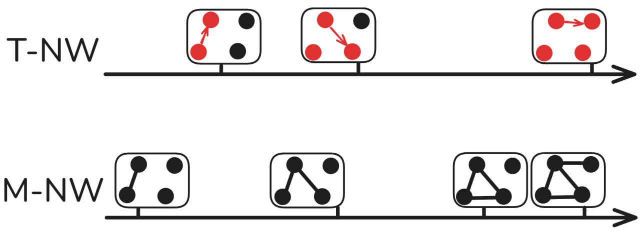

When both the T-NW and the M-NW are event-based, diffusion analysis can be performed at full temporal resolution. Transmission events as well as structural interactions between entities are represented as timestamped events, preserving exact timing and ordering. This configuration enables fine-grained causal reasoning about diffusion processes, including source identification, reconstruction of transmission chains, branching behavior, and inspection of how local medium interactions enable or constrain transmission at specific moments in time. Within our corpus, this combination comprises **6 papers** and occurs most frequently in epidemiology, social media analysis, and finance, where high-resolution temporal data is available and precise timing is central to the analytical task.

From a **visualization perspective**, event-based T-NW visualizations in combination with event-based M-NW configurations rely heavily on time-to-space mappings to manage temporal density. Node-link diagrams remain common for representing transmission structure [CLS*12, LHS*15, BPW*21], but are frequently augmented or replaced by storylines [BPW*21], Sankey-like flows [LHS*15], and other timeline-based layouts [DBDDP*15, BPW*21] to explicitly encode temporal ordering. Encodings emphasize exact timestamps, duration, and sequential dependency rather than aggregated intensity. Color is predominantly used to encode categorical state or event type [BPW*21], while spatial position and connection geometry convey temporal sequence and causality. Compared to time-sliced configurations, animation, and interaction play a more central role [BPW*21, CLS*12, DBDDP*15], enabling users to navigate dense event streams through filtering, rolling windows, or progressive disclosure.

Epidemiological applications account for one paper in this category and exemplify the analytical value of fully event-based representations. Here, both the M-NW and the T-NW are modeled as temporally precise sequences. In particular, patient co-location and infection status changes are visualized using a storyline metaphor, where horizontal lines represent individuals along a shared time axis and proximity encodes contact events [BPW*21]. Transmission events are marked explicitly at their occurrence time, and potential infection pathways are shown as dashed arcs between events, enabling detailed reconstruction of plausible transmission chains and inspection of alternative explanations (see Figure 5).

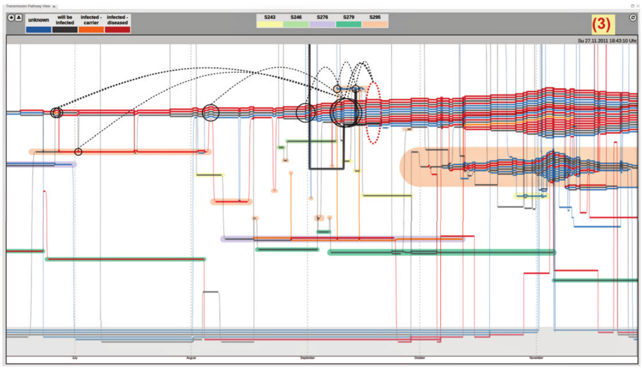

Figure 5: *Storyline visualization of the medium network (patients) as horizontal lines on the timeline. Close lines show contacts (structure of the network). The infection status is indicated by line coloring. Potential transmission pathways are depicted by dashed arcs, connecting infection status change events of patients. Reprinted from Baumgartl et al. [BPW*21], with permission.*

Social media analysis contributes two papers and demonstrates how event-based diffusion supports real-time monitoring and egocentric reasoning. In this setting, the M-NW is often only partially visualized, while the T-NW captures reposting or interaction events with exact timestamps. Whisper traces diffusion in real time using a radial node-link metaphor inspired by a sunflower, where retweet events propagate outward from original posts and are animated along curved pathways to convey timing, sentiment, and geographic spread [CLS*12]. EgoNetCloud [LHS*15] focuses on egocentric event-based networks, where discrete interaction events activate clique-like subgraphs around a focal node. Temporal dynamics are embedded into a single integrated view combining node-link layouts with stacked event timelines and trend graphs, supporting analysis of both local interaction bursts and longer-term evolution (see Figure 6).

Beyond classical diffusion domains, 1 paper addresses progression analysis of event sequences from a more **abstract, graph-theoretic** perspective, applied to a **clinical/medical** use case. Here, the M-NW corresponds to raw event sequences, while the T-NW captures inferred transitions between progression stages derived from unsupervised segmentation [GJG*19]. The visualization combines tabular event views, node-link diagrams of stage transitions, and scatterplots of event embeddings, illustrating how event-based T-NWs can generalize beyond explicit contagion scenarios.

Financial applications contribute 2 papers and highlight the suitability of event-based models for transaction-driven diffusion. In cryptocurrency analysis, individual transactions are treated as events and visualized using Gantt-chart-like layouts, where bar width encodes transaction volume and vertical position encodes block time [DBDDP*15]. This design emphasizes exact ordering, temporal clustering, and flow magnitude. In venture capital analysis, event-based investment relations are aggregated into flow-based

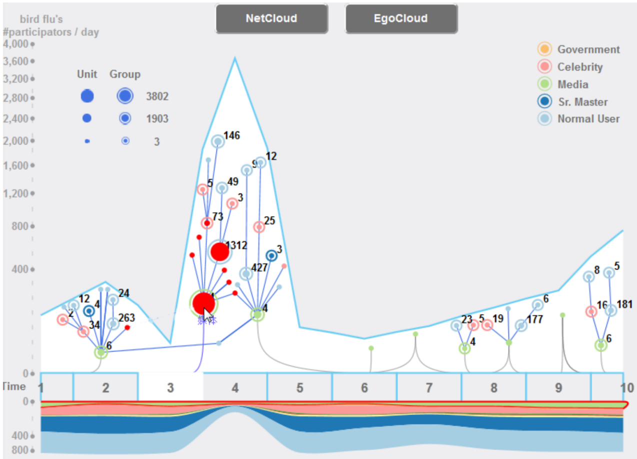

Figure 6: *Event-based egocentric diffusion pattern highlighting message forwarding initiated by media accounts during the H7N9 bird flu outbreak on Sina Weibo. Nodes represent aggregated user groups colored by account type, and edges depict dominant forwarding relationships, revealing the media-driven amplification phase in the overall diffusion process. Reprinted from Liu et al. [LHS*15], with permission.*

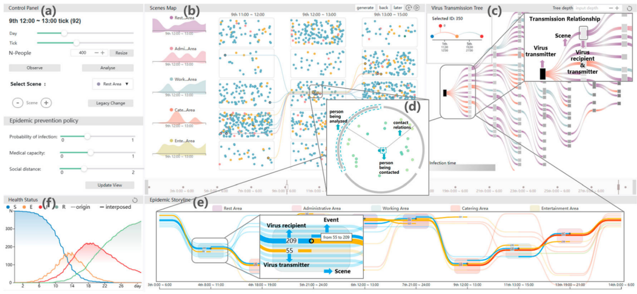

Figure 7: *VIVIAN: Multi-view visual analytics system for simulated epidemic spread, integrating scene-based mobility, contact networks, transmission trees, storylines, and population-level health dynamics to support tracing, comparison, and decision-making. Reprinted from Li et al. [LCZ*24], with permission.*

representations, such as Sankey diagrams, to show capital movement between sectors and entities over time [TLZ*23]. While aggregation is applied for scalability, the underlying model remains event-based, allowing analysts to trace investment dynamics at fine temporal granularity when needed.

Overall, event-based T-NW combined with event-based M-NW visualizations provide maximal temporal precision and support detailed causal analysis of diffusion processes. They excel at reconstructing individual transmission chains, aligning transmission with momentary interaction opportunities, and supporting (near) real-time analysis. However, this expressiveness comes at the cost of scalability and visual complexity, often requiring sophisticated interaction, filtering, or aggregation strategies. As such, this configuration is best suited for high-resolution datasets with manageable scope, while hybrid approaches may be needed to bridge event-level insight with higher-level overview tasks.

5.2.2. Event-Based Transmission Network and Time-Sliced Medium Network

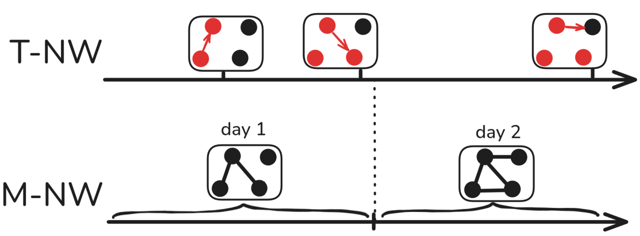

This configuration combines an event-based T-NW with a temporally aggregated representation of the M-NW. Individual transmission events are represented at full temporal resolution, while the underlying interaction structure is discretized into time windows. As a result, transmission timing is precise, but contact opportunities and structural context are only available at slice granularity. Causal reasoning about individual infection events remains possible, yet attribution to specific medium-level interactions and structure may become ambiguous when multiple contacts are aggregated within the same time-slice.

Only 1 paper in our corpus employs this temporal combination, indicating that it is a rare and specialized design choice. The sole instance originates from epidemic spread simulation, where transmission timing is explicitly generated by a model, while contact structure is abstracted to a sliced level.

Li et al. introduce *Vivian* [LCZ*24], a VA system to simulate and analyze **epidemic spread** in contact networks (see Figure 7). The M-NW is regularly time-sliced into "scenes", while transmission is simulated using SIR models mediated through the number of contacts at the time of transmission. Confirmed infection events are represented explicitly and linked through a storyline visualization, enabling analysts to trace who infected whom, when, and in which scene. Additional views, including layered transmission trees, scatterplots, and temporal line charts, provide complementary perspectives on simulated diffusion dynamics and population-level trends.

Overall, event-based T-NW combined with time-sliced M-NW offers a compromise between temporal precision and structural abstraction. This approach is particularly suited to simulation-driven analyses, where precise transmission events are available or generated, but the medium network is uncertain, incomplete, or intentionally simplified. The shortage of this configuration in the literature highlights an opportunity for future work to explore hybrid temporal abstractions that retain event-level transmission detail while selectively refining structural resolution when data or analytical tasks demand it.

5.2.3. Event-Based Transmission Network and Flattened Medium Network

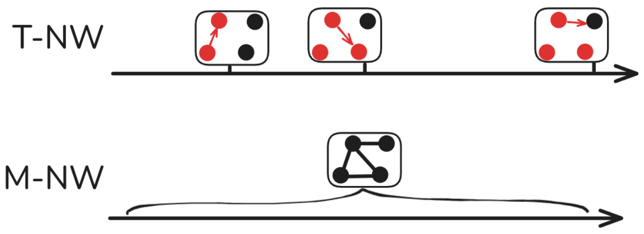

In event-based T-NW visualizations combined with a flattened M-NW, individual transmission events are represented at full temporal resolution, while the underlying interaction structure is assumed and visualized to be static over the observed interval. This configuration preserves precise timing and ordering of transmissions, but suppresses temporal variation in the medium network itself. As a result, causal reasoning focuses on event sequences unfolding over a fixed structural substrate rather than on co-evolving dynamic network structure. In our corpus, this combination comprises **7 papers** and occurs most frequently in social media analysis, cybersecurity, and infrastructure monitoring, where either the medium network evolves slowly relative to transmission dynamics or its temporal evolution is unavailable or secondary to the analysis task.

Across domains, node-link diagrams dominate both T-NW and M-NW representations in this category [TMW03, KSBT12, USK21, BBB24, LLZ*16, HSS*20, OW00]. Transmission events are typically encoded as temporally activated and visually highlighted edges or paths on top of a static network layout. Common visual channels include color [HSS*20, USK21, LLZ*16] and animation [HSS*20, USK21] to indicate event timing or state changes, and edge width or opacity [LLZ*16, HSS*20, USK21] to encode transmission volume, strength, or confidence.

Social media applications contribute three papers and illustrate different interpretations of diffusion over a static follower or influence structure. Liu et al. [LLZ*16] visualize hashtag and topic propagation on microblogging platforms, where the M-NW is a static follower graph. Transmission is inferred computationally and visualized through color encodings and flow-like patterns, explicitly incorporating uncertainty in both post similarity and hashtag diffusion (see Figure 8). Huang et al. [HSS*20] introduce *Eiffel*, where discrete influence events, such as citations or reposts, are modeled as an event-based T-NW on top of a static influence M-NW. Influence strength is encoded via edge width, while temporal emergence is conveyed through animated edge growth and node halos that emphasize newly activated transmission paths. Baum et al. [BBB24] analyze misinformation and health-related discussions on Twitter. A node-link visualization approach shows topic evolution, encoded through colored and different sized nodes and edges.

Cybersecurity and computer network analysis account for three papers in this category and strongly emphasize event-level inspection of transmission over stable infrastructure. Teoh et al. [TMW03] analyze Internet routing data by visualizing timestamped routing events over a largely static autonomous system topology. These event sequences are visualized on a timeline, using additional glyphs and links, to identify anomalies, correlations, and potential causal chains. Transmission paths are highlighted with arcs to examine individual nodes and links. Koyama et al. [KSBT12] visualize packet flows in mobile ad-hoc networks, where the M-NW is treated as static for visualization purposes, using a node-link diagrams overlaid on a map. Packet transmissions are animated as discrete events, node states are encoded through color, and transmission paths are shown via animated flows. Ulmer et al. [USK21] present a progressive visual analytics system for live *border gateway protocol* updates, where the M-NW is a flattened, geospatially embedded autonomous system network. The visualization is node-link based over a map. Event-based transmission paths are highlighted dynamically as routing updates arrive, with edge width encoding connection importance and color indicating *autonomous systems* hierarchy or selection state.

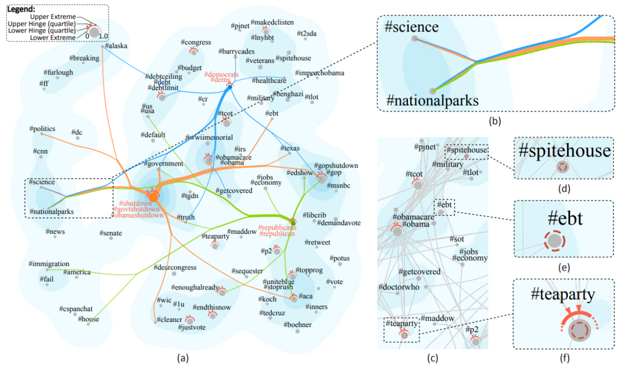

Figure 8: *Uncertainty-aware visualization of social media diffusion, combining a hashtag network with glyphs and flow maps to depict uncertainty and its propagation in ranking-based diffusion analysis. Reprinted from Liu et al. [LLZ*16], with permission.*

Only one paper addresses **electric power infrastructure**. Overbye and Weber [OW00] visualize power transmission over a static grid topology, where individual operating states and flow conditions are event-based. A node-link diagram on top of a map represents the M-NW. Transmission is encoded through animated flows, contouring, and color on the fixed network layout, enabling analysts to inspect specific system states and stress conditions.

Overall, event-based T-NW visualizations on flattened M-NWs prioritize precise temporal inspection of transmission events while relying on structural stability assumptions. This configuration is well-suited for domains where infrastructure changes slowly or is difficult to observe, hence they are not visualized, such as communication networks and power grids. However, it limits the ability to reason about how evolving interaction structures shape diffusion dynamics.

5.2.4. Event-Based Transmission Network and Implicit Medium Network

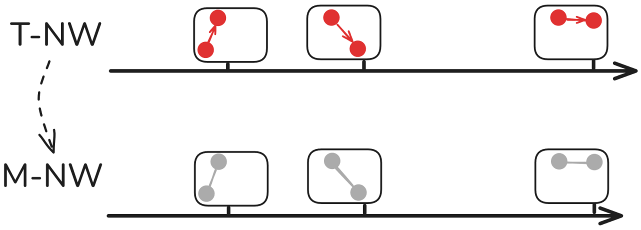

In this configuration, the T-NW is modeled and visualized at event-level temporal resolution, while the underlying M-NW is not explicitly represented. Structural context is either unknown, abstracted away, or completely omitted, and the diffusion process is instead inferred directly from event sequences, temporal proximity, or model-based reconstruction. This setting supports fine-grained temporal reasoning about propagation order and timing, but limits analysis of alternative transmission opportunities or structural constraints. In our corpus, this combination comprises **9 papers** and occurs across epidemiology, social media analysis, transportation, cybersecurity.

Across this category, node-link diagrams [VBF*17, VRHGM*24, WLY*14, DWL*22, OGGB25], Sankey-style flows [WLY*14], timeline-based sequences [MB18, VRHGM*24], and map-embedded cascades are used [XSS*24, DWL*22]. Color is the primary channel [MB18, WLY*14, VRHGM*24, JPAP21, DWL*22] for encoding event state, category, or uncertainty, while spatial position, ordering, and animation [VRHGM*24, WLY*14, JPAP21, DWL*22, OGGB25] convey temporal progression. The absence of an explicit M-NW shifts analytical focus from structural opportunity to observed or inferred propagation enables detailed event-level reasoning but limits assessment of alternative diffusion paths.

Epidemiological applications contribute two papers and focus on reconstructing transmission processes directly from case reports and clinical event data, without visualizing an explicit contact or interaction network. Valencia et al. [VBF*17] infer probable Ebola transmission links based on temporal proximity and reported relationships between cases. The resulting T-NW is visualized as a node-link diagram, where nodes represent infected individuals and directed edges encode inferred transmission events. The serial interval between transmissions is labeled in days directly on the edges. Edge color distinguishes relationship types such as household or community contact, while node color encodes case attributes. Jang et al. [JPAP21] similarly reconstruct infection cascades using a risk-aware optimization model to identify likely asymptomatic carriers. Transmission is visualized as a directed, hierarchical cascade graph, where nodes represent patients at specific event times and edges encode inferred disease-flow paths. Across both approaches, temporal order and causal structure are emphasized through layout depth, directionality, and sequencing, while the medium network remains implicit due to incomplete or unavailable contact data.

Social media analysis contributes three papers and illustrates different strategies for visualizing event-based diffusion without

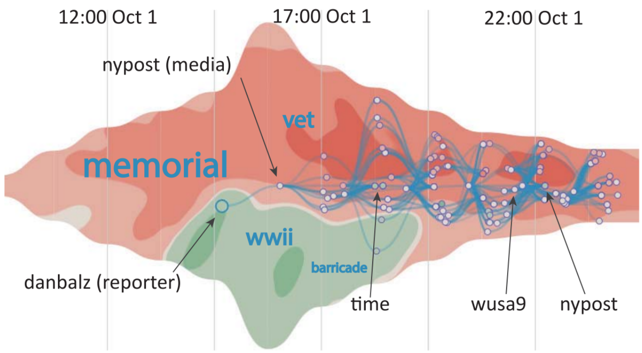

Figure 9: *OpinionFlow visualization of opinion diffusion during the U.S. government shutdown, focusing on the event where World War II veterans crossed memorial barricades. The view shows how a positively framed narrative around the veterans (green regions) coexists and competes with predominantly negative opinions criticizing the shutdown (red regions), highlighting the role of influential media accounts in propagating and amplifying opinion shifts. Reprinted from Wu et al. [WLY*14], with permission.*

explicit follower or interaction networks. OpinionFlow [WLY*14] models opinion diffusion assuming implicit, global exposure and visualizes transmission using Sankey-style flow diagrams (see Figure 9). Hierarchically organized topic bands form the backbone of the visualization, while flow width encodes opinion volume and temporal shifts. Detailed user-level T-NWs are shown on demand as embedded node-link diagrams within selected time intervals. DisTrack [VRHGM*24] visualizes misinformation cascades extracted via semantic similarity and repost relations. Here, the T-NW is shown as a node-link diagram where nodes represent individual posts, positioned along a horizontal time axis and vertically by engagement metrics such as likes. Edges encode reposting, replying, or quoting relationships (see Figure 10). Moats and Borra [MB18] avoid explicit network metaphors altogether and instead visualize URL diffusion as color-coded temporal sequences aligned on a timeline. Despite differing visual encodings, all three approaches prioritize event order and content-level propagation over structural exposure, using color, ordering, and flow width as primary channels.

Transportation-focused analysis is represented by one paper and conceptualizes diffusion as the propagation of temporal deviations rather than discrete interactions. Xiao et al. [XSS*24] analyze uncertainty propagation in bus operations by modeling arrival-time deviations as event-based transmission sequences. Transmission is visualized using Marey's graphs and Nested Tracking Graphs, where deviations propagate along routes over time, while spatial uncertainty is shown through geospatial contour maps. The underlying route structure acts as an implicit medium, but is not shown, allowing analysts to focus on temporal propagation patterns and delay amplification rather than topological connectivity.

Spatio-temporal cascade studies contribute one paper and derive event-based transmission networks from temporal correlations in large-scale data streams. Deng et al. [DWL*22] extract cascading influence structures from spatio-temporal phenomena such as

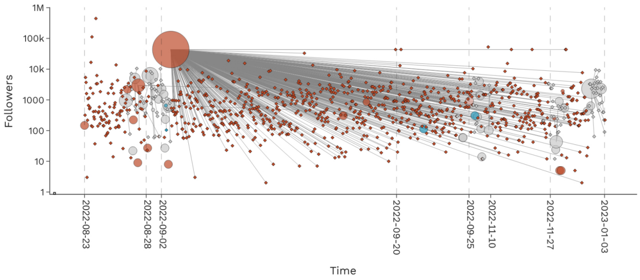

Figure 10: *Visualization of a misinformation cascade generated by DisTrack, showing the temporal evolution of posts related to the claim "Zelensky sold 17 million hectares of land to Monsanto, Dupont and Cargill". Nodes represent tweets, positioned by publication order and author influence, while directed edges indicate repost and reply relations. Node color encodes stance toward the claim (entailment, contradiction, neutral), highlighting the structure, persistence, and key spreaders of the diffusion process. Reprinted from Villar-Rodriguez et al. [VRHGM*24], with permission.*

traffic congestion or air pollution. The T-NW is visualized using coordinated views, including map-embedded node-link diagrams, cascade tables, and influence graphs, where edges encode inferred influence with associated durations and node color represents event intensity.

A general approach is presented by one paper and proposes a domain-independent approach for visualizing event-based diffusion on dynamic networks. Oh et al. [OGGB25] present *TPVis*, which computes temporal paths from a selected source and visualizes them in a node-link diagram with a timeline-based tree layout. Rather than showing the full M-NW, the system focuses on valid transmission paths only, with nodes aligned by event time and edges encoding chronological diffusion steps. The approach is demonstrated on contact, communication, and blockchain networks.

Overall, event-based T-NW visualizations with implicit M-NWs emphasize detailed temporal ordering, cascade reconstruction, and content- or event-centric analysis. They are well suited for exploratory tracing, anomaly detection, and qualitative inspection of diffusion processes, but highlight a gap for techniques that could reintroduce structural uncertainty or alternative transmission opportunities without requiring fully specified medium networks.

5.3. Time-Sliced Transmission Network Visualizations

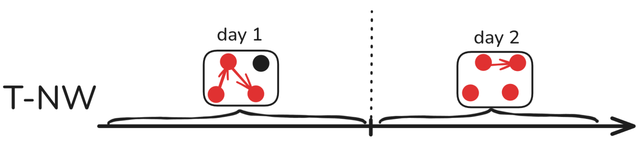

Sliced (or window-based) Transmission Network (T-NW) visualizations represent diffusion processes by aggregating transmission events into discrete temporal windows. These windows may be equidistant (e.g., daily or weekly) or irregular (e.g., policy phases or reporting intervals). Time-sliced T-NWs preserve coarse temporal ordering and allow phase-wise comparison, while suppressing event-level ordering and fine-grained causal detail within each slice. As such, they occupy a middle position between event-based representations and fully flattened temporal abstractions (see also section 2).

In this section, we discuss **33 approaches** that employ time-sliced T-NWs in combination with different temporal abstractions of the Medium Network (M-NW).

From an **application domain perspective**, epidemiology, public health, and disease spread (14 of 33) [Yan21, GGZZ22, YZGW22, DC24, HXF*21, SMSR20, KLM24, FNV22, ASGK21, AC17, ZL21, WLS*22, AME11, STX*22] dominate this category, reflecting common reporting intervals and modeling assumptions in infectious disease analysis. Social media (12 of 33) [CSNW24, ZCW21, YJZ*25, HWZ19, CCW*16, WLC*16, SMSR20, TGA*23, KLM24, CDBM*06, ASGK21, XWW*13] form the second largest groups, while additional isolated examples appear in analysis and environmental monitoring/air pollution (3 of 33) [BDPC20, HBY*23, RWZ*20], biology (4 of 33) [KLM24, FBL*18, AC17, SKKS08], cybersecurity (2 of 33) [USK19, CDBM*06], transportation/traffic (2 of 33) [CAD21, SPL*18], finance (2 of 33) [NCZZ18, FNV22], citation analysis (3 of 33) [CLYL18, HWZ19, KLM24], and general/other/creative domains (3 of 33) [ZCW21, KLM24, SKKS08].

From a **visualization perspective**, node-link diagrams are the dominant representation for time-sliced T-NWs and appear in the majority of cases (23 of 33) [SKKS08, CSNW24, Yan21, GGZZ22, YJZ*25, HWZ19, CLYL18, YZGW22, CCW*16, FBL*18, USK19, HXF*21, SMSR20, TGA*23, KLM24, FNV22, ASGK21, AC17, ZL21, WLS*22, NCZZ18, STX*22, SPL*18]).

Beyond standard node-link diagrams, a smaller number of approaches employ alternative visualization techniques for specific analytical goals. Tree-like visualizations are used to highlight cascade structure and branching behavior in aggregated diffusion processes (4 of 33) [STX*22, CLYL18, WLC*16, FNV22]. Flow- or river-based metaphors encode competitive influence or topic dynamics over time, particularly in social media analysis (3 of 33) [WLC*16, XWW*13, ZL21]. Storyline-inspired layouts appear in egocentric diffusion scenarios, where transmissions are centered around a focal entity (1 of 33) [KLM24].

Node-link diagrams are frequently enhanced with **additional encodings** such as color/opacity (12 of 23) [SKKS08, CSNW24, Yan21, GGZZ22, FBL*18, USK19, SMSR20, KLM24, FNV22, ASGK21, NCZZ18, STX*22], or edge width (9 of 23) [CLYL18, YZGW22, USK19, HXF*21, TGA*23, KLM24, AC17, WLS*22, NCZZ18] to represent aggregated transmission strength, risk, or influence. Geographic embedding is common in spatial domains, where node-link diagrams or flow representations are overlaid on maps (8 of 33) [FNV22, CDBM*06, ZL21, BDPC20, RWZ*20, CCW*16, HBY*23, AME11].

From a **temporal perspective**, transmission networks visualized as node-link diagrams are typically presented either as small multiples supporting direct comparison between temporal windows (7 of 23) [CSNW24, Yan21, CCW*16, HXF*21, SMSR20, AC17, ZL21], or as interactive views controlled via time sliders (2 of 23) [FBL*18, RWZ*20]. Animation-driven representations (5 of 33) [CDBM*06, FNV22, CCW*16, FBL*18, SPL*18] of time-sliced T-NWs typically serve as auxiliary rather than primary views.

Regarding the **combinations of time-sliced T-NWs with M-NW**,time-sliced T-NWs are most frequently combined with either time-sliced (19 of 33) [YJZ*25, HWZ19, CLYL18, YZGW22, FBL*18, DC24, ZCW21, USK19, KLM24, CDBM*06, AC17, ZL21, WLS*22, XWW*13, NCZZ18, BDPC20, HBY*23, RWZ*20, STX*22] or flattened (10 of 33) [SKKS08, CCW*16, CSNW24, CAD21, HXF*21, SMSR20, TGA*23, FNV22, SPL*18, GGZZ22] M-NWs. Event-based and step-based M-NWs were not found in this category, suggesting a tendency to align temporal abstraction levels between transmission and medium networks for reasons of interpretability and scalability. In a notable subset of papers, the M-NW remains implicit or only partially visualized (4 of 33) [WLC*16, ASGK21, AME11, Yan21], shifting analytical emphasis toward aggregated transmission outcomes rather than the medium structure.

Missing T-NW and M-NW combinations. We did not find examples for two combinations: (1)time-sliced T-NW with event-based M-NW and (2)time-sliced T-NW with step-based M-NW. In the first case, aggregating transmissions into time-slices while retaining event-level structure in the M-NW obscures temporal detail in the T-NW. In the second case, this again reflects a representational mismatch, as an ordered but time-less M-NW does not align well with temporally aggregated transmissions.

In the following subsections, we further differentiate time-sliced T-NW visualizations by the temporal abstraction of the M-NW visualization. For each combination, we summarize the number of papers, dominant domains, and characteristic visualization strategies. Combinations for which no literature was found are omitted.

5.3.1. Time-Sliced Transmission Network and Time-Sliced Medium Network

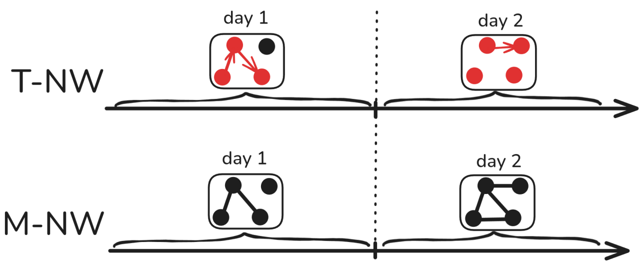

When both the T-NW and the M-NW are temporally sliced, diffusion analysis is constrained to slice-level reasoning. Transmission events are aggregated within each time window, and changes in the underlying interaction structure are likewise represented as discrete snapshots (see also section 2). This combination is the most prevalent among time-sliced T-NW visualizations, comprising **19 papers** in our corpus. It occurs most frequently in epidemiology dashboards, simulation-driven analyses, and spatial diffusion studies (e.g., air pollution), where data availability, reporting conventions, or scalability requirements favor temporal aggregation.

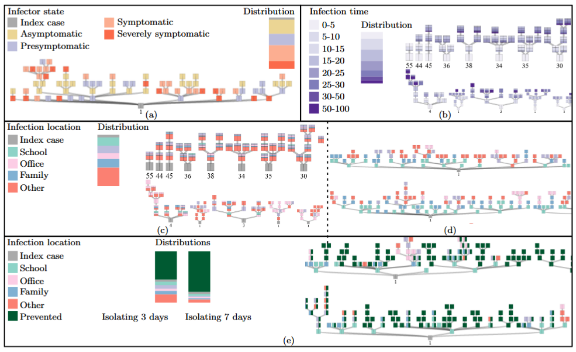

Figure 11: *Visual analytics system for exploring and comparing simulated infection diffusion processes on contact networks. The visualization combines aggregated network representations with multivariate summaries to support analysis of transmission patterns and policy effects across different simulation scenarios. Figure by Sondag et al. [STX*22]. Licensed under CC BY 4.0.*

Across domains, this setting is characterized by a strong reliance on node-link representations for both T-NW and M-NW views [HWZ19, YZGW22, FBL*18, KLM24, AC17, ZL21, WLS*22, NCZZ18]. Temporal evolution is typically conveyed via small multiples [AC17, ZL21], animated transitions [FBL*18, CDBM*06], or interactive time sliders [FBL*18, RWZ*20, NCZZ18, BDPC20, HBY*23]. Encodings predominantly emphasize aggregated transmission intensity, risk, influence, or hotspot structure rather than fine-grained propagation chains. Common channels include color/opacity [ZCW21, FBL*18, USK19, KLM24, CDBM*06, ZL21, XWW*13, NCZZ18, BDPC20, RWZ*20, STX*22] for categorical state (e.g., infection status, risk class) and size/width for aggregated volume, importance, or strength [YJZ*25, FBL*18, ZL21, USK19]. Directionality is shown through arrows, gradients, or temporally ordered highlighting across time slices.

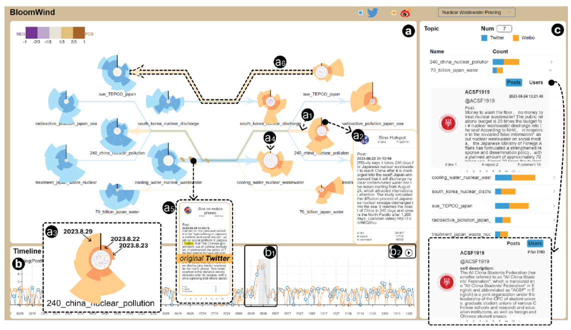

Figure 12: *Overview of a visual analytics system for implicit cross-platform information diffusion. The visualization aggregates posts into topic clusters and depicts estimated propagation between social media platforms using a metaphor-based network representation. Reprinted from Yin et al. [YJZ*25], with permission.*

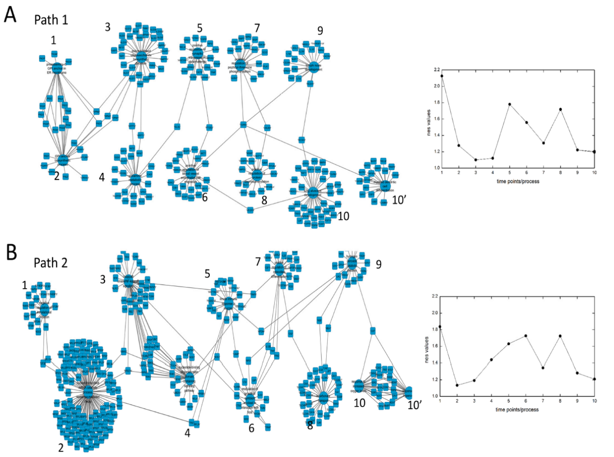

Figure 13: *Visualization of temporally linked biological processes forming dominant progression paths. Figure by Anand and Chatterjee [AC17]. Licensed under CC BY 4.0.*

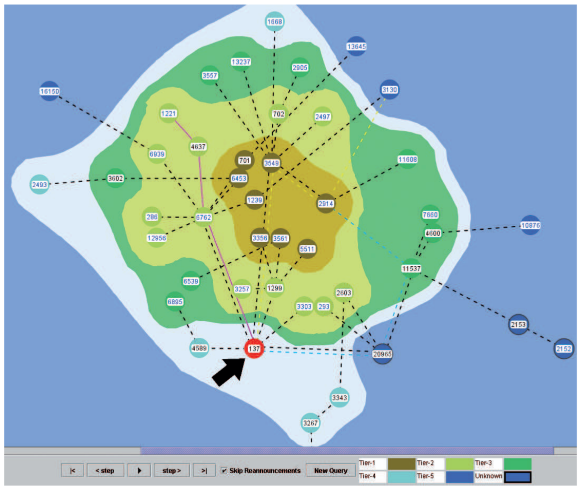

Figure 14: *A topographic map with an embedded node-link diagram showing the hierarchy of autonomous systems. When analyzing prefix propagation, its routing path is highlighted in red. This process is animated. Reprinted from Cortese et al. [CDBM*06], with permission.*

From **epidemiology and public health** originate the largest share of papers (five papers). This prevalence aligns with the common availability of case and contact data at daily or phase-based reporting intervals. Many systems visualize the time-sliced M-NW as a contact, mobility, or region adjacency structure and overlay time-sliced transmission states to identify evolving hotspots and influential spreaders. For example, influence-based analyses aggregate transmission structure to emphasize influential regions and phase-wise differences [DC24]. **Policy-oriented systems** compare multiple scenario-specific transmission structures across time intervals, enriched by per-node attribute encodings such as stacked bars for risk or policy impact [STX*22] (see Figure 11). Other works encode infection and transmission states directly on top of sliced contact graphs using node and edge color, coupled with timelines and metric views to align structural changes with population-level indicators [WLS*22]. When geographic semantics dominate, spatial embedding becomes central: transmission is shown as map-based flows or curved edges between regions, and within-region composition is summarized using glyphs such as pies, with additional risk classification encoded through color [YZGW22, ZL21].

Social media analysis contributes three papers to this category and illustrates how slicing is used to manage high-frequency activity while supporting phase-wise attention analysis. Compared to epidemiology, diffusion is often analyzed at the level of topics, clusters, or cascades rather than explicit user-to-user opportunity. Topic- and cluster-based systems infer transmission probabilistically between aggregated entities and visualize diffusion using node-link like structures between clusters, glyph-based metaphors (see Figure 12), and flow-like representations whose width encodes competitiveness or influence over time [YJZ*25, XWW*13]. Cascade-oriented approaches instead represent diffusion as sequences of tree-like graphs, where depth and branching structure are salient visual variables, complemented by auxiliary charts for growth metrics and prediction-related summaries [HWZ19].

Biological applications (two papers) interpret transmission as influence or progression within rule-based or process-based systems. Both T-NW and M-NW are explicit and commonly visualized as weighted and directed node-link diagrams per slice. Dynamic influence networks aggregate probabilistic rule interactions into time windows and encode influence magnitude via edge width and direction via color gradients [FBL*18]. Progression-oriented biological process networks use node size, color, and shape to encode activity and entity type, while paths across slices support reasoning about trajectories rather than isolated events [AC17] (see Figure 13).

In **cybersecurity and network infrastructure analysis** (two papers), slicing is tightly coupled to scale and operational monitoring. Packet- and routing data is aggregated into equidistant windows and represented as node-link diagrams, often with interaction-dependent aggregation levels. Spatial or structural context is frequently preserved across slices, while propagation is shown through temporal highlighting. For example, Cortese et al. explore prefix propagation by highlighting evolving paths over an autonomous system graph embedded in a topographic layout, using color to encode hierarchy and propagation state (see Figure 14). Similar design choices appear in web-based progressive analysis systems for network traffic [USK19].

Environmental diffusion studies on air pollution (three papers) strongly favor geospatial M-NW representations. Here, the M-NW is typically a map-based network visualization of monitoring stations or regions, while transmission is inferred from temporal correlations and represented as propagation paths or flows per time window (see Figure 15). Encodings emphasize concentration and transport strength via node color/size, heatmaps, and multivariate glyphs. Coordinated views such as calendars, timelines, and line charts support temporal selection and contextualization [BDPC20, HBY*23, RWZ*20].

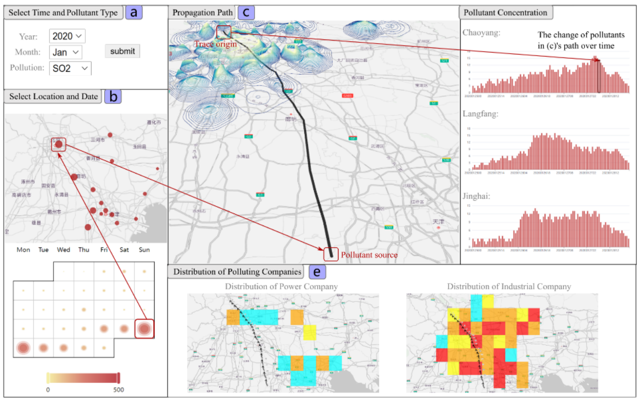

Figure 15: *Interactive visual analytics interface for tracing air pollution propagation and identifying potential emission sources. Reprinted from Hao et al. [HBY*23], with permission.*

Single instances occur in finance, citation networks, music influence analysis, and general diffusion scenarios (one paper each). These works still follow the same principle of slice-wise aggregation and comparative reasoning, but vary in layout and metaphor. **Financial risk diffusion** relies on strong quantitative encodings and is often complemented by Sankey or flow diagrams [NCZZ18]. **Citation diffusion** adopts a radial, year ring structure that embeds time-slices into the layout geometry [CLYL18]. **Music influence analysis** (one paper) emphasizes multivariate temporal charts rather than explicit topology [ZCW21]. **General diffusion** exemplars may employ storyline-based overviews with optional structural drill-down [KLM24] (see Figure 17). As an example, Xu et al. [XWW*13] model information diffusion as a time-sliced topic competition process rather than explicitly visualizing the transmission between individual actors (media sources) or messages. Diffusion is derived from a model that estimates shifts of attention among competing topics across media outlets, including news and social media, within discrete and regular temporal intervals (see Figure 16). The underlying M-NW is time-sliced and implicit, the diffusion is visualized using a themeriver-like representation showing how topic prominence evolves over time.

Overall, time-sliced T-NW combined with time-sliced M-NW visualizations favor robustness and scalability over temporal precision. They support reliable phase-wise comparison and integration of multivariate context, but largely omit event-level narratives and fine-grained causal tracing. This makes the configuration well-suited for monitoring, overview, and policy comparison tasks, while highlighting opportunities for techniques that connect slice-level overviews with finer-grained temporal evidence when such data is available.

5.3.2. Time-Sliced Transmission Network and Flattened Medium Network

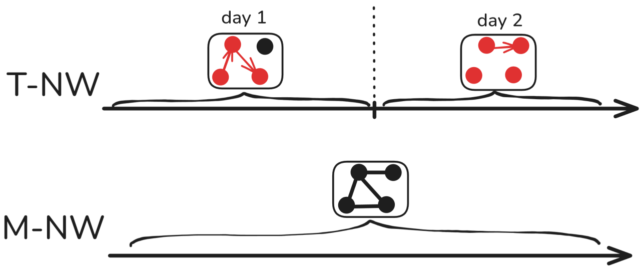

In this configuration, the transmission network (T-NW) evolves over time (represented as time windows), while the medium network (M-NW) is assumed to be static. This abstraction is comprised of **10 papers** and is prevalent in domains where the medium structure changes slowly relative to diffusion dynamics (e.g., transportation infrastructure [CAD21, SPL*18], follower networks [CSNW24, SMSR20, TGA*23]) or where the analytical focus lies on temporal changes in outcomes rather than co-evolution of structure. From a visualization perspective, the static M-NW typically acts as a stable frame of reference, while temporal change is communicated through a timeline [CCW*16], small multiples [CSNW24, CCW*16, HXF*21, SMSR20], and animation [SPL*18, FNV22, CCW*16, GGZZ22]. Encodings emphasize *where* and *how strongly* diffusion manifests on the fixed substrate using color [HXF*21] and edge emphasis [CCW*16, GGZZ22, TGA*23].

A common use case is **epidemiological analysis** on top of mobility, social, or travel networks (three papers). Geng et al. [GGZZ22] study COVID-19 spread via transportation networks, using a static infrastructure M-NW and time-sliced overlays of measured or derived transmission-relevant signals. Similarly, Han

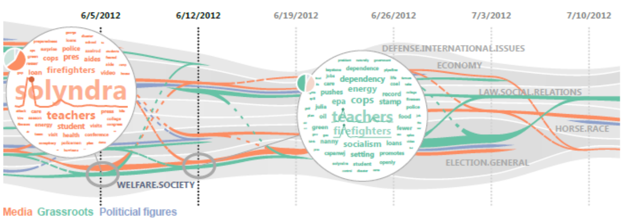

Figure 16: *Topic diffusion modeled as time-sliced competition across media sources. Topic prominence is visualized using continuous flows whose width encodes relative attention over time. Reprinted from Xu et al. [XWW* 13], with permission.*

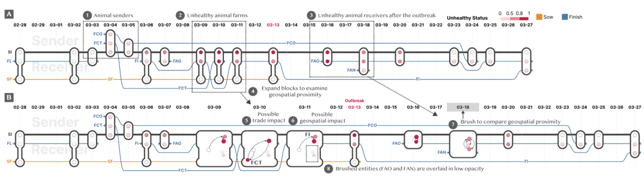

Figure 17: *SpreadLine visualization illustrating egocentric influence over time in an animal disease surveillance scenario. The storyline-based layout reveals potential transmission pathways and influential entities around a focal node. Reprinted from Kuo et al. [KLM24], with permission.*

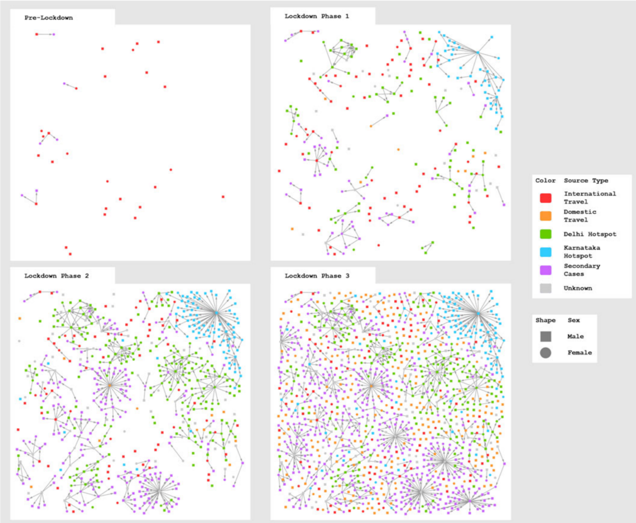

Figure 18: *Temporal evolution of the COVID-19 transmission network across successive lockdown phases in Karnataka. Each panel shows an irregular time-slice of a transmission phase, with nodes representing patients and directed edges indicating inferred transmission links. Node color encodes the source of infection (e.g., international travel, domestic travel, regional hotspots), illustrating how isolated cases progressively evolve into clustered transmission patterns over time. Figure by Saraswathi et al. [SMSR20]. Licensed under CC BY-NC-ND 4.0.*

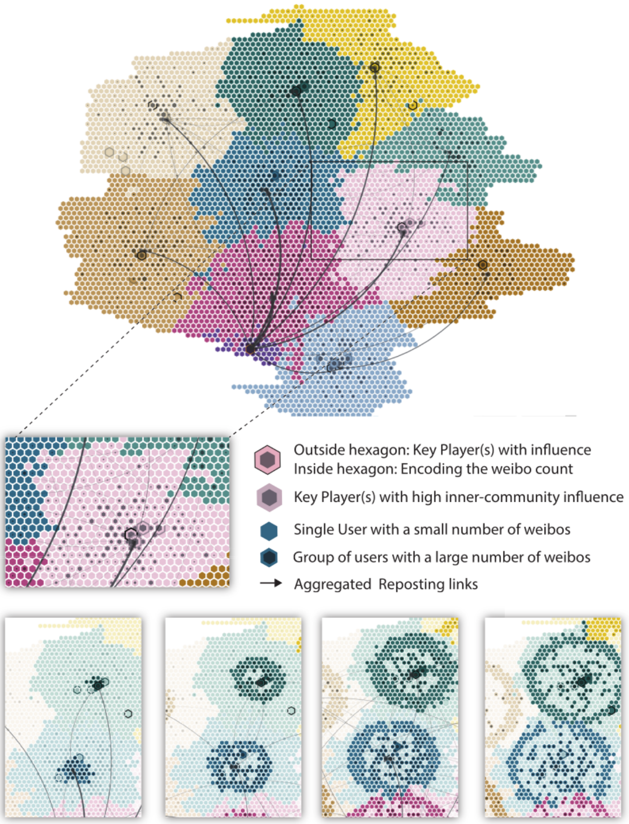

Figure 19: *Visual encodings of D-Map for a central user. Each hexagonal cell represents an individual user or an aggregated group of users participating in the diffusion process. Hexagon size encodes activity (number of reposts), color denotes community membership, and bundled links summarize reposting interactions between communities, providing a compact overview of ego-centric diffusion structure. Reprinted from Chen et al. [CCW*16], with permission.*

et al. [HXF*21] visualize case numbers on a travel network, where the static M-NW provides the structural baseline and time-slicing enables phase-wise comparison of spread intensity across locations. Saraswathi et al. [SMSR20] explicitly leverage policy phases as irregular slices, presenting small multiple node-link diagrams of transmissions (including attributed causes such as travel or hotspots) across lockdown periods while keeping the M-NW static (see Figure 18). The paper further provides flattened views of aggregated transmissions for subgroup comparison, illustrating how the time-sliced T-NW view is often complemented by summary abstractions within the same system.

Social media applications frequently adopt this combination (three papers) because follower graphs are commonly treated as static at the temporal resolution of diffusion analysis. D-Map [CCW*16] analyzes ego-centric repost diffusion: the static M-NW provides the local social context around an ego user, while the T-NW is explored via time-slicing using a timeline (see Figure 19). A notable design choice is the use of *adaptive* temporal windows (short windows for early diffusion and longer ones later), which supports analysis of the crucial initial burst while still showing long-term effects. Tabassum et al. [TGA*23] also treat the M-NW as static (friendship structure with community coloring) while examining topic-based influence and diffusion through sliding windows and slice-wise network views (see Figure 20). Temporal change is emphasized through multiple slice-specific network renderings and auxiliary summaries rather than changes in the underlying structure. Chen et al. [CSNW24] similarly assume a stable interaction substrate and focus on longitudinal slice-wise comparisons of ego networks and topic usage patterns via auxiliary views (e.g., word clouds, metrics).

Beyond social media and epidemiology, the same logic appears in **transportation and infrastructure monitoring** (two papers). Cai et al. [CAD21] analyze the propagation of air traffic delays on top of a static route structure, quantifying propagation via metrics (magnitude, severity, speed) and using temporal slicing to study how propagation evolves. Shan et al. [SPL*18] analyze traffic congestion propagation on a static road network. The medium is the road infrastructure by definition, while time-sliced transmission states represent congestion evolution. The system emphasizes likely propagation paths and uses edge weights/probabilities and interactive selection to forecast cascade effects.

Static M-NW assumptions also occur in domains where the medium is naturally stable or defined by curated structure (one paper each). Streit et al. [SKKS08] provide an example in

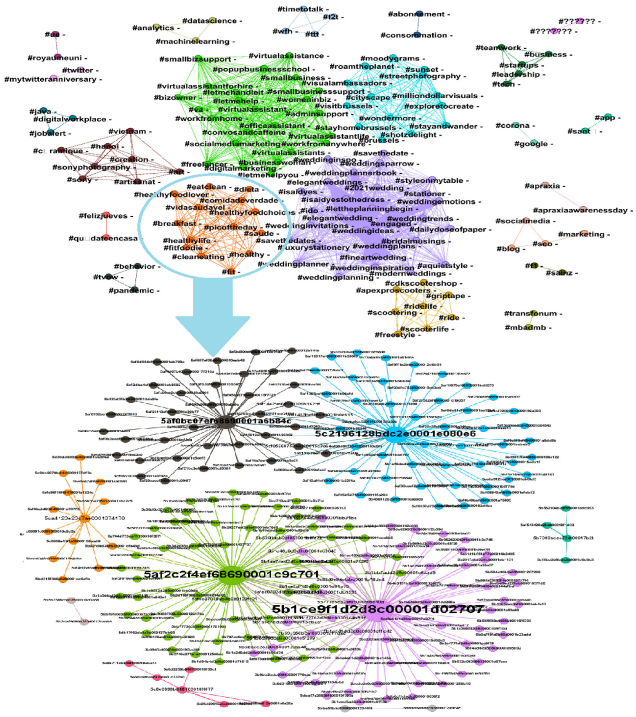

FIGURE 9 Illustration of topic modelling and finding influential nodes in a topic cluster using a sliding window

Figure 20: *Overview of topic-based influence analysis in an evolving microblog network, visualized as a node-link diagram. Reprinted from Tabassum et al. [TGA*23], with permission.*

biomedicine, where the structural substrate is treated as stable and temporal evolution is explored via time-sliced representations and layered network views, primarily supporting comparison and navigation across multiple related pathway structures. Financial contagion analysis similarly often treats dependencies as static at the time scale of interest. Franch et al. [FNV22] visualize temporal **financial risk transmissions** using time-sliced small multiple node-link diagrams over a map, while a flattened radial overview summarizes aggregated transmissions.

This illustrates a recurring theme across the category: time-sliced T-NW views for temporal comparison, complemented by summary views for accumulated effects, all grounded in a stable structural substrate. Overall, time-sliced T-NW combined with flattened M-NW visualizations enable robust temporal comparison while preserving a stable reference structure for interpretation. They are well-suited for monitoring and phase comparison tasks, but they limit reasoning between diffusion and changing medium structure. The prevalence of this category suggests that either structural change is often unavailable in the data, or it is treated as a secondary concern compared to understanding temporal variation in transmission outcomes.

5.3.3. Time-Sliced Transmission Network and Implicit Medium Network

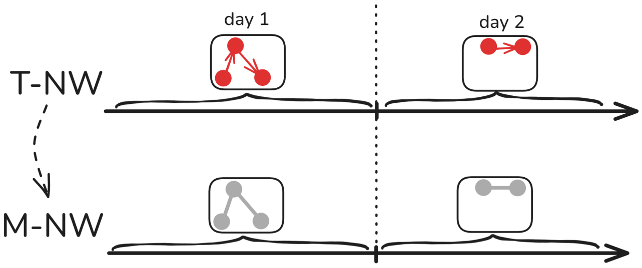

In this configuration, the transmission network (T-NW) is visualized using time-slices, while the medium network (M-NW) is implicit, unknown, or intentionally omitted. In practice, this occurs when the medium structure is unavailable (e.g., missing or privacy-restricted), when diffusion is modeled or inferred without an explicit medium, or when the analytical focus lies primarily on outcomes and temporal phases rather than on structural mechanisms. As a result, visualization designs in this category (**4 papers**) often compensate for the missing M-NW temporal through context views (timelines, event charts, Gantt charts) and by encoding uncertainty or inference status directly on transmission links.

In **epidemiological analyses** (three papers), this category is common when contact opportunities cannot be fully reconstructed. Yang [Yan21] visualizes COVID-19 spread via node-link representations of time-sliced T-NWs derived from contact routes, using irregular temporal intervals as small multiples to show increasing case networks over time. Antweiler et al. [ASGK21] focus on infection cluster detection and missing link analysis. Their system combines a time-filtered node-link view of the transmission/contact network with a Gantt-like event view capturing per person temporal events (e.g., symptom onset, infectious periods). A key encoding strategy in this work is to distinguish confirmed versus predicted contacts using visual link attributes (e.g., color), explicitly communicating uncertainty in the absence of a complete M-NW and supporting investigative tasks such as hypothesis testing and cluster validation.
Decision support- and simulation-oriented systems for epidemic modeling provide a more abstract variant, where diffusion is not shown primarily as an explicit network structure. Afzal et al. [AME11] represent time-sliced transmission outcomes (e.g., daily disease metrics) within a branching decision history tree that encodes alternative intervention paths. Here, temporal slicing on a timeline is used to compare scenario trajectories, while the M-NW remains implicit inside the simulator. Auxiliary views such as choropleth maps and line charts contextualize the outcomes, reflecting a common design choice in this category: prioritizing comparative evaluation of temporal outcomes over explicit representation of the medium structure.

In **social media and idea diffusion** (one paper), implicit M-NWs arise when diffusion is studied between groups, communities, or topics inferred from activity rather than explicit ties. IdeaFlow [WLC*16] studies how ideas diffuse within and across social groups over time. The M-NW is implicit because the underlying population structure is not presented as an explicit graph. Instead,

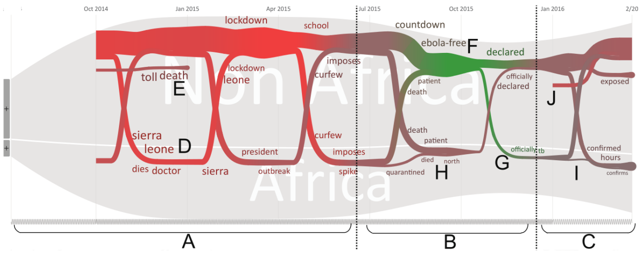

Figure 21: *The visualization combines aggregated topic clusters with flow-based representations to reveal lead-lag relationships and shifts of influence between groups within a temporally evolving diffusion process. Reprinted from Wang et al. [WLC*16], with permission.*

group membership and interactions are inferred from textual activity and idea occurrences (see Figure 21). Diffusion between groups is visualized using time-sliced abstractions and flow-based representations on a timeline.

Overall, time-sliced T-NW combined with implicit M-NW visualizations remain analytically meaningful even without visualizing the structure of the underlying M-NW. They support tasks such as cluster detection, phase comparison, and intervention evaluation through slice-wise transmission views and strong temporal context. However, they inherently limit reasoning about why transmissions were possible (M-NW) and shift attention to how diffusion manifests over time. This prevalence highlights an important opportunity: visualization techniques that can integrate partial, uncertain, or inferred M-NW representations could significantly improve explanatory power without sacrificing the robustness that makes time-sliced transmission views attractive.

5.4. Step-Based Transmission Network Visualizations

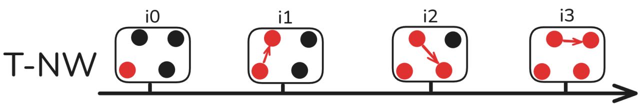

Step-based Transmission Network (T-NW) visualizations represent diffusion processes as ordered sequences of discrete propagation steps without explicit timestamps. Conceptually, these T-NWs emphasize ordered progression and dependency between steps rather than temporal duration, which distinguishes them from the other time representations (see also section 2).

In this section, we discuss **22 approaches** that employ step-based T-NWs in combination with different temporal abstractions of the Medium Network (M-NW).

From an **application domain perspective**, epidemiology (10 of 22) [Wu21, SGM*23, NW14, BASD21, RRP*21, PVL21, NSS*24, PVL22, WBv*19, PnABP20] clearly dominates this category, followed by social media (6 of 22) [LLM*19, SKOM12, XZX*24, ADL*22, AP16b, VKPM15], graph theory, environment, and flow modeling (6 of 22) [VKPM15, Gro24, XZX*24, DWC*20, WYG*11]. Isolated examples appear in finance (2 of 22) [vDBF15, ZXL23]. and biology (1 of 22) [LKB*14]. This distribution is not surprising: 17 of the 22 approaches rely on generated and simulation-based data, where diffusion unfolds as a sequence of model iterations rather than as timestamped observations. In such settings, explicit temporal information is often unavailable, uncertain, or secondary to causal ordering, making step-based representations a natural fit.

From a **visualization perspective**, node-link representations (17 of 22) are mainly used to represent T-NWs [VKPM15, DWC*20, WYG*11, Wu21, SGM*23, NW14, LLM*19, SKOM12, ZXL23, XZX*24, ADL*22, RRP*21, AP16b, NSS*24, vDBF15, LKB*14], which are enhanced by maps (3 of 16) [NW14, Wu21, NSS*24, WBv*19] for showing the spatial facet.
A few approaches replace node-link diagrams with alternative encodings. Timeline or Gantt-like sequence views (2 of 22) [PVL22, PVL21] are used to show stepwise diffusion as ordered activation sequences, spatial trajectories areas on a map can represent propagation (2 of 22) [Gro24, PnABP20], and a heatmap is used (1 of 22) [BASD21] to encode node states and propagation intensity per step through color rather than explicit transmission paths.

The **temporal dimension** is shown as small multiples (6 of 17) [DWC*20, Wu21, ZXL23, XZX*24, AP16b, NSS*24], animation (3 of 17) [SGM*23, AP16b, vDBF15], color and heatmaps (2 of 17) [ADL*22, RRP*21], or on a timeline (2 of 17) [vDBF15, WBv*19].

Regarding the **combinations of step-based T-NWs with M-NW**, there is a broader range of temporal abstractions than sliced and flattened variants. Flattened M-NWs are the most common pairing (8 of 22) [WYG*11, SGM*23, ZXL23, XZX*24, ADL*22, AP16b, vDBF15, WBv*19], followed by implicit M-NWs (9 of 22) [PnABP20, LLM*19, SKOM12, BASD21, Gro24, VKPM15, NSS*24, DWC*20, LKB*14], where the analytical focus shifts almost entirely to the sequential diffusion process rather than the underlying structure. Sliced M-NWs appear less frequently (4 of 22) [NW14, RRP*21, PVL21, PVL22], typically in epidemiological and simulation-based settings where stepwise transmission is evaluated against temporally aggregated contact structures. Only a single approach combines a step-based T-NW with a step-based M-NW (1 of 22) [Wu21], indicating that the visualization of two explicit stepwise models of both M-NW and T-NW is comparatively rare.

Missing T-NW and M-NW combinations. No papers were found that combine a step-based T-NW with an event-based M-NW. This likely reflects a conceptual mismatch: event-based medium networks preserve precise temporal information, whereas step-based transmission models deliberately abstract away from time, making their joint use analytically and visually uncommon.

In the following subsections, we categorize step-based T-NW visualizations in the context of the specific temporal information treated in the M-NW visualization. For each category, we enumerate the corresponding papers, identify the primary application domains, and describe the visualization techniques commonly employed. Categories for which no publications were identified are not included.

5.4.1. Step-Based Transmission Network and Time-Sliced Medium Network

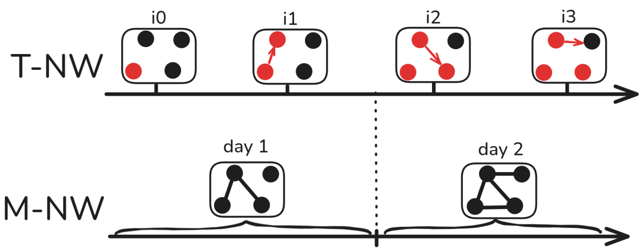

When a step-based T-NW is combined with a time-sliced M-NW, transmission is modeled as an ordered progression across discrete simulation or tracing steps, while the underlying interaction structure is aggregated into temporal windows. This configuration supports reasoning about the sequential unfolding of diffusion processes, but suppresses precise temporal duration within and between steps. Across the corpus, this combination comprises **4 papers**, all originating from epidemiology and veterinary disease analysis, where diffusion is typically studied through simulation or iterative contact tracing rather than timestamped event data.

A defining characteristic of this category is the explicit separation between structural aggregation and transmission progression. The M-NW is represented as a sequence of temporal snapshots, capturing evolving contact opportunities between entities such as farms, markets, or individuals. On top of these time-slices, the T-NW advances step-by-step, with each step corresponding to a simulation iteration, infection wave, or tracing depth. Visualization techniques therefore emphasize ordering and propagation stages rather than absolute time.

Across all approaches in this category, node-link representations remain central for conveying structural context [PVL22, PVL21, RRP*21, NW14], while alternative visualizations are employed to manage scale and temporal complexity [PVL22, PVL21]. Transmission is consistently encoded through edges. Node color is the dominant channel for representing infection state or tracing status [PVL22, PVL21, NW14], while edge presence denotes possible or simulated transmission [RRP*21, NW14]. Map-based embeddings are used when spatial semantics are essential [RRP*21], whereas matrix- and sequence-based views are favored for highlighting temporal progression and comparative dynamics [PVL22, PVL21].

Epidemiology and disease spread contribute two papers, visualizing the propagation of disease stepwise on a time-sliced underlying M-NW. Ponciano et al. [PVL22, PVL21] apply SIR models on top of a time-sliced network of contacts to simulate the spread of a disease, with color encoding the infection state given by the SIR model at the time of transmission for each step of the simulation. The T-NW is visualized as an overlay on the M-NW where the transmission process is shown through colored edges (see Figure 22). The authors provide different visualizations (i.e., sequence-oriented views (massive sequence view), temporal activity maps, and node-link diagrams), showing that slice-wise node-link diagrams support structural interpretation, while matrix- or sequence-like visualizations scale better and highlight temporal trends.

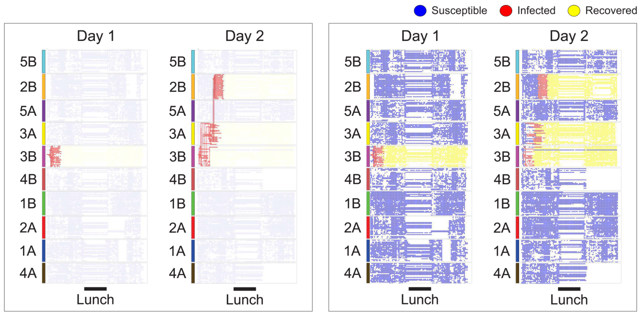

Figure 22: *A massive sequence view on the left showing the infection path between students of different classes (grouped on the y-axis) in a primary school network. The right side shows the temporal activity map where edges are omitted. Node colors show the infection status, the x-axis denotes time. Figure by Ponciano et al. [PVL22]. Licensed under CC BY-NC 4.0.*

Livestock epidemiology further exemplifies the combination of step-based T-NW visualization with time-sliced M-NW representations to study disease spread driven by animal movements (two papers). Ruget et al. [RRP*21] analyze multi-species livestock movement among farms and markets in Scotland, where the M-NW is aggregated into equidistant four-week snapshots and visualized as map-embedded node-link diagrams. On top of these time-slices, step-based epidemic simulations model transmission iteratively across successive periods, enabling comparison of contact structures, transmission pathways, and outbreak risk over time. Edge color distinguishes animal species, while pie charts summarize incoming and outgoing movements (see Figure 23). In con-

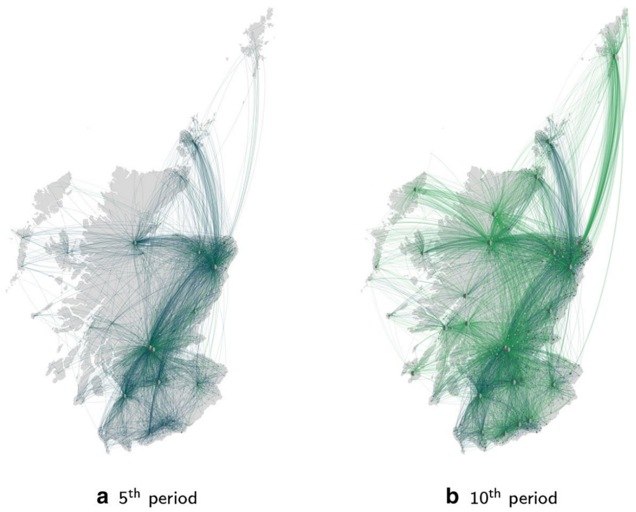

Figure 23: *Animal movements between premises for different periods during the year. Edge colors denote the animal type (blue for cattle, green for sheep). Pie charts show the number of incoming (dark grey) and outgoing (light grey) movements. Figure by Ruget et al. [RRP*21]. Licensed under CC BY 4.0.*

trast, Nöremark and Widgren [NW14] focus on contact tracing during livestock outbreaks using user-defined temporal windows rather than fixed time-slices. This T-NW is constructed step-wise through forward and backward tracing from the root farm, with node-link and map-based views revealing direct and indirect contacts. Transmissions are represented as edges between color-coded node roles, thereby emphasizing discrete infection chains over continuous temporal evolution.

Overall, step-based T-NW visualizations on time-sliced M-NWs support robust analysis of simulated and inferred diffusion processes, particularly in epidemiological contexts where exact timing is secondary to propagation order and scenario comparison. While this configuration enables scalable and interpretable reasoning about transmission pathways, it also abstracts away fine-grained temporal causality, suggesting opportunities for hybrid approaches that integrate step-wise progression with richer temporal annotations when such data becomes available.

5.4.2. Step-Based Transmission Network and Step-Based Medium Network

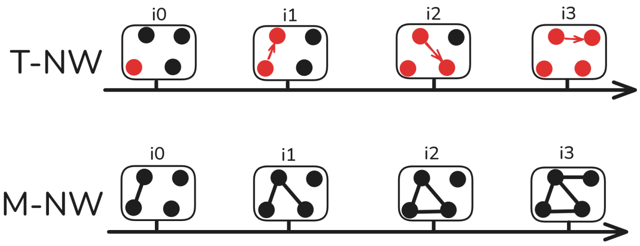

In this subcategory, both the T-NW and the M-NW are visualized using step-based representations. Temporal progression is expressed through a sequence of discrete network states rather than continuous timelines or aggregated views. Visualization techniques primarily rely on node-link diagrams to show evolving relationships between entities, complemented by spatial trajectory views (e.g., maps) that depict stepwise movement and co-presence events.

Epidemiology contributes the single paper in this category. Wu [Wu21] presents a knowledge-graph-based visual analysis approach for tracking COVID-19 patient information, focusing on infection-related events and patient interactions (see Figure 24). Both the M-NW and T-NW are modeled as event-based networks, but are visualized using step-based/sequential representations. The M-NW, illustrating potential transmission opportunities, consists of patient contacts/co-presence at the same location, travels between different locations, and diagnosis events. From these events, the T-NW is derived as explicit infection and causal relationships between patients. Temporal progression is expressed through successive network state visualizations (step-by-step) rather than through continuous time or explicit temporal scales. A node-link diagram is used for patient- and event-related relationships, and a map-based trajectory view complements the analysis of stepwise movement and interaction sequences. The transmissions are visualized as edges.

The core visualizations consist of node-link diagrams showing patients, events, and their relationships, combined with map-based

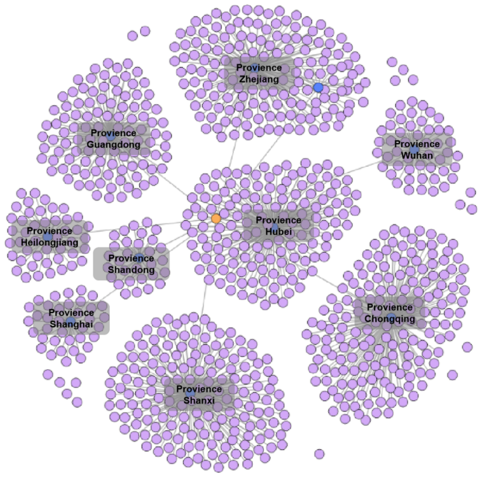

Figure 24: *Regional case node-link illustrating spatial clustering of confirmed COVID-19 cases. Nodes correspond to patients grouped by province or city, and edges represent inferred epidemiological relationships, revealing dominant regional outbreak clusters and inter-regional connections. Figure by Wu et al. [Wu21]. Licensed under CC BY-NC 3.0.*

trajectory views that illustrate stepwise movement between locations. Transmissions are encoded as edges between patient nodes, while event types and locations provide contextual grounding. This representation supports detailed inspection of individual infection chains and causal sequences, but does not emphasize aggregation or large-scale diffusion patterns.

5.4.3. Step-Based Transmission Network and Flattened Medium Network

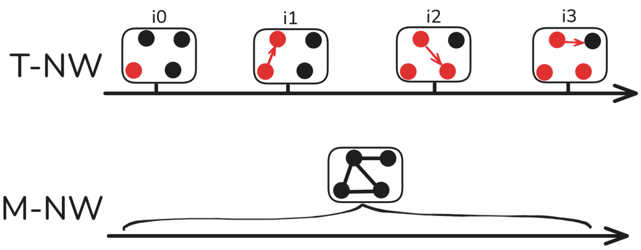

In step-based T-NW visualizations combined with a flattened M-NW, diffusion is modeled as an ordered sequence of discrete propagation steps unfolding on top of a static interaction structure. The M-NW provides a fixed substrate of potential connections, while the T-NW captures how state changes or influences propagate iteratively from one step to the next. This configuration preserves ordering and dependency between transmission steps, but omits both fine-grained event timing and temporal evolution of the M-NW itself. As a result, analysis focuses on the progression of diffusion processes rather than on precise temporal causality. In our corpus, this combination comprises **8 papers** and appears most frequently in epidemiology, financial contagion analysis, and social network diffusion modeling, where iterative simulation or algorithmic propagation is central to the analytical task.

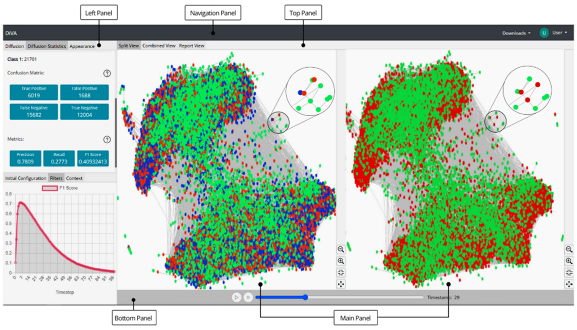

Figure 25: *Side-by-side comparison view of different diffusion algorithms in DiVA. Node colors show their status (susceptible (green), infected (red), and recovered (blue)). The zoomed-in parts reveal differences in the infection status of nodes within a specific cluster for the different algorithms. Reprinted from Sehnan et al. [SGM*23], with permission.*

Across domains, node-link diagrams are the dominant representation for both the flattened M-NW and the step-wise T-NW [WYG*11, SGM*23, WBv*19, ZXL23, XZX*24, ADL*22, AP16b, vDBF15]. Transmission is consistently encoded as edge-based propagation between nodes, with node color representing state changes such as infection, activation, risk, or default. Temporal progression is conveyed either through animation across steps [SGM*23, vDBF15, AP16b] or through small multiples that juxtapose successive propagation states [AP16b,ZXL23,XZX*24]. Additional encodings include edge width to indicate transmission strength or influence [WYG*11, ADL*22] and glyphs and bars to summarize cumulative vulnerability or probability [vDBF15, WBv*19].

Epidemiology and health-related diffusion form a substantial portion of this category (two papers). Simulation-based systems visualize disease spread as a sequence of discrete iterations over a static contact or social network. DiVA [SGM*23] overlays step-wise SIR-style diffusion states on a fixed social graph, using node color to encode health status and animated edge highlights to show newly activated transmissions, while enabling side-by-side comparison of different diffusion models at identical iteration steps (see Figure 25). Wunderlich et al. [WBv*19] aggregate Monte Carlo simulation outcomes into ensembles of step-based T-NWs, visualizing probabilities of infection and transmission through color-coded nodes, weighted edges, and glyph-based summaries that convey uncertainty and variability across simulations (see Figure 38). Both approaches emphasize comparative reasoning across steps and scenarios rather than reconstruction of individual transmission events.

Financial contagion analysis contributes two papers with structurally similar but semantically distinct approaches. Zhang et al. [ZXL23] model systemic risk propagation as a ripple-spreading process over a static network of financial institutions, visualizing each step as a separate node-link diagram where node color encodes risk state and directed edges indicate contagion pathways. Von Landesberger et al. [vDBF15] combine animated node-link views with hierarchical causal layouts, where institutions are

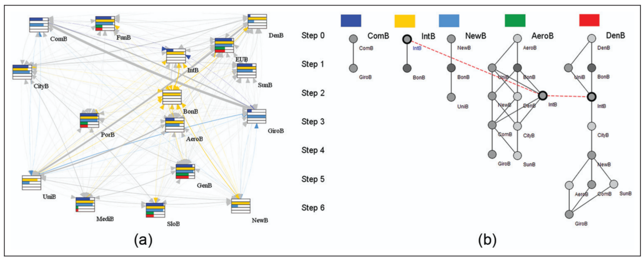

Figure 26: *A node-link and hierarchical diagram showing the defaulting nodes across different simulations. Reprinted from Von Landesberger et al. [vDBF15], with permission.*

aligned by propagation step and visual variables such as bars, colors, and edge highlights indicate default status, vulnerability, and cascading effects (see Figure 26).

In **flow simulation and modeling** (1 paper), Wang et al. [WYG*11] analyze influence transfer between variables in time-varying multivariate data by visualizing entropy-based transmission on top of a flattened M-NW. The T-NW is shown at discrete simulation steps as small multiple node-link diagrams, where edge width encodes the magnitude of information transfer and edge color distinguishes incoming and outgoing influence. Additional node-level glyphs summarize total transferred entropy per variable, supporting step-wise comparison of influence patterns rather than continuous temporal tracing.

Social network and influence analysis further illustrate the flexibility of this configuration (three papers). Archambault and Purchase [AP16b] study dynamic attribute cascades on static graphs, comparing animation and small multiples for step-based propagation and showing node color changes as attributes spread across the network. Influence maximization systems such as IMVis [XZX*24] and the approach by Arleo et al. [ADL*22] visualize iterative activation processes on static (hyper)graphs, where nodes change activation state step by step and edges represent potential influence paths. Here, heatmap-style encodings, edge direction, and small multiples support comparison of alternative seed selections and propagation outcomes.

Overall, step-based T-NW visualizations on flattened M-NWs emphasize iterative reasoning, model comparison, and sensitivity analysis over precise temporal alignment. They are particularly well-suited for simulation-driven domains where diffusion unfolds in conceptual steps rather than measurable time units. However, the assumption of a static medium network limits the ability to study feedback between evolving interaction structures and propagation dynamics.

5.4.4. Step-Based Transmission Network and Implicit Medium Network

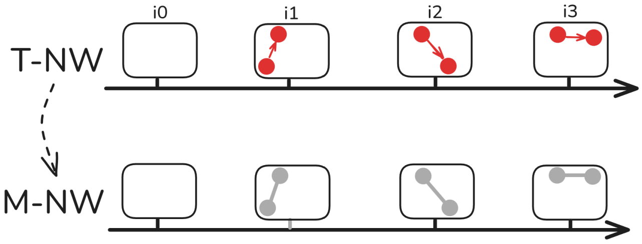

In step-based T-NW visualizations with an implicit M-NW, diffusion is modeled as a sequence of ordered propagation steps without explicit timestamps, while the underlying interaction structure is not visually represented as a reusable network substrate. Transmission is therefore interpreted directly from observed or simulated propagation chains rather than from interactions embedded in an explicit medium. This configuration supports reasoning about ordering, reachability, and progression depth, but limits analysis of alternative transmission opportunities or structural constraints. In our corpus, this is the largest step-based category, comprising **9 papers**, and spans epidemiology, environmental analysis, social media, biological mutation analysis, and synthetic or simulated diffusion scenarios.

Across domains, step-based T-NW visualizations combined with an implicit M-NW rely heavily on explicit representations of the transmission process itself, as no medium structure is available. As a consequence, visualization design focuses on making propagation order, branching structure, and step-wise state changes perceptually prominent. Node-link diagrams are the dominant representation for the T-NW in this category [LLM*19, SKOM12, LKB*14, Gro24, DWC*20], often arranged as trees, layered graphs, or force-directed layouts that emphasize reachability and cascade depth. Alternative encodings include adjacency-matrix-based views for dense or large-scale simulations [BASD21], as well as map-based layouts where spatial embedding substitutes for explicit medium structure [DWC*20, NSS*24, PnABP20].

Step progression is typically conveyed through juxtaposition or animation rather than explicit time axes. Small multiples, layered layouts, or concentric encodings visualize successive steps as discrete states [SKOM12, LKB*14, PnABP20, NSS*24], while animated transitions are used to illustrate propagation order and speed without introducing precise timestamps [DWC*20, PnABP20]. Encodings primarily target node-level attributes, with color indicating activation state, infection status, sentiment, or onset time [LLM*19, BASD21, NSS*24], and node size or glyphs used to represent influence, prevalence, or contribution. Edges encode transmission relationships and are occasionally augmented with width or opacity to indicate strength, frequency, or probabilistic relevance [DWC*20, LKB*14].

Epidemiology and public health applications constitute the largest group in this category (two papers). Several approaches focus on step-wise simulation or reconstruction of disease spread where contact structure is implicit or derived only locally. Browne et al. [BASD21] model infection percolation processes and visualize diffusion progression using adjacency-matrix-based representations, where pixel color encodes epidemiological states across simulation steps. Nasution et al. [NSS*24] analyze respiratory infection spread using epidemic forests rendered as trees over maps, where nodes represent cases or regions, node size encodes prevalence, and color denotes outbreak onset time across discrete steps (see Figure 27).

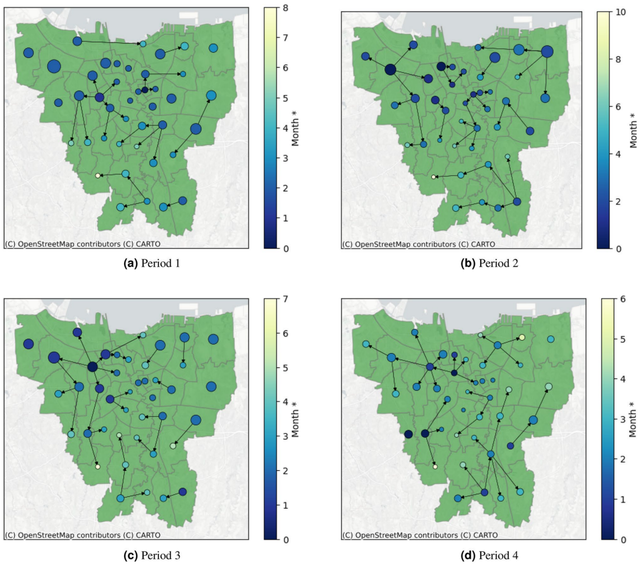

Figure 27: *Result of epidemic forest for 4 periods. Node sizes denote the number of cases, node colors indicate the time of the outbreak (darkest nodes show the earliest outbreaks). Figure by Nasution et al. [NSS*24]. Licensed under CC BY 4.0.*

Environmental and geographical diffusion studies apply similar principles to spatio-temporal propagation phenomena (two papers). Deng et al. [DWC*20] analyze air pollution spread driven by wind dynamics, where the T-NW is constructed from inferred spatial contagion events. Transmission is visualized using node-link diagrams, chord diagrams, and map-based flows, with edges representing pollution transfer between regions and glyphs encoding temporal distribution and contribution ratios across steps. Although the underlying atmospheric transport structure exists conceptually, it remains implicit. Peña-Araya et al. [PnABP20] compare multiple visualization techniques for geographic diffusion, including animation, small multiples, and glyph-based maps, where diffusion intensity per step is encoded via color while transmission paths remain implicit (see Figure 28). Across these works, step-based ordering is emphasized over exact timing, and spatial embedding substitutes for an explicit contact network.

Social media diffusion (two papers) is represented through interaction-driven transmission chains rather than explicit follower graphs. Loyola-González et al. [LLM*19] visualize tweet propagation as step-wise conversational cascades, using force-directed node-link layouts where nodes represent tweets and edges represent reply relations. Node size encodes influence or activity, while color encodes sentiment, allowing comparison of propagation patterns

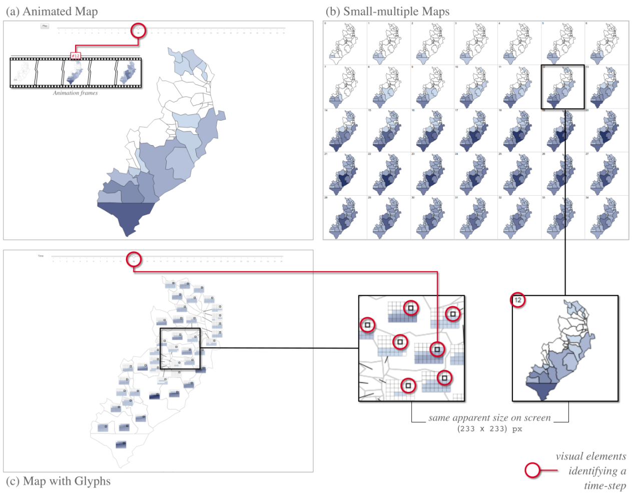

Figure 28: *Comparison of geographic diffusion visualization strategies for a step-based transmission process with an implicit medium network. Diffusion is shown over discrete propagation steps using animation, small-multiples, and map-based glyphs, with color encoding diffusion intensity to support tasks such as identifying spread direction, peaks, and spatial jumps. Reprinted from Peña-Araya et al. [PnABP20], with permission.*

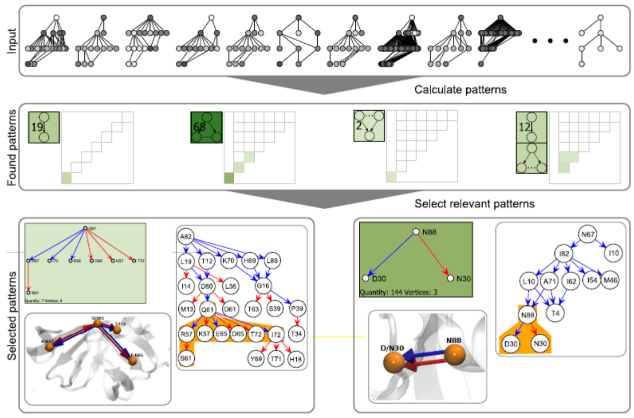

Figure 29: *Patterns in mutation graphs. The top shows input mutation graphs where it is difficult to see patterns. The middle shows the number of found patterns grouped according to their structure. At the bottom, patterns can be viewed in more detail. Reprinted from Lenz et al. [LKB*14], with permission.*

across users and topics. Saito et al. [SKOM12] model diffusion as activation cascades and visualize step-wise propagation using radial node-link diagrams embedded in spherical layouts, where concentric rings encode activation steps and special glyphs highlight mediator nodes.

Synthetic and theoretical diffusion models form another subset (two papers). Grosfils [Gro24] studies information transmission time in drone swarms using step-based propagation models. Transmission paths are visualized through node-link diagrams per iteration and aggregated glyph-based summaries, where node color distinguishes source and target roles and edges encode message transfer. Similarly, Vallet et al. [VKPM15] visualize graph rewriting processes as step-wise transformations of a single evolving network, where node-link diagrams encode active, inactive, or visited states through color, and transmission is implicit in the rule application sequence rather than in a separate medium network.

Biological mutation analysis represents a structurally distinct but conceptually aligned case (one paper). Lenz et al. [LKB*14] analyze mutation chain reactions in proteins, where transmission corresponds to dependency-induced mutation sequences. The T-NW is visualized as a node-link diagram, with nodes representing amino acids and edges encoding mutation dependencies. Additional coordinated views support pattern detection across multiple mutation graphs, while the protein structure provides spatial context without functioning as an explicit medium network (see Figure 29).

Overall, step-based T-NW visualizations with implicit M-NWs consistently emphasize ordered propagation, reachability, and comparative pattern analysis over structural completeness. Node-link diagrams dominate, complemented by matrices, maps, radial layouts, and glyph-based encodings. Transmission is almost exclusively encoded through edges, while node color, size, or shape represent state, influence, or temporal ordering. This configuration is well-suited for simulated processes and domains, where interaction opportunities are unknown or secondary. However, it limits the ability to assess how alternative or evolving medium structures might enable or constrain diffusion.

5.5. Flattened Transmission Network Visualizations

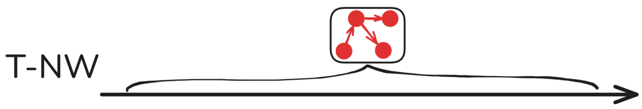

Flattened Transmission Network (T-NW) visualizations represent diffusion processes in a temporally aggregated form, where temporal ordering, duration, or sequencing of transmission events is suppressed in favor of cumulative or summary representations (terminology adapted from Bach et al. [BDA*17], see also section 2). Instead of explicitly encoding time, transmission intensity, frequency, or importance is collapsed into static edge or node attributes. This abstraction prioritizes structural overview and comparative analysis over temporal reconstruction and causal tracing.

In this section, we discuss **21 approaches** that employ flattened T-NWs in combinations with different temporal abstractions of the Medium Network (M-NW).

From an **application domain perspective**, flattened T-NWs are most prevalent in social media analysis (10 of 21) [MZK19, FH16, BLRM19, SKM08, SYM24, PMA*22, WM21, Wue21, SV20, RIDS25], where diffusion is often inferred from aggregated interaction logs rather than reconstructed as explicit event sequences. Epidemiology constitutes the second largest group (5 of 21) [AAA*24, WTF*16, TMK14, WM21, LMJ*21], typically focusing on summarizing transmission intensity or reach across populations or regions. Further heterogeneous domains include finance (4 of 21) [CSS*25, QHD26, GNX25, YLZ*25], cybersecurity (1 of 21) [RBJ*23], air pollution (1 of 21) [DCX*24], and citation networks (1 of 21) [SSXS15].

From a **visualization perspective**, flattened T-NWs are in all of our found cases represented using node-link diagrams (21 of 21) [MZK19, AAA*24, RBJ*23, FH16, BLRM19, SKM08, WTF*16, SYM24, SSXS15, PMA*22, DCX*24, TMK14, WM21, Wue21, LMJ*21, SV20, RIDS25, CSS*25, QHD26, GNX25, YLZ*25].

Additional attributes, such as transmission values, e.g., relative importance or volume, are most commonly encoded through edge width (8 of 21) [MZK19, SSXS15, SV20, RBJ*23, CSS*25, QHD26, GNX25, YLZ*25] or color and opacity (12 of 21) [RBJ*23, BLRM19, SKM08, WTF*16, SSXS15, PMA*22, DCX*24, TMK14, WM21, Wue21, LMJ*21, YLZ*25].

Flattened T-NW are combined with few types of M-NW: The medium network (M-NW) is either flattened (7 of 21) [MZK19, AAA*24, RBJ*23, FH16, WTF*16, PMA*22, SV20] or remains implicit (14 of 21) [BLRM19, SKM08, SYM24, SSXS15, DCX*24, TMK14, WM21, Wue21, LMJ*21, CSS*25, QHD26, GNX25, YLZ*25, RIDS25], reflecting a design choice to emphasize aggregate transmission outcomes rather than explicit contact opportunities or interaction dynamics.

From a **temporal perspective**, overall, flattened transmission network visualizations favor robustness, scalability, and interpretability over temporal fidelity. They are well suited for overview tasks, influence ranking, and comparative analysis across entities or scenarios, but inherently limit reasoning about transmission order, timing, and causality. As such, this abstraction is most effective when temporal detail is either unavailable, unreliable, or secondary to structural summarization goals.

Missing T-NW and M-NW combinations. We did not identify examples for three combinations: (1) flattened T-NW with event-based M-NW, (2) flattened T-NW with time-sliced M-NW, and (3) flattened T-NW with step-based M-NW. For the first case, flattening the T-NW removes temporal ordering that is essential when the M-NW provides event-level timing, making meaningful transmission reasoning difficult [HS12]. The second case is typically addressed by deriving step-based simulations on top of time-sliced M-NWs rather than fully flattening transmissions. The third case again reflects a representational mismatch, as an ordered but time-agnostic M-NW does not align well with fully aggregated transmission representations.

In the following subsections, we further differentiate flattened T-NW visualizations according to the temporal abstraction of the M-NW visualization. For each combination, we summarize the number of papers, dominant application domains, and characteristic visualization strategies. Combinations for which no literature was identified are omitted.

5.5.1. Flattened Transmission Network and Flattened Medium Network

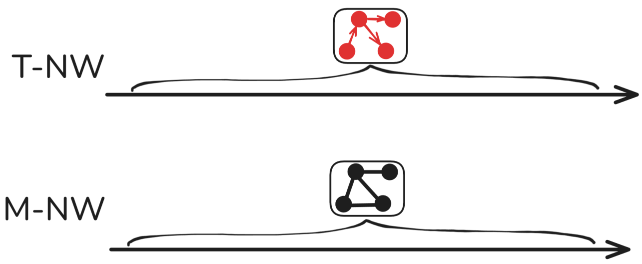

When both the T-NW and the M-NW are flattened, diffusion is analyzed without any explicit temporal encoding. All transmission events are aggregated into a single structure, and the underlying interaction network is likewise represented as a static snapshot. As a consequence, temporal ordering and duration are not visualized, and analytical reasoning focuses on structural properties such as connectivity, influence, and reach. This configuration represents the most temporally abstracted form of diffusion visualization in our taxonomy and comprises **7 papers** in the corpus. It occurs most frequently in social media analysis and cybersecurity, where the primary analytical goal is to identify influential actors, or potential propagation reach rather than to reconstruct temporal diffusion processes.

Across domains, flattened T-NW combined with flattened M-NW visualizations are dominated by node-link representations [FH16, MZK19, PMA*22, RBJ*23, SV20, WTF*16, AAA*24]. Diffusion is typically inferred computationally and encoded through structural metrics rather than explicit propagation sequences. Common visual channels include node size for influence, centrality, or volume [MZK19, SV20, AAA*24], node color for cluster membership, role, or diffusion sta-

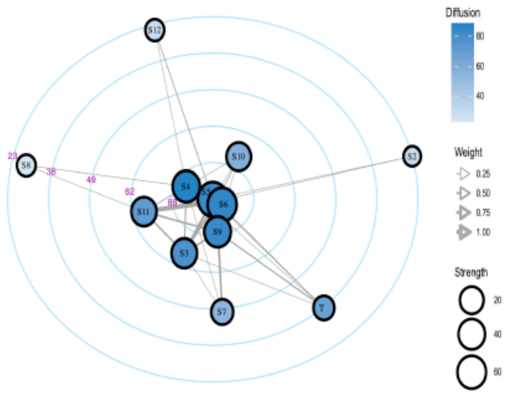

Figure 30: *Diffusion-based network visualization of information exchange in a computer-supported collaborative learning (CSCL) setting. Nodes represent participants, and edges represent interactions, while diffusion-centric encodings highlight differing levels of influence and participation within the learning network. Reprinted from Saqr and Viberg [SV20], with permission.*

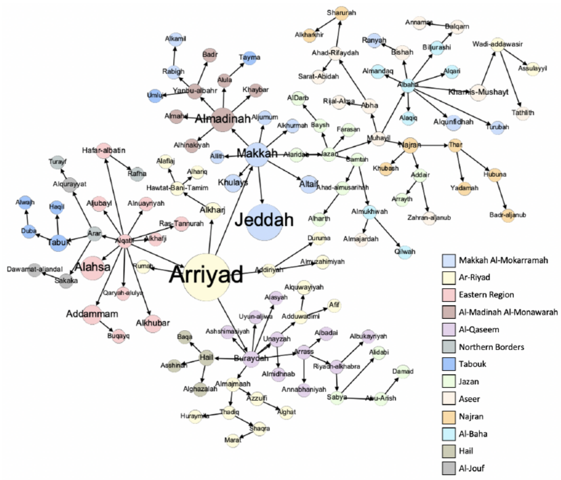

Figure 31: *City-level transmission network illustrating inferred disease spread between cities in a node-link diagram. Nodes represent cities, edges indicate transmission pathways derived from infection order and spatial proximity, with node size reflecting population and color denoting administrative regions. Figure by Alrasheed et al. [AAA*24]. Licensed under CC BY 4.0.*

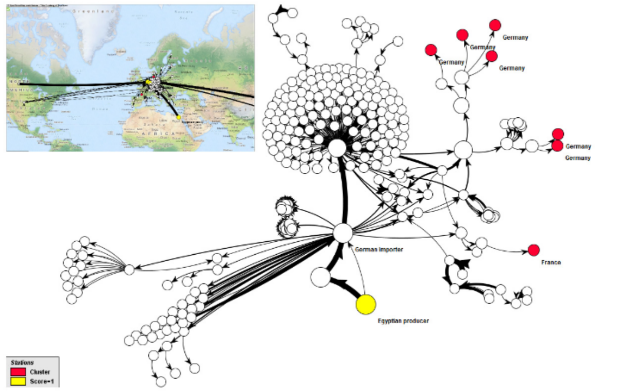

Figure 32: *Trace-back and trace-forward network of the 2011 EHEC outbreak generated with FoodChain-Lab, showing outbreak clusters (red) and their connections to the identified source in Egypt (yellow). Node size encodes the tracing score, highlighting the most likely contamination source, and the network view is synchronized with a geographic map to support spatial reasoning. Figure by Weiser et al. [WTF*16]. Licensed under CC BY 4.0.*

tus [PMA*22, RBJ*23], and edge width or opacity for transmission strength or frequency [SV20, WTF*16]. Temporal information, when present in the data, is either discarded or summarized into aggregate statistics and additional views, such as bar charts, Sankey diagrams, scatterplots, or word clouds [PMA*22, WTF*16, AAA*24].

Social media applications account for four papers and emphasize influence detection and reach estimation over large user populations. Francalanci and Hussain [FH16] analyze Twitter data using a flattened author–topic network, where influence is inferred from retweet behavior and content specificity. Although diffusion is conceptually multi-hop, the visualization collapses all activity into a single node-link snapshot, arranged using a force-directed layout with k-shell-inspired layering to highlight influential users. Mrsic et al. [MZK19] study Facebook fan page interactions at scale, encoding diffusion-related centrality measures such as PageRank and betweenness directly through node size, without any temporal differentiation. *MeVer NetworkX* [PMA*22] focuses on disinformation tracking, flattening the M-NW to highlight suspicious actors and their potential reach. Here, the flattened T-NW supports neighborhood inspection, while additional charts and textual summaries provide semantic context. In educational settings, Saqr et al. [SV20] visualize knowledge exchange in collaborative learning as a flattened diffusion network, where edge weights encode interaction strength and node position and size reflect diffusion centrality, enabling role identification without temporal analysis (see Figure 30).

Epidemiological diffusion at an aggregated spatial level appears in two papers. Alrasheed et al. [AAA*24] model city-to-city disease transmission using a flattened network, where directed edges encode inferred spread between regions (see Figure 31). Node size and color reflect population and regional clustering, while transmission strength is derived from outgoing flows and centrality measures. Although multiple transmission trees can be explored, each is shown as a static structure, and temporal dynamics are not explicitly visualized. Weiser et al. [WTF*16] visualize contamination propagation through static trace-back and trace-forward paths (see Figure 32). The flattened T-NW highlights potential contamination routes using node-link diagrams and Sankey-style flow representations, supporting scenario comparison rather than temporal reconstruction.

Cybersecurity and infrastructure monitoring contributes one paper and adopt flattened representations to emphasize structural attack or flow patterns. Rabzelj et al. [RBJ*23] model cyberattacks observed in distributed honeypot networks, representing attackers, targets, malware servers, and artifacts as heterogeneous node types in a single aggregated graph. Although attacks are inherently temporal, time is deliberately omitted to focus on connectivity, attack frequency, and structural relationships between entities. In supply-chain and food safety analysis,

Overall, flattened T-NW combined with flattened M-NW visualizations prioritize scalability, simplicity, and structural interpretability over temporal fidelity. They are well-suited for tasks such as influence ranking, hotspot identification, pathway enumeration, and comparative scenario analysis across large heterogeneous systems. However, by collapsing diffusion into a single aggregated view, these approaches cannot support temporal reasoning about causality, ordering, or evolution, highlighting a clear trade-off between analytical tractability and temporal expressiveness.

5.5.2. Flattened Transmission Network and Implicit Medium Network

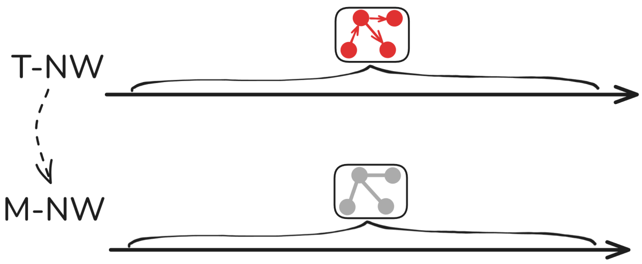

In flattened T-NW visualizations with an implicit M-NW, transmission structures are shown as aggregated, time-collapsed networks without explicit representation of the underlying interaction substrate. The M-NW is assumed rather than visualized and is only indirectly reflected through observed transmission relations. This configuration suppresses both temporal ordering and medium-network dynamics, shifting analytical focus toward structural diffusion patterns, influence, clustering, and comparative outcomes. In our corpus, this combination comprises **14 papers** and occurs most frequently in social media analysis and epidemiology, with additional isolated examples from citation analysis, healthcare logistics, and environmental monitoring.

Across domains, flattened node-link diagrams dominate the visualization of the T-NW [BLRM19, SKM08, SYM24, SSXS15, DCX*24, TMK14, WM21, LMJ*21, Wue21, CSS*25, QHD26, GNX25, YLZ*25, RIDS25]. Transmission is encoded through edges representing observed interactions (e.g., replies, citations, contacts, or transitions), while node attributes such as size, color, or position encode influence, cluster membership, origin, or diffusion strength. Because neither event timing nor step ordering is visually preserved, additional views, such as Sankey diagrams [WM21], statistical summaries [BLRM19, SYM24, DCX*24, Wue21, WM21, GNX25, YLZ*25, CSS*25], or geographic embeddings [WM21], are frequently employed to contextualize propagation patterns and support comparative analysis.

Social media applications contribute four papers and focus on understanding diffusion structure, topical communities, and influence without exposing the full social graph. Babvey et al. [BLRM19] and Würschinger [Wue21] analyze topic and lexical diffusion on Twitter using flattened node-link diagrams in which nodes represent tweets or users and edges encode reposting or interaction relations. Color and layout emphasize communities, topics, or neologisms, while influence is inferred from structural position rather than temporal sequence. Soga et al. [SYM24] extend this paradigm toward explainable fake-news detection, combining flattened propagation graphs with node-level details and coordinated statistical views. Saito et al. [SKM08] compare diffusion outcomes across different models and embeddings using flattened visualizations, explicitly prioritizing comparative diffusion behavior over reconstruction of the underlying medium network (see Figure 33). Similarly, Rasel et al. [RIDS25] investigate in tourism-focused social media the role of influential users and hashtag diffusion patterns. They visualize interactions as a flattened network, nodes representing users and edges encoding engagement relationships,

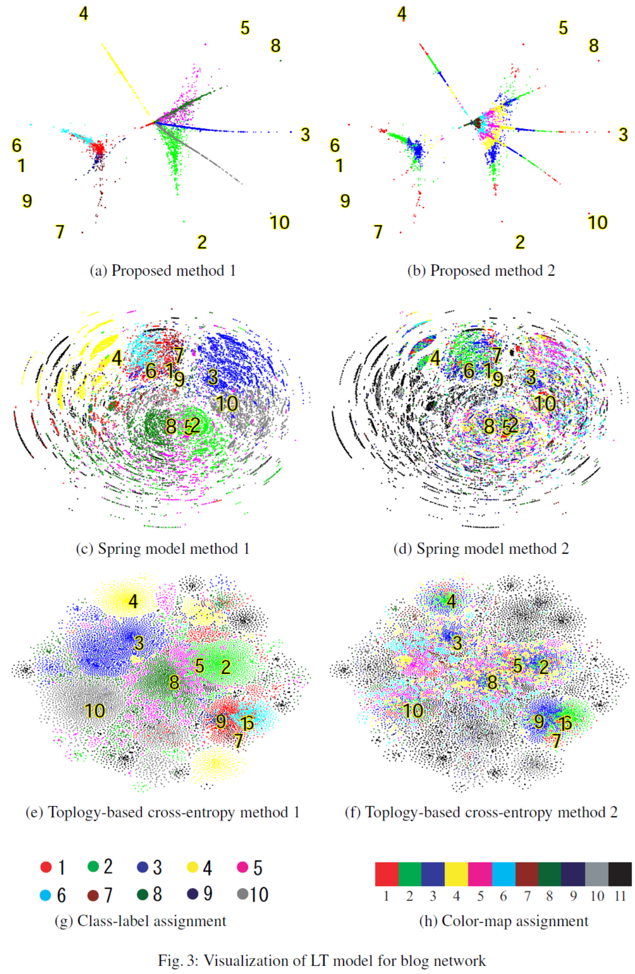

Figure 33: *Visualization of information diffusion on a blog network using different embedding strategies. The proposed diffusion-aware embedding emphasizes continuity and separability of influence paths, while topology-based baselines produce less interpretable diffusion structures. Reprinted from Saito et al. [SKM08], with permission.*

such as mentions or hashtag co-usage. Visual encodings, such as layout and color, emphasize central actors, community structures, and engagement intensity rather than temporal propagation. Across these works, the implicit M-NW enables scalability and abstraction, while diffusion is treated as a structural pattern rather than a temporally unfolding process.

Financial applications contribute four papers and visualize the diffusion of risk, impact, or substitution dynamics across transaction and market networks. Cao et al. [CSS*25] present *NFTracer* to analyze NFT marketplaces through substitutive transaction-flow systems. Projects are represented as nodes, and directed edges encode stakeholder migration and substitution effects between collections. Their system combines a node-link diagram embedded into a substitution view with other coordinated views to trace how

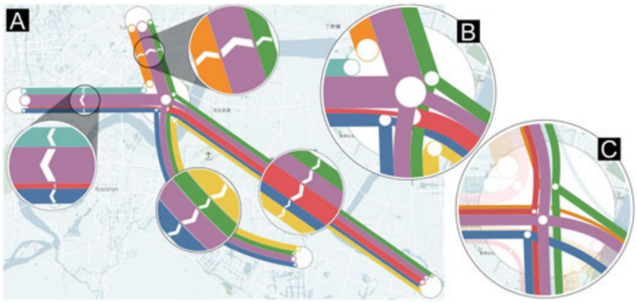

Figure 34: *Multilevel analysis of air pollution event cascades using GeoNetverse. (A) Overview of all geo-networks, showing cascades originating from a central district. (B) Zoomed view of the central node, revealing multiple outgoing cascading patterns to surrounding districts. (C) Drill-down to individual geo-networks of interest, enabling detailed inspection of specific cascade structures and their spatial context. Reprinted from Deng et al. [DCX*24], with permission.*

project impact diffuses and decays over time. Qiu et al. [QHD26] and Gong et al. [GNX25] focus on financial contagion across cryptocurrencies and stock markets, showing geopolitical risk. Nodes represent individual indices or whole markets, and edges encode spillover strength derived from risk-variance decomposition. The visualization emphasizes contagion pathways, influential transmitters, and community structure rather than individual transactions. Yu et al. [YLZ*25] address financial risk propagation in dynamic networks, visualizing risk spread across a flattened network and providing visualization tools for quantifying and validating cascading effects. Across these works, diffusion is treated as a structural and systemic process, with node-link representations used to reveal contagion channels, substitution relations, and influential entities in finance markets.

Epidemiological studies account for three papers and similarly rely on implicit medium networks to emphasize outbreak structure and clustering. Wickramasinghe et al. [WM21] visualize global COVID-19 spread using flattened node-link diagrams embedded in geographic maps, complemented by Sankey diagrams to compare community-detection results. Luo et al. [LMJ*21] construct time-flattened transmission networks of infected individuals, using node color to encode infection origin and cluster affiliation. Takagi et al. [TMK14] analyze patient flow through hospital wards, visualizing transitions as weighted edges in a flattened node-link diagram, where edge width encodes transition frequency. In all cases, the underlying contact or organizational structure is assumed rather than visualized, allowing analysts to focus on propagation topology and aggregation patterns.

Beyond these dominant domains, individual works adopt the same abstraction strategy in different contexts (one paper each). Su et al. [SSXS15] visualize influence diffusion in **citation networks** using flattened node-link diagrams, where edge width encodes influence strength and node size reflects citation impact. Deng et al. [DCX*24] analyze **air pollution and traffic diffusion** using aggregated transmission graphs embedded in geographic space, where color distinguishes diffusion instances and temporal ordering is intentionally omitted (see Figure 34). In both cases, the implicit M-NW allows the transmission structure itself to define the visible network, emphasizing influence and flow over infrastructure.

Overall, flattened T-NW visualizations with implicit M-NWs favor abstraction, scalability, and structural comparison over temporal fidelity and medium-network reasoning. By omitting explicit representations of M-NW structure and temporal progression, these approaches support the identification of influential actors, clusters, and comparative diffusion outcomes across large and heterogeneous datasets. However, this configuration limits causal reasoning about how transmission dynamics interact with evolving M-NW structure or temporal order.

6. Additional Aspects of Visualization

In addition to the visual representations of the medium network (M-NW) and transmission network (T-NW), the surveyed papers identify several recurring design aspects important for information diffusion (ID) analysis. These include the use of additional views and derived statistics, specialized interaction techniques, layout strategies for the network, and task-driven requirements. Together, they complement the core medium and transmission network representations and shape how analysts explore, interpret, and compare diffusion processes.

6.1. Visualization of Derived Values and Additional Charts

A wide range of papers use additional statistics to provide the user with additional information, employing a variety of visual encodings. This entails showing additional facets of the data and derived measures (e.g., network and process statistics) beyond the M-NW and T-NW. About 85% of papers included at least one chart of additional data, models, or statistics. One paper even had 7 different chart types to show additional facets of the data [CVV*21].

Additional views include bar charts [SGM*23, RBJ*23, NCZZ18], line charts [SGM*23, ZXL23, CDBM*06], scatterplots [TGA*23, HWZ19, SV20], radial and PCP plots [XZX*24, SV20, LHS*15]. Interestingly, node-link diagrams were also used to show additional data, such as topic-links for text data or the compartment model for the ID process of infection spread [HSS*20, FH16, YJZ*25]. Line charts are the most commonly used additional chart type, followed by bar charts.

The distribution of node degree is shown as a histogram [ZXL23] or scatterplot [SGM*23]. Zhang et al. [ZXL23] show the temporal evolution of node-degree for a time-sliced M-NW in a line chart. Xu et al. [XZX*24] show network statistics as Nightingale Rose Diagram-based glyph (see Figure 35). Ren et al. [RWZ*20] overlay a map on top of the M-NW node-link diagram to show the spatial distribution of the data for further analysis. This is the case not only in transportation M-NWs, but also in other cases, e.g., showing spatial distribution of cattle in case of disease spreading [RRP*21] or computer networks [USK21]. Additional measures about M-NWs can also be shown using additional encodings within the node-link representation, e.g., node size.

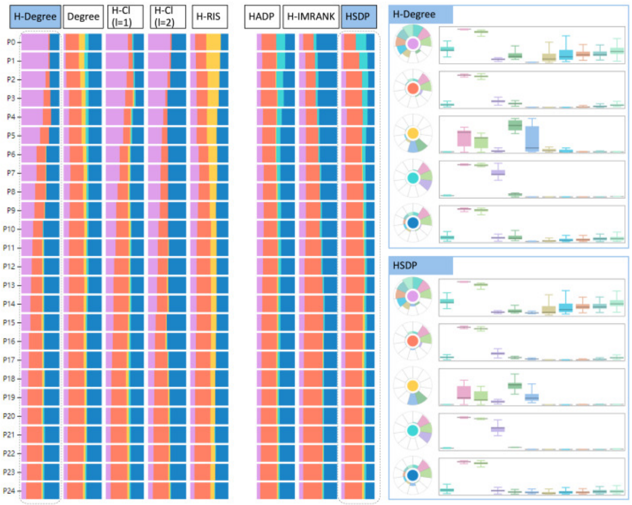

Figure 35: *Overview-level comparison of multiple information maximization (IM) algorithms in Algebra. The transmission processes of IM algorithms in the left group evolved gradually, while those in the right group remained basically unchanged. Figure by Xu et al. [XZX*24]. Licensed under CC BY-NC-ND 4.0.*

The T-NW is also often shown as a node-link diagram with additional data shown within or as an additional chart. Additional facets, such as spatial context, are often shown in additional views. For example, Deng et al. [DWL*22] and Alrasheed et al. [AAA*24] embed the T-NW both in a map and in a separate node-link visualization (see Figure 31). Lenz et al. [LKB*14] show the T-NW both as a node-link diagram and as edges overlaid over a 3D protein view (see Figure 36). This is designed to show both the topology and the spatial embedding of the network in protein folding.

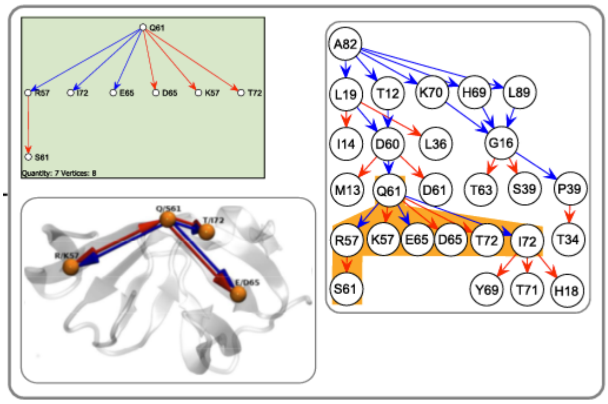

Figure 36: *User-selected relevant patterns in T-NWs can be examined in detail both in the node-link diagram of the full T-NW and in the 3D protein structure. Reprinted from Lenz et al. [LKB*14], with permission.*

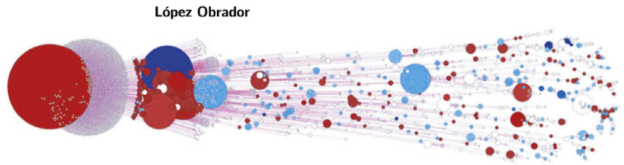

Figure 37: *Largest constellations of Lopez Obrador galaxy of tweets. Reprinted from Loyola-González et al. [LLM*19], with permission.*

ID process analysis often requires identifying and assessing influential nodes [GHFZ13]. This can be done using additional visual mappings within the T-NW node-link view or in additional charts. Loyola-González et al. [LLM*19] encode the influence of a tweet as node size, while node color encodes tweet sentiment (see Figure 37). Saqr et al. [SV20] present a specially designed radial plot to show diffusion statistics per network node. Color, size, and position of the node encode several diffusion measures.

In many cases, ID processes are simulated, e.g., for prediction or model parameter exploration. Papers that discuss visualization methods to explore ID simulations often deal with COVID-19 spreading, such as Sondag et al. [STX*22]. Sometimes, the T-NW is based on a derived network and data, such as in topic and word modeling, where they are visualized in a word cloud or node-link diagram [WLC*16, HSS*20, FH16, YJZ*25].

Additional charts and tables are also used for showing statistics and derived measures of the transmission process, such as the number of infected nodes per process step, total number of infected nodes per transmission process simulation, the duration of the transmission process, min-average-maximum number of infected nodes per transmission event, etc. Process-based statistics are often shown in line charts (with time on the x-axis and measures on the y-axis) [SGM*23, ZXL23, CDBM*06], or bar charts [WBv*19]. Interesting charts about the clustering of transmission processes for ensemble simulations are shown by Wunderlich et al. [WBv*19] (see Figure 38).

6.2. Interaction

This section discusses interaction techniques in ID visualization, with a particular focus on how common interaction primitives are adapted to diffusion-specific analytical objects such as sources and seeds, transmission paths, cascades, and simulation scenarios. Standard techniques such as pan/zoom, hovering, sorting, filtering, and multiple coordinated views of the raw network or additional data are common across the surveyed systems (in particular, in the case of M-NWs) and are not interesting in themselves. We therefore consider them here only when they are coupled to diffusion-specific analytical objects, for example, when selection is used to define source posts or seed sets, highlighting is used to trace propagation paths, drill-down is used to move from aggregate cascades to individual events, or comparison is used to inspect alternative simulation scenarios.

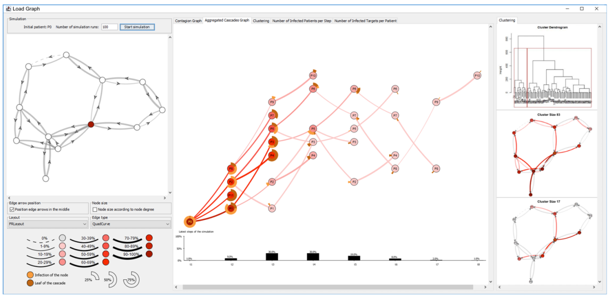

Figure 38: *Visual Interface of probabilistic T-NWs created by monte carlo simulation - ensembles. The infection transmission in the patient contact graph (M-NW left) is simulated. The development of the transmission process is shown with an Aggregated Cascades Graph (center). The T-NW results are clustered and displayed with so-called Contagion Graphs (right), and the clustering is shown as a dendrogram on the top right. The bottom bar chart shows the number of finished transmissions per time step. Reprinted from Wunderlich et al. [WBv*19], with permission.*

Diffusion-specific interactions are comparatively rare. Based on our coding of the 98 papers, only about one quarter of the papers (24/98) describe at least one interaction tailored to diffusion-related reasoning tasks, and only 17 papers make such interactions a clear part of their contribution. In other words, relatively few papers describe interactions that act directly on diffusion-specific objects rather than only supporting generic navigation or inspection. Example classes of interactions include source or seed selection [CCW*16, WLY*14, YJZ*25, LHS*15, SGM*23, ADL*22, AME11, LCZ*24, STX*22], backward/forward path tracing and diffusion trace highlighting [CLS*12, WLY*14, BPW*21, WTF*16, ASGK21], diffusion scenario comparison [DWC*20, DWL*22, YJZ*25], and cascade-specific drill-down from aggregate patterns to individual transmission events or posts [SGM*23, ADL*22, vDBF15, AME11, STX*22].

One prominent class of diffusion-specific interaction concerns source or seed selection. Examples include filtering results of diffusion processes for specific seeds or selecting seeds for a diffusion simulation scenario.

In social media systems, seed selection interaction often means selecting source posts, topics, platforms, or user groups from which the diffusion process is explored. For example, D-Map [CCW*16] allows users to select source Weibos (original posts on the Chinese microblogging platform Weibo, similar to Twitter/X) and related re-posting communities, while OpinionFlow [WLY*14] supports topic selection in a stacked tree and subsequent selection of user groups for detailed propagation analysis (see Figure 19 and Figure 9. BloomWind [YJZ*25] supports selecting events, platforms, and time ranges before exploring cluster-level and post-level cross-platform propagation (see Figure 12). EgoNetCloud [LHS*15] uses topic-based interactions to isolate forwarding networks initiated by celebrities, media, or ordinary users, thereby enabling comparisons of which actor groups dominate different phases of a Weibo information cascade (see Figure 6).

A second important class of interaction for diffusion exploration is path tracing and trace highlighting. Here, analysts select a user, patient, or transmission chain and then trace diffusion or transmission paths backward and forward to identify origins, key mediators, and affected entities. This interaction pattern is particularly central in systems designed for social media, contagion analysis, and contact tracing. Whisper [CLS*12] supports monitoring a diffusion topic in real time and focusing individual diffusion pathways to inspect detailed retweet series along a configurable timeline. OpinionFlow [WLY*14] allows analysts to select a user and trace that user's influence path through the diffusion view, and even to test *what if* hypotheses by modifying opinions and immediately updating the projected propagation. In epidemic settings, the interaction becomes even more explicitly source-oriented: *In Search of Patient Zero* [BPW*21] introduces dedicated backward and forward tracing interactions to reconstruct transmission pathways and identify candidate index patients. Related trace-back/trace-forward workflows are also found in FoodChain-Lab [WTF*16] for outbreak investigations and in the COVID-19 infection-cluster system with linked contact network and Epi-Gantt views from Antweiler et al. [ASGK21]. These examples show that interaction is often essential for ID analysis because the analytical question is not only what the network looks like, but also who infected, influenced, or triggered whom, and along which path.

Another recurring pattern is interaction for cascade-specific drill-down from aggregate structures to concrete instances. The key interactions here are selecting, filtering, brushing, hovering, and clicking on aggregate diffusion structures in order to open more detailed views. This is most clearly visible in systems for spatiotemporal propagation. AirVis [DWC*20] supports interactive mining of propagation motifs, filtering by district or polygon selection, and hierarchical drill-down from motifs to patterns to concrete pollution instances. Lenz et al. [LKB*14] allow the extraction of diffusion patterns, showing an overview of the patterns by their structure, selecting interesting pattern structures, and drilling down to individual instances that are shown in the context of original data – protein structures (see Figure 29). VisCas [DWL*22] allows users to lasso locations, tune inference parameters, filter or select cascade groups, brush time windows, and switch from uncertainty views to influence views for detailed cascade inspection. BloomWind [YJZ*25] likewise combines overview and detail by allowing analysts to hover and click on cross-platform propagation paths to reveal salient instances, and then open a post-level propagation view for the selected relationship. In all these cases, the drill-down is not generic details-on-demand, but is tightly coupled to the analytical abstraction of the diffusion process itself, i.e., motifs, cascades, pathways, or cluster-to-cluster propagation links.

In simulation settings, seed selection interactions are explicit: DiVA [SGM*23] allows analysts to upload custom seed sets and compare the resulting diffusion simulations side-by-side (see Figure 25), while VAIM [ADL*22] lets users change the seed set interactively and iterate the simulate-evaluate-compare loop. The system by von Landesberger et al. [vDBF15] allows the user to select seed banks and compare their diffusion processes in a specialized view. It also allows users to select nodes of the diffusion processes to compare their existence across diffusion processes using linking (see Figure 26).

Finally, interactive scenario setting and scenario comparison are key interaction techniques in papers concerned with modeled or simulated diffusion. Several systems explicitly support the creation and comparison of multiple runs, policies, or contagion scenarios. Decision-support systems for epidemic spread, such as the visual analytics decision-support environment for epidemic modeling by Afzal et al. [AME11], VIVIAN [LCZ*24], and the contact-tracing policy simulation system by Sondag et al. [STX*22], allow analysts to vary mitigation measures, model parameters, or policy settings and directly inspect how the transmission process changes. DiVA [SGM*23] and VAIM [ADL*22] compare alternative seed sets, algorithms, or diffusion models. The system for visual analysis of contagion in networks by von Landesberger et al. [vDBF15] supports the comparison of multiple contagion processes and their final effects under user-defined simulation conditions (see Figure 26). The epidemic decision-support environment from Afzal et al. [AME11] links geospatial views, temporal views, and a decision-history tree to compare simulation branches over time.

In summary, these examples indicate that some of the most distinctive interaction contributions in ID visualization do not merely support navigation, but provide concrete mechanisms for source and seed selection, path tracing and highlighting, cascade-aware drill-down, and scenario comparison. Overall, diffusion-specific interaction appears whenever users need to move between overview and causal detail, follow propagation paths, or actively manipulate assumptions about how diffusion starts or evolves.

6.3. Layouts

Graph layout is a central aspect of network visualization. It concerns calculating the coordinates of the nodes in the 2D plane when adopting a node-link visualization, which can have a significant impact on understanding the topology of the graph, including relationships between nodes, neighborhoods, and paths between nodes. Empirical studies identified quality *aesthetic* criteria for layouts that affect their readability. These cannot all be satisfied in a single layout, consequently, tradeoffs are required. These include the number of crossings, edge length variability, crossing angles, area, and more [WPCM02, Pur02, BRSG07, vKS*11]. The readability of graph structure and graph topology, as well as network properties, is of special interest to the visualization of the medium network (M-NW). However, for the purpose of understanding ID, specialized layouts are needed that convey data about diffusion properties such as transmission pathways, sources, and targets of diffusion, or the importance of nodes in the diffusion, as well as other properties of the transmission network (T-NW) [SKM08, ADL*22]. Our survey revealed interesting trends and solutions for the layout of nodes and edges, especially regarding ID.

Layouts focusing on highlighting features related to the transmission process (sources, transmission paths, and targets of the diffusion) vary according to the type of T-NW. Flattened T-NWs do not have information about the time/step of the process, thus, a standard force-directed layout [AAA*24, SMSR20] is used (see Figure 18 and Figure 31). This, however, makes it difficult to perceive parent-child relationships and the whole process. For step-based T-NWs, even though the process can be shown with standard layouts, Sugiyama-like [STT81] layouts are widely used [vDBF15, LKB*14, STX*22] (see Figure 36 and Figure 38). The transmission process is naturally a directed-acyclic graph (DAG) or, in special cases, a tree with sources of diffusion being the ultimate parent nodes, and the transmissions creating parent-child relationships. In the DAG case, one child can possibly have several parents if the diffusion runs in parallel and the target nodes of diffusion are the ultimate children. In these cases, Sugiyama-like, top-down, or radial tree layouts are used. The Sugiyama-style top-down layout offers the advantages of providing a bird's-eye view of the cascading process, supporting source identification, targets, transmission pathways, and superspreaders, as well as the sequence of diffusion. For continuous time, other types of visualization, such as storylines, are used [BPW*21, XWW*13, KLM24]. They also have special layouts that help to see the transmissions, such as placing contact lines close to each other or ordering lines according to the time of first contact [BPW*21] (see Figure 5). Here, the interesting aspect is also the layout of transmission links. While standard network links are drawn as straight lines, in this case, transmission links are drawn as arcs on top of the medium network to differentiate and emphasize the transmission between entities.

Showing the diffusion properties of nodes, such as influence and number of followers, can also be conveyed by specialized layouts. For example, Liu et al. [LHS*15] and Villar-Rodriguez [VRHGM*24] use the y-axis position to show the number of followers in the transmission network (see Figure 6 and Figure 10). This enables spotting superspreader nodes easily.

When available, the spatial context of diffusion processes is typically visualized using geographical maps. In such representations, nodes are positioned according to their real-world locations, and links indicate transmission between these geolocated nodes (see Figure 27 and Figure 23). Alternatively, spatial context can be conveyed through topographic maps or hexbin cartograms (see Figure 14 and Figure 19). Spatial information may also be represented directly as 3D structures, such as protein folding landscapes [LKB*14] (see Figure 36). These map-based and 3D visualizations prioritize the spatial embedding of the diffusion over the structural characteristics of the diffusion process itself.

It is interesting to note that when choosing a layout for ID, the goal (e.g., features highlight, cascade analysis) impacts the prioritization of the different aesthetic criteria. From this analysis, it also emerges that there is no specialized "diffusion-aware" layout method specifically designed to highlight diffusion features. The only exception to the work by Saito et al. [SKM08], which proposes an embedding method based on conditional probabilities of ID. However, it is limited to processes generated under independent cascade or linear threshold diffusion models.

6.4. Task & Requirements

In our literature review, we found that the analytical tasks supported by the systems are rarely explicitly stated. Therefore, a limitation of this survey is the lack of a specific task-centered categorization.

However, we can infer some high-level tasks and goals from each approach's visualization techniques, interaction design, and evaluation methods, and we discuss and summarize these in the following.

One of the most common and high-level analytical tasks is to trace diffusion processes and transmission events to reconstruct or reason about which paths of propagation were essential and contributing to the overall spread, and to identify the sources of transmission [CLS*12,WLY*14,BPW*21]. Following that, understanding macro patterns, such as spread dynamics, speed, extent, and branching structure, emerged as the next most common analysis supported by the systems [CLS*12,CCW*16,DWC*20, YJZ*25]. Once diffusion processes are traced and macro patterns identified, a common next step in the analysis is to dive into details and understand the temporal aspects of diffusion processes, including order of events, delays, and propagation, as well as distinct phases of the processes [CLS*12,WLY*14,BPW*21,DWL*22,LCZ*24]. At the lowest level, most analytical tasks focused on determining the influence that specific entities in the network had on the diffusion process (i.e., identifying key spreaders/influencers) [CCW*16, LHS*15, ADL*22]. In addition, comparative analysis, exploratory tasks, and assessment of intervention strategies [AME11, vDBF15, ADL*22,STX*22,LCZ*24] were reflected in some of the surveyed systems' goals and visualization designs, but were not as common. These tasks were closely related to simulations of diffusion scenarios, where analysts and experts would define simulation parameters and seed nodes, run batches of these, accumulate hypothetical outcomes, and need to compare these ensembles to identify the most probable outcomes [SGM*23,ADL*22,AME11,STX*22, LCZ*24].

These common tasks impose constraints and requirements on the visualization approaches and interaction techniques. Specifically, a central aspect is how time is modeled and represented, ranging from event-based models to preserve precise ordering of events, to time-sliced, step-based, or flattened approaches [LHS*15, BPW*21, CLS*12, WLY*14, SGM*23, DWL*22]. These present increasing levels of temporal aggregation, which require a specific visualization method to showcase continuity of diffusion processes versus abrupt changes between time-slices [CLS*12, WLY*14, DWL*22, SGM*23]. Furthermore, many of the common tasks contain path tracing or discuss causal reasoning, which requires the visualization to depict the relationships and sequences of events occurring due to the diffusion process [BPW*21, WTF*16, CLS*12, WLY*14]. Depending on the size and density of the network, certain scalability concerns need to be considered so that the approach may effectively tackle denser structures [SGM*23, LHS*15, DWL*22]. Finally, there was significant variability between how much structural context was required or depicted by the surveyed publications. This ranged from explicit medium networks to transmission-specific views, and there was a frequent requirement to support multi-level analysis for both global patterns and local details [CCW*16, YJZ*25, DWL*22, BPW*21, SGM*23].

7. Summary and Future Work

Our survey reveals that visualizing ID over dynamic networks is not only a question of appropriate visual encodings, but more so about the choices of modeling diffusion processes and which aspects of these are central to the analysis objective. This section synthesizes the main insights from our categorization and identifies directions for future research. We provide a summary of the differences in strategies to model and represent time in diffusion networks in Table 3, specifically focusing on the approaches' strengths and weaknesses.

7.1. Takeaways

Medium vs. Transmission Networks A core contribution of this survey is defining and making the distinction between medium (M-NW) and transmission (T-NW) networks. Across the surveyed literature, this distinction is rarely explicitly discussed or articulated.

Implicit (*hidden*) M-NWs are surprisingly common in related literature. In contrast to initial expectations that T-NWs are visualized as processes unfolding over explicit M-NWs, we found many approaches exclusively visualize the transmission events and patterns without representing (or discussing) the role of the underlying structure supporting the diffusion. Particularly prevalent in the application domain of social media [WLY*14, WLC*16], where visualization of the underlying follower or friend networks that define the set of all possible transmissions is omitted and instead the approaches focus on the cascades or propagation of topics and opinions. These design choices have consequences; without explicitly providing the M-NW an analyst can only have partial reasoning about *why* a certain transmission occurred or *why* a certain pattern emerged. In the context of contact-tracing, attributes such as uncertainty, delay, or confidence directly affect how events propagate and accumulate throughout the M-NW and influence the transmission patterns that can be observed [BFR*25]. It is also not always clear what alternative scenarios and pathways are possible. Few approaches tackle this challenge and visualize the relationship between the M-NW and T-NW networks, demonstrating the value within an analytical context by explicitly visualizing them [ASGK21, LLZ*16]. Further examples demonstrate how the visualization approaches heavily depend on the characteristics of the M-NW. In cases when the M-NW is well-defined and changes slowly (e.g., power grids [OW00], computer networks & infrastructure [KSBT12, TMW03]), the M-NWs can be visualized in a spatial substrate and employ animation or highlighting to draw the viewer's attention to transmission events. However, when the M-NW rapidly changes, such as in social media applications, it is often omitted (implicit) [HWZ19, XWW*13, YJZ*25], flattened across time [SKM08,LLM*19], or the dynamics can be leveraged to compute and identify important flow paths in the T-NW [WLC*16].

Temporal Asymmetry In our categorization, we notice an asymmetric relationship between the time models of the M-NW and T-NW networks. Across literature, T-NWs are modeled at equal or finer temporal granularity than their corresponding M-NWs (see diagonal matrix pattern in Table 2). This suggests that the details of transmissions cannot exceed the resolution supported by the M-NW, though this constraint is rarely discussed. We further identify missing combinations in related literature (compare empty cells in Table 2): event-based T-NWs and step-based M-NWs cannot coexist since they create ambiguity (i.e., how can precise transmission times be assigned when contact timing is unknown?). Simi-

Strategy	Well-suited for	Limitations
Event-based	• Fine-grained temporal analysis • Tracing diffusion paths and causality • Reconstructing transmission chains • Identifying precise ordering of events	• Limited scalability for dense datasets (high computational costs) • High visual complexity and clutter • Requires significant interaction and filtering • Fine temporal details might obfuscate overview patterns and global trends
Time-sliced	• Trend analysis and summarization • Comparing diffusion between time intervals • High-level view of spread dynamics • Global patterns overview	• Loss of fine temporal ordering • Sensitive to slice temporal resolution • Ambiguity within slices (no order of events) • Reduced causal interpretability
Step-based	• Propagation order and dependencies • Model-driven or iterative processes • Simplified progression analysis	• No explicit temporal meaning • Limited real-world time interpretation • Less suitable for dynamics • Often used in specific domains and models
Flattened	• Global structure and overview • Identifying key nodes and influence • Static comparison of diffusion processes	• No temporal information • No causality or ordering • Cannot trace diffusion paths • Risk of oversimplification

Table 3: *Comparison of temporal modeling strategies for transmission networks, highlighting their strengths and limitations with respect to task of interest to ID.*

larly, time-sliced T-NWs cannot appear with event-based or step-based M-NWs, as this requires aggregating transmission events while preserving finer-grained structural changes occurring to the M-NW. Flattened T-NWs collapse the temporal dimensions. Consequently, event-based, time-sliced, and step-based M-NWs cannot be mapped (compare other empty cells in Table 2).

We also found that step-based M-NWs are rare occurrences, despite the existence of algorithms and approaches to visualize these in dynamic network visualization literature [BBDW17]. This may reflect domain- and application-specific characteristics, specifically in epidemiology [WLS*22, YZGW22], social media [CCW*16, TGA*23], and infrastructure [USK21, CAD21], where data is typically provided with precise time stamps or natural time windows as opposed to having a purely sequential order of events. Exceptions to this are discussed in related literature on simulations and diffusion models [Wu21], where the results produce step-based simulation data.

The COVID-19 Effect Throughout our literature collection, a common trend is how dominant the application domain of epidemiology is; particularly prominent are contributions on COVID-19 contact tracing, outbreak analysis, and intervention evaluation [STX*22, WLS*22, YZGW22, CARA*22, DARA*22]. This reflects a sense of urgency related to pandemics and how VA has developed capabilities for crisis responses [BGv*25, KAD*25]. However, this also raises questions about how these contributions could be generalized across application domains. Many epidemic-focused systems incorporate assumptions, such as SIR models, contact definitions, intervention scenarios, and prevention strategies, that may not transfer easily to other diffusion contexts. Social media forms our second most popular application domain cluster. The analytical focus in this domain is more on influence and sentiment analysis [FH16, BLRM19], rather than transmission mechanics. It is common to use glyphs in these contexts to depict multiple variables or facets of the data [LLM*19, XWW*13, YJZ*25].

Across domains, multiple coordinated views dominate the visual designs: almost all the surveyed papers include auxiliary charts beyond network visualizations, such as line charts of derived network measures, maps as additional views to node-link diagrams for assessing spatial data facets, linking M-NWand T-NW network views, views on parameter implications, etc. However, distributing information across views imposes cognitive integration costs, highlighting opportunities for more novel approaches combining structural, temporal, and statistical facets [KLM24].

7.2. Opportunities for Future Research

Current approaches visualize either M-NW or T-NW networks. Techniques to encode how diffusion processes unfold over M-NWs to show the relationship between the two are underinvestigated in related literature. This could improve causal reasoning and support further analysis techniques such as counterfactuals and "what if" analysis.

Furthermore, we need approaches for uncertainty-aware diffusion visualizations. We have established a conceptual framework [BFR*25], however, we discovered that visualization approaches and systems to convey uncertainty within dynamic transmission networks are still lacking. Wunderlich et al. [WBv*19] present an exception, visualizing probabilistic infection propagation through ensemble-based representations with color-coded and glyph-based encodings of transmission probabilities. Given the prevalence of inference in related work [WLC*16, YJZ*25] and prediction [ZL21, HWZ19], we need systematic approaches to encode uncertainty in transmission pathways since they affect both the timing and possible outcomes of the transmission events. A way forward could be to consider interaction techniques for exploring uncertainty or ensemble visualizations for probabilistic networks [SNG*17].

Guidance and influence-aware analysis also present a notable open challenge. While many systems compute influence measures, such as centrality metrics [MZK19, SV20], betweenness [FH16], or custom metrics [ADL*22, DC24], few approaches attempt to actively guide toward influential nodes [CCW*16], critical transmission pathways [BPW*21, WTF*16], or temporally salient events [LHS*15]. Analysts manually search for patterns rather than being directed. We need intelligent navigation systems that proactively highlight super-spreaders [WLS*22], identify bottleneck transmission events whose removal would most disrupt cascades [vDBF15], flag temporal anomalies (unexpected acceleration, delayed propagation [CLS*12]), and recommend intervention points [STX*22, SPL*18]. Promising directions exist, e.g., TimeLighting [FCAA25] demonstrates how guidance can highlight interesting temporal intervals and network elements in event-based graphs, supporting pattern identification.

Scalability limitations are discussed across temporal and structural dimensions. Related literature commonly addresses these primarily by filtering and temporal/spatial aggregation (*flattening*) [ZL21, YZGW22, USK19]. However, this comes at the cost of detail and can obscure critical patterns. We need more sophisticated approaches, integrated selection techniques for fluid overview-detail navigation [CCW*16, YJZ*25] and progressive approaches for real-time monitoring during crises [USK21, BGv*25].

Finally, although there is some initial work [AP16b, LAN21], more empirical studies and evaluations for comparing the effectiveness of the developed techniques and approaches across domains need to be conducted. Does a storyline visualization that is effective at conveying contact tracing within hospital settings [BPW*21] work equally well for botnet propagation and cyber attacks [RBJ*23]?; Do flow metaphors from air pollution [RWZ*20, HBY*23] transfer to financial contagion and systematic risk [vDBF15, FNV22]?

The COVID-19 pandemic demonstrated both the potential and limitations of current approaches. Visualization techniques were rapidly deployed [KAD*25] as systems for contact tracing [ASGK21], policy evaluation [STX*22], and risk assessment [ZL21], showing how our field can respond to urgent societal needs. Many systems present many different visualizations, views, encodings, and metaphors. The challenge now is consolidating these diverse approaches into explicit, validated design patterns that can guide future work across domains. The next crisis, epidemic, financial contagion, or misinformation campaign will arrive without warning. When it does, we need visualization approaches that are validated and transferable.

Visualization and analysis of information diffusion is not a solved problem; it's an active area of research where interdisciplinary research is conducted. This survey maps the landscape we have explored so far, providing a practical resource for researchers and practitioners with a structured overview of existing techniques and the critical distinction between the M-NW and T-NW networks.

8. Conclusion

This survey provides a systematic overview of VA approaches for understanding ID and transmission phenomena unfolding over dynamic networks. We distinguish between M-NW and T-NW networks and categorize visualizations according to what is diffused, where, and how it spreads. We further offer a structured perspective on a rapidly evolving and diverse field. Our review clarifies terminology, consolidates concepts, and identifies popular visualization paradigms as well as innovative approaches, providing both researchers and practitioners with a practical resource for diffusion and network visualization.

Through our systematic literature review, we identify several pressing research directions, including supporting multivariate diffusion data, improving uncertainty representation, enabling interactive exploration of large-scale transmission networks, as well as integrating predictive and prescriptive analytic capabilities. We hope this survey serves as a foundation for future work in the design, evaluation, and application of visualizations for ID, advancing the understanding of these complex processes across domains and supporting evidence-based decision-making.

Acknowledgments This research was partially funded by the Österreichischen Wissenschaftsfonds (FWF, Austrian Science Fund) [10.55776/I6635] and the Deutsche Forschungsgemeinschaft (DFG, German Research Foundation) [527250730] within the joint project "SANE", BMFTR Project RiskPrincipe [01ZZ2323J], FWF project ArtVis [10.55776/P35767], and FWF doc.funds.connect Visual Heritage [10.55776/DFH37]. This work involves the reflection on UK Research and Innovation Engineering and Physical Sciences Research Council (UKRI EPSRC) grant EP/V033670/1. For the purpose of open access, the authors have applied a Creative Commons Attribution (CC-BY) license to any Author Accepted Manuscript version arising from this submission. Open Access funding enabled and organized by Projekt DEAL.

References

[AAA*24] ALRASHEED H., ALBALLA N., AL-TURAIKI I., ALMUTLAQ F., ALABDULJABBAR R.: City Transmission Networks: Unraveling Disease Spread Dynamics. *ISPRS International Journal of Geo-Information 13*, 8 (Aug. 2024), 283. doi:10.3390/ijgi13080283. 9, 25, 26, 27, 30, 32

[AC17] ANAND R., CHATTERJEE S.: Tracking disease progression by searching paths in a temporal network of biological processes. *PLOS ONE 12*, 4 (Apr. 2017), e0176172. doi:10.1371/journal.pone.0176172. 9, 14, 15, 16

[ADL*22] ARLEO A., DIDIMO W., LIOTTA G., MIKSCH S., MONTECCHIANI F.: Influence Maximization With Visual Analytics. *IEEE Transactions on Visualization and Computer Graphics 28*, 10 (Oct. 2022), 3428–3440. doi:10.1109/TVCG.2022.3190623. 2, 5, 9, 20, 23, 31, 32, 33, 35

[AGJS*20] AFZAL S., GHANI S., JENKINS-SMITH H. C., EBERT D. S., HADWIGER M., HOTEIT I.: A Visual Analytics-based Decision Making Environment for COVID-19 Modeling and Visualization . In *IEEE Visualization Conference* (2020), IEEE, pp. 86–90. doi:10.1109/VIS47514.2020.00024. 2

[AL20] AHN Y., LIN Y.-R.: PolicyFlow: Interpreting Policy Diffusion in Context. *ACM Trans. Interact. Intell. Syst. 10*, 2 (2020). doi:10.1145/3385729. 5

[AMA22] ARLEO A., MIKSCH S., ARCHAMBAULT D.: Event-based dynamic graph drawing without the agonizing pain. *Computer Graphics Forum 41*, 6 (2022), 226–244. doi:10.1111/cgf.14615. 3

[AME11] AFZAL S., MACIEJEWSKI R., EBERT D. S.: Visual analytics decision support environment for epidemic modeling and response evaluation. In *2011 IEEE Conference on Visual Analytics Science and Technology (VAST)* (2011), pp. 191–200. doi:10.1109/VAST.2011.6102457. 2, 9, 14, 15, 19, 31, 32, 33

[AP12] ARCHAMBAULT D., PURCHASE H. C.: Mental map preservation helps user orientation in dynamic graphs. In *International Symposium on Graph Drawing* (2012), Springer, pp. 475–486. doi:10.1007/978-3-642-36763-2_42. 3

[AP16a] ARCHAMBAULT D., PURCHASE H. C.: Can animation support the visualization of dynamic graphs? *Information Sciences 330* (2016), 495–509. doi:10.1016/j.ins.2015.04.017. 3

[AP16b] ARCHAMBAULT D., PURCHASE H. C.: On the effective visualisation of dynamic attribute cascades. *Information Visualization 15*, 1 (Jan. 2016), 51–63. doi:10.1177/1473871615576758. 9, 20, 23, 35

[ASGK21] ANTWEILER D., SESSLER D., GINZEL S., KOHLHAMMER J.: Towards the Detection and Visual Analysis of COVID-19 Infection Clusters. *EuroVis Workshop on Visual Analytics (EuroVA)* (2021), 5 pages. doi:10.2312/EUROVA.20211097. 9, 14, 15, 19, 31, 33, 35

[BASD21] BROWNE C. A., AMCHIN D. B., SCHNEIDER J., DATTA S. S.: Infection Percolation: A Dynamic Network Model of Disease Spreading. *Frontiers in Physics 9* (2021). doi:10.3389/fphy.2021.645954. 9, 20, 24

[BBB24] BAUM K., BAUMANN A., BATZEL K.: Investigating Innovation Diffusion in Gender-Specific Medicine: Insights from Social Network Analysis. *Business & Information Systems Engineering 66*, 3 (2024), 335–355. doi:10.1007/s12599-024-00875-6. 8, 9, 12

[BBDW17] BECK F., BURCH M., DIEHL S., WEISKOPF D.: A Taxonomy and Survey of Dynamic Graph Visualization. In *Computer Graphics Forum* (2017), vol. 36, Wiley Online Library, pp. 133–159. doi:10.1111/cgf.12791. 4, 5, 34

[BDA*17] BACH B., DRAGICEVIC P., ARCHAMBAULT D., HURTER C., CARPENDALE S.: A descriptive framework for temporal data visualizations based on generalized space-time cubes. *Computer Graphics Forum 36*, 6 (2017), 36–61. doi:10.1111/cgf.12804. 3, 4, 5, 25

[BDPC20] BACHECHI C., DESIMONI F., PO L., CASAS D. M.: Visual analytics for spatio-temporal air quality data. In *2020 24th International Conference Information Visualisation (IV)* (Sept. 2020), pp. 460–466. doi:10.1109/IV51561.2020.00080. 9, 14, 15, 16

[BFR*25] BAUMGARTL T., FILIPOV V., RAJENDRAN S., MIKSCH S., ARCHAMBAULT D., ARLEO A., VON LANDESBERGER T.: Layers of Doubt: Typology of Temporal Uncertainty in Dynamic Diffusion Networks. In *2025 IEEE Workshop on Uncertainty Visualization: Unraveling Relationships of Uncertainty, AI, and Decision-Making* (2025), pp. 53–57. doi:10.1109/UncertaintyVisualization68947.2025.00012. 2, 33, 35

[BGG*11] BROECK W. V. D., GIOANNINI C., GONÇALVES B., QUAGGIOTTO M., COLIZZA V., VESPIGNANI A.: The GLEaMviz Computational Tool, a Publicly Available Software to Explore Realistic Epidemic Spreading Scenarios at the Global Scale . *BMC Infectious Diseases 11* (2011), 1–14. doi:10.1186/1471-2334-11-37. 5

[BGG19] BHATTACHARYA S., GAURAV K., GHOSH S.: Viral Marketing on Social Networks: An Epidemiological Perspective. *Physica A: Statistical Mechanics and its Applications 525* (2019), 478–490. doi:10.1016/j.physa.2019.03.008. 5

[BGv*25] BAUMGARTL T., GHONIEM M., VON LANDESBERGER T., MARAI G. E., MIKSCH S., MOHR S., SCHEITHAUER S., SRIVASTAVA N.: Empowering Communities: Tailored Pandemic Data Visualization for Varied Tasks and Users. *IEEE Computer Graphics and Applications 45*, 1 (2025), 130–138. doi:10.1109/MCG.2024.3509293. 34, 35

[BLRM19] BABVEY P., LIPIZZI C., RAMIREZ-MARQUEZ J. E.: Dissecting Twitter Discussion Threads with Topic-Aware Network Visualization. In *2019 International Conference on Computational Science and Computational Intelligence (CSCI)* (2019), pp. 1359–1364. doi:10.1109/CSCI49370.2019.00254. 9, 25, 26, 28, 34

[BM11] BRANDES U., MADER M.: A quantitative comparison of stress-minimization approaches for offline dynamic graph drawing. In *International Symposium on Graph Drawing* (2011), Springer, pp. 99–110. doi:10.1007/978-3-642-25878-7_11. 3

[BPW*21] BAUMGARTL T., PETZOLD M., WUNDERLICH M., HOHN M., ARCHAMBAULT D., LIESER M., DALPKE A., SCHEITHAUER S., MARSCHOLLEK M., EICHEL V. M., MUTTERS N. T., CONSORTIUM H., VON LANDESBERGER T.: In Search of Patient Zero: Visual Analytics of Pathogen Transmission Pathways in Hospitals. *IEEE Transactions on Visualization and Computer Graphics 27*, 2 (Feb. 2021), 711–721. doi:10.1109/TVCG.2020.3030437. 2, 8, 9, 10, 31, 32, 33, 35

[BRSG07] BENNETT C., RYALL J., SPALTEHOLZ L., GOOCH A.: The aesthetics of graph visualization. pp. 57–64. doi:10.2312/COMPAESTH/COMPAESTH07/057-064. 32

[CAD21] CAI Q., ALAM S., DUONG V. N.: A Spatial-Temporal Network Perspective for the Propagation Dynamics of Air Traffic Delays. *Engineering 7*, 4 (2021), 452–464. doi:10.1016/j.eng.2020.05.027. 9, 14, 15, 17, 18, 34

[CARA*22] CHEN M., ABDUL-RAHMAN A., ARCHAMBAULT D., DYKES J., RITSOS P., SLINGSBY A., TORSNEY-WEIR T., TURKAY C., BACH B., BORGO R., ET AL.: RAMPVIS: Answering the challenges of building visualisation capabilities for large-scale emergency responses. *Epidemics 39* (2022), 100569. doi:10.1016/j.epidem.2022.100569. 2, 5, 34

[CCL*17] CHEN S., CHEN S., LIN L., YUAN X., LIANG J., ZHANG X.: E-map: A visual analytics approach for exploring significant event evolutions in social media. In *IEEE Conference on Visual Analytics Science and Technology (VAST)* (2017), IEEE, pp. 36–47. doi:10.1109/VAST.2017.8585638. 5

[CCW*16] CHEN S., CHEN S., WANG Z., LIANG J., YUAN X., CAO N., WU Y.: D-Map: Visual analysis of ego-centric information diffusion patterns in social media. In *2016 IEEE Conference on Visual Analytics Science and Technology (VAST)* (Baltimore, MD, USA, Oct. 2016), IEEE, pp. 41–50. doi:10.1109/VAST.2016.7883510. 5, 9, 14, 15, 17, 18, 31, 33, 34, 35

[CCW*18] CHEN S., CHEN S., WANG Z., LIANG J., WU Y., YUAN X.: D-map+ interactive visual analysis and exploration of ego-centric and event-centric information diffusion patterns in social media. *ACM Transactions on Intelligent Systems and Technology (TIST) 10*, 1 (2018), 1–26. doi:10.1145/3183347. 5

[CDBM*06] CORTESE P. F., DI BATTISTA G., MONETA A., PATRIGNANI M., PIZZONIA M.: Topographic Visualization of Prefix Propagation in the Internet. *IEEE Transactions on Visualization and Computer Graphics 12*, 5 (Sept. 2006), 725–732. doi:10.1109/TVCG.2006.185. 9, 14, 15, 16, 29, 30

[CLCY19] CHEN S., LI S., CHEN S., YUAN X.: R-map: A map metaphor for visualizing information reposting process in social media. *IEEE Transactions on Visualization and Computer Graphics 26*, 1 (2019), 1204–1214. doi:10.1109/TVCG.2019.2934263. 5

[CLS*12] CAO N., LIN Y.-R., SUN X., LAZER D., LIU S., QU H.: Whisper: Tracing the Spatiotemporal Process of Information Diffusion in Real Time. *IEEE Transactions on Visualization and Computer Graphics 18*, 12 (2012), 2649–2658. doi:10.1109/TVCG.2012.291. 5, 8, 9, 10, 31, 33, 35

[CLY17] CHEN S., LIN L., YUAN X.: Social Media Visual Analytics. In *Computer Graphics Forum* (2017), vol. 36, Wiley Online Library, pp. 563–587. doi:10.1111/cgf.13211. 2, 5

[CLYL18] CHOI G., LIM S., YOON T., LEE K.: Citation Network Visualization of Reference Papers Based on Influence Groups. In *2018 IEEE 8th Symposium on Large Data Analysis and Visualization (LDAV)* (Oct. 2018), pp. 96–97. doi:10.1109/LDAV.2018.8739176. 9, 14, 15, 17

[Cro25] CROSSREF: Crossref rest api, 2025. Accessed: 2025-09-25. URL: https://www.crossref.org/documentation/retrieve-metadata/rest-api/. 5

[CS14] CANNARELLA J., SPECHLER J. A.: Epidemiological Modeling of Online Social Network Dynamics. *arXiv preprint arXiv:1401.4208* (2014). doi:10.48550/arXiv.1401.4208. 5

[CSN*20] CHEN B., SHI M., NI X., RUAN L., JIANG H., YAO H., WANG M., SONG Z., ZHOU Q., GE T.: Visual Data Analysis and Simulation Prediction for COVID-19. *International Journal of Educational Excellence* (2020). doi:10.3991/ijoe.v17i08.20099. 2

[CSNW24] CHEN T., SU L. Y.-F., NG Y. M. M., WANG Y.-C.: A longitudinal analysis of usage patterns, topics, and information dissemination related to five names for cultured meat on social media. *Current Research in Food Science 9* (2024), 100859. doi:10.1016/j.crfs.2024.100859. 9, 14, 15, 17, 18

[CSS*25] CAO Y., SHI Q., SHEN L., CHEN K., WANG Y., ZENG W., QU H.: NFTracer: Tracing NFT Impact Dynamics in Transaction-Flow Substitutive Systems With Visual Analytics. *IEEE Transactions on Visualization and Computer Graphics 31*, 8 (2025), 4369–4386. doi:10.1109/TVCG.2024.3402834. 9, 26, 28

[CVV*21] CARDENAS N. C., VANDERWAAL K., VELOSO F. P., GALVIS J. O. A., AMAKU M., GRISI-FILHO J. H.: Spatio-temporal network analysis of pig trade to inform the design of risk-based disease surveillance. *Preventive Veterinary Medicine 189* (Apr. 2021), 105314. doi:10.1016/j.prevetmed.2021.105314. 29

[CWW10] CHEN W., WANG C., WANG Y.: Scalable influence maximization for prevalent viral marketing in large-scale social networks. In *Proceedings of the 16th ACM SIGKDD International Conference on Knowledge Discovery and Data Mining* (New York, NY, USA, 2010), KDD '10, Association for Computing Machinery, pp. 1029–1038. doi:10.1145/1835804.1835934. 5

[DARA*22] DYKES J., ABDUL-RAHMAN A., ARCHAMBAULT D., BACH B., BORGO R., CHEN M., ENRIGHT J., FANG H., FIRAT E. E., FREEMAN E., ET AL.: Visualization for epidemiological modeling: Challenges, solutions, reflections and recommendations. *Philosophical Transactions of the Royal Society A 380*, 2233 (2022). doi:10.1098/rsta.2021.0299. 2, 5, 34

[DBDDP*15] DI BATTISTA G., DI DONATO V., PATRIGNANI M., PIZZONIA M., ROSELLI V., TAMASSIA R.: Bitconeview: Visualization of flows in the bitcoin transaction graph. In *2015 IEEE Symposium on Visualization for Cyber Security (VizSec)* (Oct. 2015), pp. 1–8. doi:10.1109/VIZSEC.2015.7312773. 2, 8, 9, 10

[DC24] DUTTA S., CHAKRABORTY S.: Influence detection in dynamic networks: A novel overlapping community detection approach applied to COVID-19 spread analysis in India. *Social Network Analysis and Mining 14*, 1 (Sept. 2024), 198. doi:10.1007/s13278-024-01359-x. 9, 14, 15, 16, 35

[DCX*24] DENG Z., CHEN S., XIE X., SUN G., XU M., WENG D., WU Y.: Multilevel Visual Analysis of Aggregate Geo-Networks. *IEEE Transactions on Visualization and Computer Graphics 30*, 7 (2024), 3135–3150. doi:10.1109/TVCG.2022.3229953. 9, 26, 28, 29

[DG02] DIEHL S., GÖRG C.: Graphs, they are changing. In *International Symposium on Graph Drawing* (2002), Springer, pp. 23–31. doi:10.1007/3-540-36151-0_3. 3

[DGK01] DIEHL S., GÖRG C., KERREN A.: Preserving the mental map using foresighted layout. In *Data Visualization 2001* (2001), Springer, pp. 175–184. doi:10.1007/978-3-7091-6215-6_19. 3

[DWC*20] DENG Z., WENG D., CHEN J., LIU R., WANG Z., BAO J., ZHENG Y., WU Y.: AirVis: Visual Analytics of Air Pollution Propagation. *IEEE Transactions on Visualization and Computer Graphics 26*, 1 (Jan. 2020), 800–810. doi:10.1109/TVCG.2019.2934670. 9, 20, 24, 31, 33

[DWL*22] DENG Z., WENG D., LIANG Y., BAO J., ZHENG Y., SCHRECK T., XU M., WU Y.: Visual Cascade Analytics of Large-Scale Spatiotemporal Data. *IEEE Transactions on Visualization and Computer Graphics 28*, 6 (2022), 2486–2499. doi:10.1109/TVCG.2021.3071387. 8, 9, 13, 30, 31, 33

[EHK*03] ERTEN C., HARDING P. J., KOBOUROV S. G., WAMPLER K., YEE G.: GraphAEL: Graph animations with evolving layouts. In *International Symposium on Graph Drawing* (2003), Springer, pp. 98–110. doi:10.1007/978-3-540-24595-7_9. 3

[Els25] ELSEVIER: Scopus api, 2025. Accessed: 2025-09-25. URL: https://dev.elsevier.com/. 5

[Eur25] EUROGRAPHICS ASSOCIATION: Eurographics digital library, 2025. URL: https://diglib.eg.org/. 5

[FAM23] FILIPOV V., ARLEO A., MIKSCH S.: Are We There Yet? A Roadmap of Network Visualization from Surveys to Task Taxonomies . *Computer Graphics Forum 42*, 6 (2023), e14794. doi:10.1111/cgf.14794. 5

[FBL*18] FORBES A. G., BURKS A., LEE K., LI X., BOUTILLIER P., KRIVINE J., FONTANA W.: Dynamic Influence Networks for Rule-Based Models. *IEEE transactions on visualization and computer graphics 24*, 1 (Jan. 2018), 184–194. doi:10.1109/TVCG.2017.2745280. 9, 14, 15, 16

[FCAA23] FILIPOV V., CENEDA D., ARCHAMBAULT D., ARLEO A.: TimeLighting: Guidance-enhanced exploration of 2D projections of temporal graphs. In *Graph Drawing and Network Visualization* (Cham, 2023), Bekos M. A., Chimani M., (Eds.), pp. 231–245. doi:10.1007/978-3-031-49272-3_16. 3

[FCAA25] FILIPOV V., CENEDA D., ARCHAMBAULT D., ARLEO A.: TimeLighting: Guided exploration of 2d temporal network projections. *IEEE Transactions on Visualization and Computer Graphics 31*, 3 (2025), 1932–1944. doi:10.1109/TVCG.2024.3514858. 3, 35

[FGRW*15] FARAJTABAR M., GOMEZ-RODRIGUEZ M., WANG Y., LI S., ZHA H., SONG L.: Co-evolutionary Dynamics of Information Diffusion and Network Structure. In *Proceedings of the International Conference on World Wide Web* (2015), pp. 619–620. doi:10.1145/2740908.2744105. 5

[FH16] FRANCALANCI C., HUSSAIN A.: Discovering social influencers with network visualization: Evidence from the tourism domain. *Information Technology & Tourism 16*, 1 (Mar. 2016), 103–125. doi:10.1007/s40558-015-0030-3. 9, 25, 26, 27, 29, 30, 34, 35

[FKN*04] FORRESTER D., KOBOUROV S. G., NAVABI A., WAMPLER K., YEE G. V.: GraphAEL: A system for generalized force-directed layouts. In *International Symposium on Graph Drawing* (2004), Springer, pp. 454–464. doi:10.1007/978-3-540-31843-9_47. 3

[FNV22] FRANCH F., NOCCIOLA L., VOULDIS A.: Temporal Networks in the Analysis of Financial Contagion, 2022. arXiv:4125870, doi:10.2139/ssrn.4125870. 9, 14, 15, 17, 19, 35

[GGZZ22] GENG R., GAO Y., ZHANG H., ZU J.: Analysis of the Spatio-Temporal Dynamics of COVID-19 in Massachusetts via Spectral Graph Wavelet Theory. *IEEE Transactions on Signal and Information Processing over Networks 8* (2022), 670–683. doi:10.1109/TSIPN.2022.3193252. 9, 14, 15, 17

[GHFZ13] GUILLE A., HACID H., FAVRE C., ZIGHED D. A.: Information Diffusion in Online Social Networks: A Survey. *SIGMOD Rec. 42*, 2 (2013), 17–28. doi:10.1145/2503792.2503797. 5, 30

[GJG*19] GUO S., JIN Z., GOTZ D., DU F., ZHA H., CAO N.: Visual Progression Analysis of Event Sequence Data. *IEEE Transactions on Visualization and Computer Graphics 25*, 1 (2019), 417–426. doi:10.1109/TVCG.2018.2864885. 8, 9, 10

[GNX25] GONG X.-L., NING H.-Y., XIONG X.: Research on the cross-contagion between international stock markets and geopolitical risks: The two-layer network perspective. *Financial Innovation 11*, 1 (2025), 23. doi:10.1186/s40854-024-00687-3. 9, 26, 28, 29

[Gro24] GROSFILS P.: Information Transmission in a Drone Swarm: A Temporal Network Analysis. *Drones 8*, 1 (2024), 28. doi:10.3390/drones8010028. 9, 20, 24, 25

[Guo07] GUO D.: Visual Analytics of Spatial Interaction Patterns for Pandemic Decision Support . *International Journal of Geographical Information Science 21*, 8 (2007), 859–877. doi:10.1080/13658810701349037. 2

[HBY*23] HAO Y., BI C., YANG L., QIU X., LI Y., YU C.: Visual Analytics of Air Pollutant Propagation Path and Pollution Source. In *Proceedings of the 16th International Symposium on Visual Information Communication and Interaction* (New York, NY, USA, Oct. 2023), VINCI '23, Association for Computing Machinery, pp. 1–8. doi:10.1145/3615522.3615527. 9, 14, 15, 16, 17, 35

[HFZW23] HE Q., FANG H., ZHANG J., WANG X.: Dynamic opinion maximization in social networks. *IEEE Transactions on Knowledge and Data Engineering 35*, 1 (2023), 350–361. doi:10.1109/TKDE.2021.3077491. 5

[HKPC18] HOHMAN F., KAHNG M., PIENTA R., CHAU D. H.: Visual analytics in deep learning: An interrogative survey for the next frontiers. *IEEE transactions on visualization and computer graphics 25*, 8 (2018), 2674–2693. doi:10.1109/TVCG.2018.2843369. 5

[HMM00] HERMAN I., MELANCON G., MARSHALL M.: Graph visualization and navigation in information visualization: A survey. *IEEE Transactions on Visualization and Computer Graphics 6*, 1 (2000), 24–43. doi:10.1109/2945.841119. 4

[HS12] HOLME P., SARAMÄKI J.: Temporal Networks. *Physics Reports 519*, 3 (2012), 97–125. doi:10.1016/j.physrep.2012.03.001. 3, 26

[HSS15] HADLAK S., SCHUMANN H., SCHULZ H.-J.: A Survey of Multi-faceted Graph Visualization. In *EuroVis (STARs)* (2015), The Eurographics Association. doi:10.2312/eurovisstar.20151109. 2, 4, 5

[HSS*20] HUANG Y., SHI L., SU Y., HU Y., TONG H., WANG C., YANG T., WANG D., LIANG S.: Eiffel: Evolutionary Flow Map for Influence Graph Visualization. *IEEE Transactions on Visualization and Computer Graphics 26*, 10 (Oct. 2020), 2944–2960. doi:10.1109/TVCG.2019.2906900. 8, 9, 12, 29, 30

[HWZ19] HUANG Z., WANG Z., ZHANG R.: Cascade2vec: Learning Dynamic Cascade Representation by Recurrent Graph Neural Networks. *IEEE Access 7* (2019), 144800–144812. doi:10.1109/ACCESS.2019.2942853. 9, 14, 15, 16, 29, 33, 35

[HXF*21] HAN X., XU Y., FAN L., HUANG Y., XU M., GAO S.: Quantifying COVID-19 importation risk in a dynamic network of domestic cities and international countries. *Proceedings of the National Academy of Sciences 118*, 31 (2021), e2100201118. doi:10.1073/pnas.2100201118. 9, 14, 15, 17, 18

[IHK*16] ISENBERG P., HEIMERL F., KOCH S., ISENBERG T., XU P., STOLPER C. D., SEDLMAIR M., CHEN J., MÖLLER T., STASKO J.: vispubdata.org: A metadata collection about ieee visualization (vis) publications. *IEEE transactions on visualization and computer graphics 23*, 9 (2016), 2199–2206. doi:10.1109/TVCG.2016.2615308. 5

[JPAP21] JANG H., PAI S., ADHIKARI B., PEMMARAJU S. V.: Risk-aware Temporal Cascade Reconstruction to Detect Asymptomatic Cases : For the CDC MInD Healthcare Network. In *2021 IEEE International Conference on Data Mining (ICDM)* (2021), pp. 240–249. doi:10.1109/ICDM51629.2021.00034. 8, 9, 13

[KAD*25] KOZLIKOVA B., ARCHAMBAULT D., DREESMAN J., KERREN A., LUCINI B., TURKAY C.: Embarrassingly agile–data visualization methodology in emergency responses. *IEEE Computer Graphics and Applications 45*, 5 (2025), 138–146. doi:10.1109/MCG.2025.3595342. 34, 35

[KDB*24] KHODAVEISI T., DEHDARIRAD H., BOURAGHI H., MOHAMMADPOUR A., SAJADI F., HOSSEINIRAVANDI M.: Characteristics and specifications of dashboards developed for the covid-19 pandemic: a scoping review. *Journal of Public Health 32*, 4 (2024), 553–574. doi:10.1007/s10389-023-01838-z. 5

[KKC14] KERRACHER N., KENNEDY J., CHALMERS K.: The Design Space of Temporal Graph Visualisation. In *EuroVis - Short Papers* (2014), Elmqvist N., Hlawitschka M., Kennedy J., (Eds.), The Eurographics Association. doi:10.2312/eurovisshort.20141149. 5

[KKT03] KEMPE D., KLEINBERG J., TARDOS E.: Maximizing the spread of influence through a social network. In *Proceedings of the Ninth ACM SIGKDD International Conference on Knowledge Discovery and Data Mining* (New York, NY, USA, 2003), KDD '03, Association for Computing Machinery, pp. 137–146. doi:10.1145/956750.956769. 5

[KKT05] KEMPE D., KLEINBERG J., TARDOS É.: Influential Nodes in a Diffusion Model for Social Networks. In *Automata, Languages and Programming: International Colloquium* (2005), Springer, pp. 1127–1138. doi:10.1007/11523468_91. 5

[KLM24] KUO Y.-H., LIU D., MA K.-L.: SpreadLine: Visualizing Egocentric Dynamic Influence. *IEEE Transactions on Visualization and Computer Graphics* (2024). doi:10.1109/TVCG.2024.3456373. 9, 14, 15, 17, 32, 34

[KPK18] KUCHER K., PARADIS C., KERREN A.: The state of the art in sentiment visualization. *Computer Graphics Forum 37*, 1 (2018), 71–96. doi:10.1111/cgf.13217. 5

[KSBT12] KOYAMA A., SATO S., BAROLLI L., TAKIZAWA M.: An Implementation of Visualization System for Visualizing Network Topology and Packet Flow in Mobile Ad Hoc Networks. In *2012 15th International Conference on Network-Based Information Systems* (Sept. 2012), pp. 148–155. doi:10.1109/NBiS.2012.23. 8, 9, 12, 33

[LAN19] LEE A., ARCHAMBAULT D., NACENTA M.: Dynamic network plaid: A tool for the analysis of dynamic networks. In *Proceedings of the 2019 CHI Conference on Human Factors in Computing Systems* (2019), CHI '19, pp. 1–14. doi:10.1145/3290605.3300360. 3

[LAN21] LEE A., ARCHAMBAULT D., NACENTA M. A.: The effectiveness of interactive visualization techniques for time navigation of dynamic graphs on large displays. *IEEE Transactions on Visualization and Computer Graphics 27*, 2 (2021), 528–538. doi:10.1109/TVCG.2020.3030446. 3, 35

[Lan24] LANGE D.: Vispubs: A visualization publications repository, 2024. doi:10.31219/osf.io/dg3p2. 5

[LCZ*24] LI G., CHANG B., ZHAO J., WANG J., HE F., WANG Y., Xu T., Zhou Z.: VIVIAN: Virtual simulation and visual analysis of epidemic spread data. *Journal of Visualization 27*, 4 (2024), 677–694. doi:10.1007/s12650-024-00990-2. 8, 9, 11, 31, 32, 33

[Ley02] Ley M.: The dblp computer science bibliography: Evolution, research issues, perspectives. In *International symposium on string processing and information retrieval* (2002), Springer, pp. 1–10. URL: https://dblp.org/xml/. 5

[LFWT18] Li Y., Fan J., Wang Y., Tan K.-L.: Influence maximization on social graphs: A survey. *IEEE Transactions on Knowledge and Data Engineering 30*, 10 (2018), 1852–1872. doi:10.1109/TKDE.2018.2807843. 5

[LHS*15] Liu Q., Hu Y., Shi L., Mu X., Zhang Y., Tang J.: EgoNetCloud: Event-based egocentric dynamic network visualization. In *2015 IEEE Conference on Visual Analytics Science and Technology (VAST)* (Oct. 2015), pp. 65–72. doi:10.1109/VAST.2015.7347632. 8, 9, 10, 11, 29, 31, 32, 33, 35

[LKB*14] Lenz O., Keul F., Bremm S., Hamacher K., von Landesberger T.: Visual analysis of patterns in multiple amino acid mutation graphs. In *2014 IEEE Conference on Visual Analytics Science and Technology (VAST)* (2014), pp. 93–102. doi:10.1109/VAST.2014.7042485. 9, 20, 24, 25, 30, 31, 32

[LLJ*24] Lessani M. N., Li Z., Jing F., Qiao S., Zhang J., Olatosi B., Li X.: Human mobility and the infectious disease transmission: a systematic review. *Geo-Spatial Information Science 27*, 6 (2024), 1824–1851. doi:10.1080/10095020.2023.2275619. 5

[LLM*19] Loyola-González O., López-Cuevas A., Medina-Pérez M. A., Camiña B., Ramírez-Márquez J. E., Monroy R.: Fusing pattern discovery and visual analytics approaches in tweet propagation. *Information Fusion 46* (Mar. 2019), 91–101. doi:10.1016/j.inffus.2018.05.004. 9, 20, 24, 30, 33, 34

[LLZ*16] Liu M., Liu S., Zhu X., Liao Q., Wei F., Pan S.: An Uncertainty-Aware Approach for Exploratory Microblog Retrieval. *IEEE Transactions on Visualization and Computer Graphics 22*, 1 (Jan. 2016), 250–259. doi:10.1109/TVCG.2015.2467554. 8, 9, 12, 33

[LMJ*21] Luo C., Ma Y., Jiang P., Zhang T., Yin F.: The construction and visualization of the transmission networks for COVID-19: A potential solution for contact tracing and assessments of epidemics. *Scientific Reports 11*, 1 (2021), 8605. doi:10.1038/s41598-021-87802-x. 9, 25, 26, 28, 29

[LWN*20] Lo K., Wang L. L., Neumann M., Kinney R., Weld D. S.: S2orc: The semantic scholar open research corpus. In *Proceedings of the 58th Annual Meeting of the Association for Computational Linguistics (ACL)* (2020), Association for Computational Linguistics, pp. 4969–4983. doi:10.18653/v1/2020.acl-main.447. 5

[LWW*13] Liu S., Wu Y., Wei E., Liu M., Liu Y.: StoryFlow: Tracking the Evolution of Stories. *IEEE Transactions on Visualization and Computer Graphics 19*, 12 (2013), 2436–2445. doi:10.1109/TVCG.2013.196. 6

[LZ14] Liu C., Zhang Z.-K.: Information Spreading on Dynamic Social Networks. *Communications in Nonlinear Science and Numerical Simulation 19*, 4 (2014), 896–904. doi:10.1016/j.cnsns.2013.08.028. 4, 5

[LZW25] Liu Y., Zhang Q., Wang Z.: Community opinion maximization in social networks. *IEEE Transactions on Evolutionary Computation 29*, 5 (2025), 1760–1773. doi:10.1109/TEVC.2024.3431608. 5

[MB18] Moats D., Borra E.: Quali-quantitative methods beyond networks: Studying information diffusion on Twitter with the Modulation Sequencer. *Big Data & Society 5*, 1 (2018), 2053951718772137. doi:10.1177/2053951718772137. 8, 9, 13

[MBZ22] Mendonça M. R., Barreto A. M., Ziviani A.: Efficient Information Diffusion in Time-varying Graphs Through Deep Reinforcement Learning . *World Wide Web 25*, 6 (2022), 2535–2560. doi:10.1007/s11280-021-00998-w. 5

[MGM*19] McGee F., Ghoniem M., Melançon G., Otjacques B., Pinaud B.: The state of the art in multilayer network visualization. In *Computer graphics forum* (2019), vol. 38, Wiley Online Library, pp. 125–149. doi:10.1111/cgf.13610. 4, 5

[MLL*13] Monroe M., Lan R., Lee H., Plaisant C., Shneiderman B.: Temporal event sequence simplification. *IEEE transactions on visualization and computer graphics 19*, 12 (2013), 2227–2236. doi:10.1109/TVCG.2013.200. 3

[MLMdO*13] Monroe M., Lan R., Morales del Olmo J., Shneiderman B., Plaisant C., Millstein J.: The challenges of specifying intervals and absences in temporal queries: a graphical language approach. In *Proceedings of the SIGCHI Conference on Human Factors in Computing Systems* (New York, NY, USA, 2013), CHI '13, Association for Computing Machinery, pp. 2349–2358. doi:10.1145/2470654.2481325. 3

[MMH21] Masuda N., Miller J. C., Holme P.: Concurrency measures in the era of temporal network epidemiology: A review. *Journal of The Royal Society Interface 18*, 179 (2021), 20210019. doi:10.1098/rsif.2021.0019. 5

[MOM*24] Miranda F., Ortner T., Moreira G., Hosseini M., Vuckovic M., Biljecki F., Silva C. T., Lage M., Ferreira N.: The state of the art in visual analytics for 3D urban data. In *Computer Graphics Forum* (2024), vol. 43, Wiley Online Library, p. e15112. doi:10.1111/cgf.15112Digital. 5

[MZK19] Mrsic L., Zajec S., Kopal R.: Appliance of Social Network Analysis and Data Visualization Techniques in Analysis of Information Propagation. In *Intelligent Information and Database Systems* (Cham, 2019), Nguyen N. T., Gaol F. L., Hong T.-P., Trawiński B., (Eds.), Springer International Publishing, pp. 131–143. doi:10.1007/978-3-030-14802-7_11. 9, 25, 26, 27, 35

[NCZZ18] Niu Z., Cheng D., Zhang L., Zhang J.: Visual Analytics for Networked-Guarantee Loans Risk Management. In *2018 IEEE Pacific Visualization Symposium (PacificVis)* (Apr. 2018), pp. 160–169. doi:10.1109/PacificVis.2018.00028. 9, 14, 15, 17, 29

[NMSL19] Nobre C., Meyer M., Streit M., Lex A.: The state of the art in visualizing multivariate networks. In *Computer Graphics Forum* (2019), vol. 38, Wiley Online Library, pp. 807–832. doi:10.1111/cgf.13728. 4

[NSS*24] Nasution Y. N., Sitorus M. Y., Sukandar K., Nuraini N., Apri M., Salama N.: The epidemic forest reveals the spatial pattern of the spread of acute respiratory infections in Jakarta, Indonesia. *Scientific Reports 14*, 1 (2024), 7619. doi:10.1038/s41598-024-58390-3. 9, 20, 24

[NW14] Nöremark M., Widgren S.: EpiContactTrace: An R-package for contact tracing during livestock disease outbreaks and for risk-based surveillance | BMC Veterinary Research. *BMC veterinary research* (2014). doi:10.1186/1746-6148-10-71. 9, 20, 21, 22

[OGGB25] Oh J., Gaza H. L., Gang E., Byun J.: TPVis: A Temporal Path Visualization System for Intuitive Understanding of Information Diffusion Inside Temporal Networks. *IEEE Access 13* (2025), 119633–119645. doi:10.1109/ACCESS.2025.3586044. 8, 9, 13, 14

[OW00] Overbye T., Weber J.: New methods for the visualization of electric power system information. In *IEEE Symposium on Information Visualization 2000. INFOVIS 2000. Proceedings* (Oct. 2000), pp. 131–16c. doi:10.1109/INFVIS.2000.885101. 8, 9, 12, 33

[PLFT21] Ponciano J. R., Linhares C. D., Faria E. R., Travenã̆golo B. A.: An online and nonuniform timeslicing method for network visualisation. *Computers & Graphics 97* (2021), 170–182. doi:10.1016/j.cag.2021.04.006. 3

[PMA*22] Papadopoulou O., Makedas T., Apostolidis L., Poldi F., Papadopoulos S., Kompatsiaris I.: MeVer NetworkX: Network Analysis and Visualization for Tracing Disinformation. *Future*

Internet 14, 5 (2022), 147. doi:10.3390/fi14050147. 9, 25, 26, 27

[PMB*21] PAGE M. J., MCKENZIE J. E., BOSSUYT P. M., BOUTRON I., HOFFMANN T. C., MULROW C. D., SHAMSEER L., TETZLAFF J. M., AKL E. A., BRENNAN S. E., CHOU R., GLANVILLE J., GRIMSHAW J. M., HRÓBJARTSSON A., LALU M. M., LI T., LODER E. W., MAYO-WILSON E., MCDONALD S., MCGUINNESS L. A., STEWART L. A., THOMAS J., TRICCO A. C., WELCH V. A., WHITING P., MOHER D.: The PRISMA 2020 Statement: An Updated Guideline for Reporting Systematic Reviews. *BMJ 372* (2021). doi:10.1136/bmj.n71. 5

[PnABP20] PEÑA ARAYA V., BEZERIANOS A., PIETRIGA E.: A Comparison of Geographical Propagation Visualizations. In *Proceedings of the 2020 CHI Conference on Human Factors in Computing Systems* (2020), ACM, pp. 1–14. doi:10.1145/3313831.3376350. 9, 20, 24, 25

[PS20] PERRI V., SCHOLTES I.: HOTVis: Higher-order time-aware visualisation of dynamic graphs. In *Graph Drawing and Network Visualization* (Cham, 2020), Auber D., Valtr P., (Eds.), Springer International Publishing, pp. 99–114. doi:10.1007/978-3-030-68766-3_8. 3

[Pur02] PURCHASE H. C.: Metrics for graph drawing aesthetics. *Journal of Visual Languages & Computing 13*, 5 (2002), 501–516. doi:10.1006/jvlc.2002.0232. 32

[PVL21] PONCIANO J. R., VEZONO G. P., LINHARES C. D. G.: Simulating and visualizing infection spread dynamics with temporal networks. In *Simpósio Brasileiro de Banco de Dados (SBBD)* (Oct. 2021), SBC, pp. 37–48. doi:10.5753/sbbd.2021.17864. 9, 20, 21

[PVL22] PONCIANO J. R., VEZONO G. P., LINHARES C. D. G.: A Visualization Approach for Simulating and Analyzing Infection Spread Dynamics Using Temporal Networks. *Journal of Information and Data Management 13*, 2 (2022). doi:10.5753/jidm.2022.2456. 9, 20, 21

[QHD26] QIU L., HUANG Y., DONG G.: Exploring crypto-stock risk contagion via directed complex network analytics. *Physica A: Statistical Mechanics and its Applications 681* (2026), 131111. doi:10.1016/j.physa.2025.131111. 9, 26, 28, 29

[RBJ*23] RABZELJ M., BOHAK C., JUŽNIČ L. Š., KOS A., SEDLAR U.: Cyberattack Graph Modeling for Visual Analytics. *IEEE Access 11* (2023), 86910–86944. doi:10.1109/ACCESS.2023.3304640. 9, 26, 27, 29, 35

[RIDS25] RASEL M. A. B., ISLAM M. R., DAS P. C., SAINI S.: User Influence, Hashtag Trends, and Engagement Patterns: Analyzing Social Media Network Dynamics in Tourism Using Graph Analytics. *Tourism and Hospitality 6*, 2 (2025). doi:10.3390/tourhosp6020060. 9, 25, 26, 28

[RRP*21] RUGET A.-S., ROSSI G., PEPLER P. T., BEAUNÉE G., BANKS C. J., ENRIGHT J., KAO R. R.: Multi-species temporal network of livestock movements for disease spread. *Applied Network Science 6*, 1 (Feb. 2021), 15. doi:10.1007/s41109-021-00354-x. 9, 20, 21, 29

[RWZ*20] REN K., WU Y., ZHANG H., FU J., QU D., LIN X.: Visual Analytics of Air Pollution Propagation Through Dynamic Network Analysis. *IEEE Access 8* (2020), 205289–205306. doi:10.1109/ACCESS.2020.3036354. 9, 14, 15, 16, 29, 35

[SAK17] SIMONETTO P., ARCHAMBAULT D., KOBOUROV S.: Drawing dynamic graphs without timeslices. In *International Symposium on Graph Drawing and Network Visualization* (2017), Springer, pp. 394–409. doi:10.1007/978-3-319-73915-1_31. 3

[SAK20] SIMONETTO P., ARCHAMBAULT D., KOBOUROV S.: Event-based dynamic graph visualisation. *IEEE Transactions on Visualization and Computer Graphics 26*, 7 (2020), 2373–2386. doi:10.1109/TVCG.2018.2886901. 3

[SGM*23] SEHNAN D., GOEL V., MASUD S., JAIN C., GOYAL V., CHAKRABORTY T.: DiVA: A Scalable, Interactive and Customizable Visual Analytics Platform for Information Diffusion on Large Networks. *ACM Trans. Knowl. Discov. Data 17*, 4 (Feb. 2023), 47:1–47:33. doi:10.1145/3558771. 9, 20, 23, 29, 30, 31, 32, 33

[SKKS08] STREIT M., KALKUSCH M., KASHOFER K., SCHMALSTIEG D.: Navigation and Exploration of Interconnected Pathways. *Computer Graphics Forum 27*, 3 (2008), 951–958. doi:10.1111/j.1467-8659.2008.01229.x. 9, 14, 15, 18

[SKM08] SAITO K., KIMURA M., MOTODA H.: Effective Visualization of Information Diffusion Process over Complex Networks. In *Machine Learning and Knowledge Discovery in Databases*, Daelemans W., Goethals B., Morik K., (Eds.), vol. 5212. Springer Berlin Heidelberg, 2008, pp. 326–341. doi:10.1007/978-3-540-87481-2_22. 9, 25, 26, 28, 32, 33

[SKOM12] SAITO K., KIMURA M., OHARA K., MOTODA H.: Graph embedding on spheres and its application to visualization of information diffusion data. In *Proceedings of the 21st International Conference on World Wide Web* (New York, NY, USA, Apr. 2012), WWW '12 Companion, Association for Computing Machinery, pp. 1137–1144. doi:10.1145/2187980.2188253. 9, 20, 24, 25

[SMSR20] SARASWATHI S., MUKHOPADHYAY A., SHAH H., RANGANATH T. S.: Social network analysis of COVID-19 transmission in Karnataka, India. *Epidemiology & Infection 148* (2020), e230. doi:10.1017/S095026882000223X. 9, 14, 15, 17, 18, 32

[SNG*17] SCHULZ C., NOCAJ A., GOERTLER J., DEUSSEN O., BRANDES U., WEISKOPF D.: Probabilistic graph layout for uncertain network visualization. *IEEE Transactions on Visualization and Computer Graphics 23*, 1 (2017), 531–540. doi:10.1109/TVCG.2016.2598919. 35

[SPL*18] SHAN Z., PAN Z., LI F., XU H., XU H.: Visual Analytics of Traffic Congestion Propagation Path with Large Scale Camera Data. *Chinese Journal of Electronics 27*, 5 (2018), 934–941. doi:10.1049/cje.2018.04.011. 9, 14, 15, 17, 18, 35

[SSXS15] SU Y., SUN S., XUAN Y., SHI L.: Influence Visualization of Scientific Paper through Flow-Based Citation Network Summarization. In *2015 IEEE International Conference on Data Mining Workshop (ICDMW)* (2015), pp. 1652–1655. doi:10.1109/ICDMW.2015.105. 9, 26, 28, 29

[STP*17] SUN G., TANG T., PENG T.-Q., LIANG R., WU Y.: Socialwave: Visual Analysis of Spatio-temporal Diffusion of Information on Social Media . *ACM Transactions on Intelligent Systems and Technology (TIST) 9*, 2 (2017), 1–23. doi:10.1145/3106775. 2

[STT81] SUGIYAMA K., TAGAWA S., TODA M.: Methods for visual understanding of hierarchical system structures. *IEEE Transactions on Systems, Man, and Cybernetics 11*, 2 (1981), 109–125. doi:10.1109/TSMC.1981.4308636. 32

[STX*22] SONDAG M., TURKAY C., XU K., MATTHEWS L., MOHR S., ARCHAMBAULT D.: Visual Analytics of Contact Tracing Policy Simulations During an Emergency Response. *Computer Graphics Forum 41*, 3 (2022), 29–41. doi:10.1111/cgf.14520. 2, 9, 14, 15, 16, 30, 31, 32, 33, 34, 35

[Sum13] SUMMER M.: Financial contagion and network analysis. *Annu. Rev. Financ. Econ. 5*, 1 (2013), 277–297. doi:10.1146/annurev-financial-110112-120948. 5

[SV20] SAQR M., VIBERG O.: Using Diffusion Network Analytics to Examine and Support Knowledge Construction in CSCL Settings. In *Addressing Global Challenges and Quality Education* (Cham, 2020), Alario-Hoyos C., Rodríguez-Triana M. J., Scheffel M., Arnedillo-Sánchez I., Dennerlein S. M., (Eds.), Springer International Publishing, pp. 158–172. doi:10.1007/978-3-030-57717-9_12. 9, 25, 26, 27, 29, 30, 35

[SYM24] SOGA K., YOSHIDA S., MUNEYASU M.: Graph-Based Interpretability for Fake News Detection through Topic- and Propagation-Aware Visualization. *Computation 12*, 4 (Apr. 2024), 82. doi:10.3390/computation12040082. 9, 25, 26, 28

[SYPB21] SCHÖTTLER S., YANG Y., PFISTER H., BACH B.: Visualizing and Interacting with Geospatial Networks: A Survey and Design Space. *Computer Graphics Forum 40*, 6 (2021), 5–33. doi:10.1111/cgf.14198. 4, 5

[Tan18] TANG S.: When social advertising meets viral marketing: Sequencing social advertisements for influence maximization. *Proceedings of the AAAI Conference on Artificial Intelligence 32*, 1 (April 2018). doi:10.1609/aaai.v32i1.11306. 5

[TGA*23] TABASSUM S., GAMA J., AZEVEDO P. J., CORDEIRO M., MARTINS C., MARTINS A.: Social network analytics and visualization: Dynamic topic-based influence analysis in evolving micro-blogs. *Expert Systems 40*, 5 (2023), e13195. doi:10.1111/exsy.13195. 9, 14, 15, 17, 18, 19, 29, 34

[TLZ*23] TIAN Y., LIU J., ZHANG X., YANG X., KE Z., ZHANG C., LIAO L., HONG S., ZHANG H., LI Q.: InvestLens: A Visual Analytics Approach to Inspecting the Dynamics of Venture Capital Investment Network. In *2023 IEEE 39th International Conference on Data Engineering Workshops (ICDEW)* (2023), pp. 12–19. doi:10.1109/ICDEW58674.2023.00007. 8, 9, 11

[TMK14] TAKAGI H., MISUE K., KANAI Y.: Queuing Network Model and Visualization for the Patient Flow in the Obstetric Unit of the University of Tsukuba Hospital. In *2014 Annual SRII Global Conference* (2014), pp. 147–156. doi:10.1109/SRII.2014.31. 9, 25, 26, 28, 29

[TMW03] TEOH S. T., MA K.-L., WU S.: A visual exploration process for the analysis of Internet routing data. In *IEEE Visualization, 2003. VIS 2003.* (2003), pp. 523–530. doi:10.1109/VISUAL.2003.1250415. 8, 9, 12, 33

[TPL*25] TINARRAGE R., PONCIANO J. R., LINHARES C. D. G., TRAINA A. J. M., POCO J.: ZigzagNetVis: Suggesting temporal resolutions for graph visualization using zigzag persistence. *IEEE Transactions on Visualization and Computer Graphics 31*, 10 (2025), 6852–6869. doi:10.1109/TVCG.2025.3528197. 3

[UA24] USUL M., ARLEO A.: Peeking at Visualization Research on Information Diffusion. In *EuroVis 2024 - Posters* (2024), Kucher K., Diehl A., Gillmann C., (Eds.), The Eurographics Association. doi:10.2312/evp.20241089. 5

[USK19] ULMER A., SESSLER D., KOHLHAMMER J.: NetCapVis: Web-based Progressive Visual Analytics for Network Packet Captures. In *2019 IEEE Symposium on Visualization for Cyber Security (VizSec)* (2019), pp. 1–10. doi:10.1109/VizSec48167.2019.9161633. 9, 14, 15, 16, 35

[USK21] ULMER A., SESSLER D., KOHLHAMMER J.: ProBGP: Progressive Visual Analytics of Live BGP Updates. *Computer Graphics Forum 40*, 3 (2021), 37–48. doi:10.1111/cgf.14287. 8, 9, 12, 29, 34, 35

[VBF*17] VALENCIA C., BAH H., FATOUMATA B., RODIER G., DIALLO B., KONE M., GIESE C., CONDE L., MALANO E., MOLLET T., JANSA J., COULOMBIER D., SUDRE B.: Network visualization for outbreak response: Mapping the ebola virus disease (evd) chains of transmission in N Zerekore, guinea. *Journal of Infection 74*, 3 (2017), 294–301. doi:10.1016/j.jinf.2016.09.012. 8, 9, 13

[vDBF15] VON LANDESBERGER T., DIEL S., BREMM S., FELLNER D. W.: Visual analysis of contagion in networks. *Information Visualization 14*, 2 (Apr. 2015), 93–110. doi:10.1177/1473871613487087. 2, 9, 20, 23, 31, 32, 33, 35

[VKPM15] VALLET J., KIRCHNER H., PINAUD B., MELANÇON G.: A Visual Analytics Approach to Compare Propagation Models in Social Networks. *Electronic Proceedings in Theoretical Computer Science 181* (Apr. 2015), 65–79. arXiv:1504.02612, doi:10.4204/EPTCS.181.5. 9, 20, 25

[vKS*11] VON LANDESBERGER T., KUIJPER A., SCHRECK T., KOHLHAMMER J., VAN WIJK J. J., FEKETE J.-D., FELLNER D. W.: Visual Analysis of Large Graphs: State-of-the-Art and Future Research Challenges . In *Computer Graphics Forum* (2011), vol. 30, Wiley Online Library, pp. 1719–1749. doi:10.1111/j.1467-8659.2011.01898.x. 4, 5, 32

[VRHGM*24] VILLAR-RODRIGUEZ G., HUERTAS-GARCIA A., MARTIN A., HUERTAS-TATO J., CAMACHO D.: DisTrack: A New Tool For Semi-automatic Misinformation Tracking in Online Social Networks. *Cognitive Computation 17*, 1 (2024), 12. doi:10.1007/s12559-024-10378-x. 8, 9, 13, 14, 32

[WAH*19] WANG Y., ARCHAMBAULT D., HALEEM H., MOELLER T., WU Y., QU H.: Nonuniform timeslicing of dynamic graphs based on visual complexity. In *IEEE Visualization Conference (VIS) Short Papers* (2019). doi:10.1109/VISUAL.2019.8933748. 3

[WBv*19] WUNDERLICH M., BLOCK I., VON LANDESBERGER T., PETZOLD M., MARSCHOLLEK M., SCHEITHAUER S.: Visual Analysis of Probabilistic Infection Contagion in Hospitals. In *VMV* (2019), pp. 143–150. doi:10.2312/vmv.20191328. 2, 9, 20, 23, 30, 31, 35

[WDC*22] WANG R., DU K., CHEN Q., ZHAO Y., TANG M., TAO H., WANG S., LI Y., WANG Y.: Rumorlens: Interactive analysis and validation of suspected rumors on social media. In *CHI Conference on Human Factors in Computing Systems Extended Abstracts* (2022), pp. 1–7. doi:10.1145/3491101.3519712. 5

[WLC*16] WANG X., LIU S., CHEN Y., PENG T.-Q., SU J., YANG J., GUO B.: How ideas flow across multiple social groups. In *2016 IEEE Conference on Visual Analytics Science and Technology (VAST)* (Oct. 2016), pp. 51–60. doi:10.1109/VAST.2016.7883511. 9, 14, 15, 19, 20, 30, 33, 35

[WLS*22] WU M., LI C., SHEN Z., HE S., TANG L., ZHENG J., FANG Y., LI K., CHENG Y., SHI Z., SHENG G., LIU Y., ZHU J., YE X., CHEN J., CHEN W., LI L., SUN Y., CHEN J.: Use of temporal contact graphs to understand the evolution of COVID-19 through contact tracing data. *Communications Physics 5*, 1 (2022), 270. doi:10.1038/s42005-022-01045-4. 9, 14, 15, 16, 34, 35

[WLY*14] WU Y., LIU S., YAN K., LIU M., WU F.: OpinionFlow: Visual Analysis of Opinion Diffusion on Social Media. *IEEE Transactions on Visualization and Computer Graphics 20*, 12 (2014), 1763–1772. doi:10.1109/TVCG.2014.2346920. 2, 8, 9, 13, 31, 33

[WM21] WICKRAMASINGHE A. N., MUTHUKUMARANA S.: Social network analysis and community detection on spread of COVID-19. *Model Assisted Statistics and Applications 16*, 1 (2021), 37–52. doi:10.3233/MAS-210513. 9, 25, 26, 28, 29

[WPCM02] WARE C., PURCHASE H., COLPOYS L., MCGILL M.: Cognitive measurements of graph aesthetics. *Information Visualization 1*, 2 (2002), 103–110. doi:10.1057/palgrave.ivs.9500013. 32

[WTF*16] WEISER A. A., THÖNS C., FILTER M., FALENSKI A., APPEL B., KÄSBOHRER A.: FoodChain-Lab: A Trace-Back and Trace-Forward Tool Developed and Applied during Food-Borne Disease Outbreak Investigations in Germany and Europe. *PLOS ONE 11*, 3 (Mar. 2016), e0151977. doi:10.1371/journal.pone.0151977. 9, 25, 26, 27, 31, 33, 35

[Wu21] WU J.: Construct a Knowledge Graph for China Coronavirus (COVID-19) Patient Information Tracking. *Risk Management and Healthcare Policy 14* (Oct. 2021), 4321–4337. doi:10.2147/RMHP.S309732. 9, 20, 22, 34

[Wue21] WUERSCHINGER Q.: Social Networks of Lexical Innovation. Investigating the Social Dynamics of Diffusion of Neologisms on Twitter. *Frontiers in Artificial Intelligence 4* (2021). doi:10.3389/frai.2021.648583. 9, 25, 26, 28

[WYG*11] WANG C., YU H., GROUT R. W., MA K.-L., CHEN J. H.: Analyzing information transfer in time-varying multivariate data. In *2011 IEEE Pacific Visualization Symposium* (2011), pp. 99–106. doi:10.1109/PACIFICVIS.2011.5742378. 9, 20, 23

[XSS*24] XIAO S., SHI Q., SHAO L., DU B., WANG Y., SHEN Q., ZENG W.: MetroBUX: A Topology-Based Visual Analytics for Bus Operational Uncertainty EXploration. *IEEE Transactions on Intelligent*

Transportation Systems 25, 6 (2024), 5525–5538. doi:10.1109/TITS.2023.3338700. 8, 9, 13

[XWW*13] XU P., WU Y., WEI E., PENG T.-Q., LIU S., ZHU J. J., QU H.: Visual Analysis of Topic Competition on Social Media. *IEEE Transactions on Visualization and Computer Graphics 19*, 12 (2013), 2012–2021. doi:10.1109/TVCG.2013.221. 9, 14, 15, 16, 17, 32, 33, 34

[XZX*24] XU J., ZHANG C., XIE M., ZHAN X., YAN L., TAO Y., PAN Z.: IMVis: Visual analytics for influence maximization algorithm evaluation in hypergraphs. *Visual Informatics 8*, 2 (June 2024), 13–26. doi:10.1016/j.visinf.2024.04.006. 9, 20, 23, 29, 30

[YAD*18] YOGHOURDJIAN V., ARCHAMBAULT D., DIEHL S., DWYER T., KLEIN K., PURCHASE H. C., WU H.-Y.: Exploring the limits of complexity: A survey of empirical studies on graph visualisation. *Visual Informatics 2*, 4 (2018), 264–282. doi:10.1016/j.visinf.2018.12.006. 5

[Yan21] YANG Z.: Analysis of dynamic contact network of patients with COVID-19 in Shaanxi Province of China. *Scientific Reports 11*, 1 (2021), 4889. doi:10.1038/s41598-021-84428-x. 9, 14, 15, 19

[YJZ*25] YIN J., JIA H., ZHOU B., TANG T., YING L., YE S., PENG T.-Q., WU Y.: Blowing Seeds Across Gardens: Visualizing Implicit Propagation of Cross-Platform Social Media Posts. *IEEE Transactions on Visualization and Computer Graphics 31*, 1 (Jan. 2025), 185–195. doi:10.1109/TVCG.2024.3456181. 2, 9, 14, 15, 16, 29, 30, 31, 33, 34, 35

[YLZ*25] YU G., LI Q., ZHAO Y., WANG J., CHEN Y., CHEN S.: Utilizing Effective Dynamic Graph Learning to Shield Financial Stability from Risk Propagation, 2025. arXiv:2502.13979, doi:10.48550/arXiv.2502.13979. 9, 26, 28, 29

[YZGW22] YANG Z., ZHANG J., GAO S., WANG H.: Complex Contact Network of Patients at the Beginning of an Epidemic Outbreak: An Analysis Based on 1218 COVID-19 Cases in China. *International Journal of Environmental Research and Public Health 19*, 2 (Jan. 2022), 689. doi:10.3390/ijerph19020689. 9, 14, 15, 16, 34, 35

[ZCW*14] ZHAO J., CAO N., WEN Z., SONG Y., LIN Y.-R., COLLINS C.: #FluxFlow: Visual Analysis of Anomalous Information Spreading on Social Media . *IEEE Transactions on Visualization and Computer Graphics 20*, 12 (2014), 1773–1782. doi:10.1109/TVCG.2014.2346922. 2

[ZCW21] ZHENG J., CHI X., WENG S.: A Network Based Quantitative Method for the Mining and Visualization of Music Influence. In *Data Mining and Big Data* (2021), Tan Y., Shi Y., Zomaya A., Yan H., Cai J., (Eds.), Springer, pp. 59–72. doi:10.1007/978-981-16-7476-1_6. 9, 14, 15, 17

[ZL21] ZHANG T., LI J.: Understanding and predicting the spatiotemporal spread of COVID-19 via integrating diffusive graph embedding and compartmental models. *Transactions in GIS 25*, 6 (2021), 3025–3047. doi:10.1111/tgis.12803. 9, 14, 15, 16, 35

[ZM14] ZHANG J., MOURA J. M.: Diffusion in Social Networks as SIS Epidemics: Beyond Full Mixing and Complete Graphs. *IEEE Journal of Selected Topics in Signal Processing 8*, 4 (2014), 537–551. doi:10.1109/JSTSP.2014.2314858. 5

[ZSG*23] ZHANG Y., SUN Y., GAGGIANO J. D., KUMAR N., ANDRIS C., PARKER A. G.: Visualization design practices in a crisis: Behind the scenes with covid-19 dashboard creators. *IEEE Transactions on Visualization and Computer Graphics 29*, 1 (2023), 1037–1047. doi:10.1109/TVCG.2022.3209493. 5

[ZXL23] ZHANG B., XIE X., LI C.: How Connected Is China's Systemic Financial Risk Contagion Network?—A Dynamic Network Perspective Analysis. *Mathematics* (2023). doi:10.3390/math11102267. 9, 20, 23, 29, 30